

University of Central Florida

STARS

Electronic Theses and Dissertations

2017

Discovery and Characterization of Antimalarials with Novel Mechanisms of Action

Bracken Roberts

University of Central Florida



Part of the [Biochemistry, Biophysics, and Structural Biology Commons](#)

Find similar works at: <https://stars.library.ucf.edu/etd>

University of Central Florida Libraries <http://library.ucf.edu>

This Doctoral Dissertation (Open Access) is brought to you for free and open access by STARS. It has been accepted for inclusion in Electronic Theses and Dissertations by an authorized administrator of STARS. For more information, please contact STARS@ucf.edu.

STARS Citation

Roberts, Bracken, "Discovery and Characterization of Antimalarials with Novel Mechanisms of Action" (2017). *Electronic Theses and Dissertations*. 5596.

<https://stars.library.ucf.edu/etd/5596>

DISCOVERY AND CHARACTERIZATION OF ANTIMALARIAL COMPOUNDS WITH
NOVEL CELLULAR MECHANISMS OF ACTION

by

BRACKEN F. ROBERTS

M.S. Biotechnology University of Central Florida, 2012

B.S. Biotechnology University of Central Florida, 2009

B.S. Molecular and Microbiology University of Central Florida, 2009

A dissertation submitted in partial fulfillment of the requirements
for the degree of Doctor of Philosophy
in the Molecular Microbiology Division of the
Burnett School of Biomedical Sciences
in the College of Medicine
at the University of Central Florida
Orlando, Florida

Summer Term
2017

Major Professor: Debopam Chakrabarti

© 2017 Bracken Roberts

ABSTRACT

Malaria kills over 500,000 people each year and over a third of the global population is at risk of infection. Though the human race has been fighting the malaria war for over 4,000 years and we have made great strides in eliminating malaria from many countries, we are treading on the edge of what could be another malaria epidemic primarily due to widespread drug resistance. There are documented cases of resistance for every known antimalarial in use today, including Artemisinins. It is critical that we open a new window of discovery in development of next generation antimalarials that circumvent current resistance paradigms. These compounds must attack new targets, have different speeds of action, and ideally possess powerful transmission blocking potential if they are to be successful antimalarial candidates.

Screening endeavors historically focused on either synthetic or natural product libraries. Recent efforts have focused on combining privilege elements of natural products into synthetically tractable compounds to create hybrid libraries. To discover novel antimalarial pharmacophores, we have screened natural products derived from marine biodiversity as well as natural product-inspired synthetic libraries. Our phenotypic screening of 3,164 marine natural products from the Harbor Branch Oceanographic Institute, 56 high density combinatorial natural product based libraries from the Torrey Pines Institute for Molecular Studies, alkaloid, terpene, and macrocyclic libraries from Memorial Sloan Kettering Cancer Center, and 594 natural product-inspired compounds from Asinex have identified several new selective antiplasmodial hit chemotypes.

In this study, we have focused on compounds that exhibit cellular actions differing from current antimalarials. Two of the scaffolds, UCF 201 and 501, a spirocyclic chromane and a nitroquinoline, respectively, act early in the development cycle and block invasion. The alkaloid derived compound M03 blocks egress. UCF 501 cures malaria in the rodent model and significantly inhibits stage V gametocytogenesis. Given that discovery of transmission blocking agents are a priority in the malaria elimination strategies, this result is significant. This work is of high impact as it addresses a critical need in the field- next generation antimalarial scaffolds for malaria therapy and elimination campaign.

I dedicate this work:

to my parents who taught me to cherish education and to never stop learning,

to my wife, without whom I could never achieve anything of significance,

and to my children, may they learn from our progress and use our results to achieve

even greater success.

ACKNOWLEDGMENTS

I first and foremost wish to acknowledge Dr. Debopam Chakrabarti. He has taught me to expect perfection and tolerate excellence. I am the scientist I am today because of him and I will forever be grateful for the improvements he has helped me see in myself and for fire that burns in me now to continually strive to be better in every aspect of my life. He is a patient mentor and I consider it a great blessing to call him my friend.

I could not have organized and accomplished the results in this dissertation without the support of my committee. Dr. Travis Jewett, Dr. William Self, and Dr. Otto Phanstiel IV, thank you for your continual guidance.

I also wish to thank Dr. White and Mr. Greg Weigel. Their leap of faith in accepting me as a General Microbiology teaching assistant provided the financial support that allowed me to initially pursue a graduate degree. Their continued friendship and open doors provided perspective and insight throughout my progress.

Finally, I wish to thank Robert Banks at the Aria Drive Animal Facility for his patience and support as we conducted our rodent malaria efficacy studies.

TABLE OF CONTENTS

LIST OF FIGURES.....	xi
LIST OF TABLES.....	xiii
CHAPTER 1: INTRODUCTION.....	1
Malaria: An Introduction	1
The <i>Plasmodium spp.</i> Complicated Two-Host Life Cycle	2
Lessons From the Past	4
History of Malaria Control Measures	8
Current Antimalarial Therapy.....	10
CHAPTER 2: METHODOLOGY	13
Drug Lead Discovery Scheme.....	13
Screening Library Selection	13
Culturing <i>P. falciparum</i>	14
SYBR Green-I Fluorescence Assay	15
Cytotoxicity Assay.....	16
Physicochemical Profiling.....	16
Sensitivity and Reliability Statistical Analysis.....	17
Rate of Killing and Parasitocidal/Parasitostatic Studies	17
Cellular Mechanism of Action.....	18
<i>in vivo</i> Efficacy	18
β -Hematin Formation Assay.....	19
Synthesis of UCF 501	19

Resistance Profiling	20
CHAPTER 3: DISCOVERY AND CHARACTERIZATION OF ANTIPLASMODIAL COMPOUNDS FROM HARBOR BRANCH OCEANOGRAPHIC INSTITUTE PEAK- FRACTION COLLECTION	
.....	22
HBOI Marine Natural Products Library	22
Hit Identification.....	24
Physicochemical Properties of HBOI Hits.....	30
HBOI Hits Cellular Mechanism of Action	32
CHAPTER 4: DISCOVERY AND CHARACTERIZATION OF ANTIPLASMODIAL COMPOUNDS FROM THE TORREY PINES INSTITUTE FOR MOLECULAR STUDIES HIGH-DENSITY COMBINATORIAL LIBRARY.....	
.....	38
TPIMS High-Density Combinatorial Library	38
Physicochemical Properties of TPIMS 2291	43
Structure Activity Relationship Profiling	45
Cellular Mechanism of Action of TPIMS 2291	47
2291-SB1 <i>in vivo</i> Efficacy.....	49
Transmission Blocking Potential.....	49
CHAPTER 5: DISCOVERY AND CHARACTERIZATION OF ANTIPLASMODIAL COMPOUNDS FROM THE MEMORIAL SLOAN KETTERING CANCER CENTER NATURAL PRODUCT BASED ALKALOID LIBRARY	
.....	51
MSKCC Natural-Inspired Alkaloid Library.....	51
Physicochemical Properties of MSKCC-M03.....	53
Pharmacokinetic Properties of MSK-M03.....	55

Structure Activity Relationship Profiling for MSKCC-M03	57
Rate of Killing and Parasitocidal/Parasitostatic Evaluation	59
Cellular Mechanism of Action of MSKCC-M03	61
CHAPTER 6: DISCOVERY AND CHARACTERIZATION OF ANTIPLASMODIAL	
COMPOUNDS FROM NATURAL PRODUCT-INSPIRED ASINEX BIODESIGN	
LIBRARY	64
Asinex Natural Product-Inspired Library	64
Physicochemical Properties of UCF 201 and UCF 501	69
Structure Activity Relationship Profile for UCF 201	71
Determining Structure Activity Relationships for UCF 501	73
Synthesis of UCF 501	76
Cellular Mechanism of Action	76
UCF 501 Inhibition of β -Hematin Formation	86
Rate of Killing and Parasitocidal/Parasitostatic Evaluation	88
<i>in vivo</i> Efficacy	90
Transmission Blocking Potential.....	94
CHAPTER 7: TARGET IDENTIFICATION OF ANTIPLASMODIAL HITS	
96	
Necessity of Target ID.....	96
Resistance Line Generation	96
Screening for Activity Against Targets Involved in Stage-Specific Interaction Profile.....	101
Affinity Pull-Down	109
CHAPTER 8: DISCUSSION.....	
114	
The Search for New Libraries.....	114
Characteristics of Our Novel Antiplasmodial Hits.....	118

Breaking the Failing Paradigm of Current Antimalarials.....	122
Known Target Necessity	123
REFERENCES.....	125

LIST OF FIGURES

Figure 1 <i>Plasmodium spp.</i> Life Cycle	3
Figure 2 Distribution of Malaria in the United States, 1882-1935.	6
Figure 3 Drug Lead Discovery Scheme.....	13
Figure 4 HBOI Johnson Sea Link Manned Submersible	23
Figure 5 Selectivity of HBOI Dereplicated Hits.	29
Figure 6 Stage Specific Interaction of HBOI Antiplasmodial Hits.	33
Figure 7 Nitenin and Microsclerodermin A Cellular Mechanism of Action.	35
Figure 8 TPIMS Positional Scanning Library Design.....	39
Figure 9 Antiplasmodial Activity of 2291-SB1.....	42
Figure 10 Stage-Specific Activity of TPIMS 2291.....	48
Figure 11 TPIMS 2291-SB1 Gametocyte Inhibition.....	50
Figure 12 Diversity Oriented Synthesis	52
Figure 13 MSKCC Hits Antiplasmodial Activity.	53
Figure 14 MSKCC-M03 SAR.....	58
Figure 15 MSK-M03 Rate of Killing and Parasitostatic Evaluation.	60
Figure 16 Stage Specific Interaction of MSK-M03.....	63
Figure 17 UCF 201 Selectivity.....	66
Figure 18 UCF 501 Antiplasmodial Activity.	68
Figure 19 UCF 501 and SAR Analogs Synthetic Scheme.....	74
Figure 20 UCF 201 Cellular Mechanism of Action.	79
Figure 21 UCF 501 Cellular Mechanism of Action.	84

Figure 22 UCF 501 Rate of Killing and Parasitocidal Evaluation.....	89
Figure 23 <i>in vivo</i> efficacy of UCF 201.....	91
Figure 24 UCF 501 <i>in vivo</i> Efficacy.	92
Figure 25 UCF 501 <i>in vivo</i> Efficacy <i>P. berghei</i> luciferase.....	93
Figure 26 UCF 501 Gametocyte Inhibition	95
Figure 27 UCF 201 Resistance Lines and Activity.	99
Figure 28 MSK-M03 Resistant Lines and Activity.	100
Figure 29 PfPKG and PfCDPK5 Activation Triggers Parasite Egress	102
Figure 30 Plasmodium Egress and Invasion	103
Figure 31 <i>PfCDPK5</i> Cloning.....	106
Figure 32 <i>PfPKG</i> Cloning	107
Figure 33 <i>PfCDPK5</i> Expression	108
Figure 34 Affinity Probe Labeling Strategies for Target Identification.....	110
Figure 35 Likely Tolerable Affinity Probe Linker Site	112
Figure 36 Natural Product-Based Synthetic Libraries Occupy Unique Regions of Chemical Space	117

LIST OF TABLES

Table 1 Antimalarial Chemical Classes and Resistance	12
Table 2 HBOI Antiplasmodial Hit Selectivity.....	25
Table 3 Source Organisms for HBOI Antiplasmodial Hits.	27
Table 4 Physicochemical Properties of HBOI Hits	31
Table 5 Flow Cytometry Analysis of Stage-Specific Interaction of Nitenin and Microsclerodermin A.....	37
Table 6 Antiplasmodial Activity and Selectivity of Top TPIMS Libraries.....	41
Table 7 Physicochemical Properties of 2291-SB1	44
Table 8 TPIMS 2291 SAR	46
Table 9 Physicochemical Properties of MSK-M03	54
Table 10 MSK-M03 <i>in vivo</i> PK (mouse)	56
Table 11 MSK-M03 <i>in vivo</i> PK (human serum)	56
Table 12 Physicochemical Properties of UCF 201	70
Table 13 Physicochemical Properties of UCF 501	70
Table 14 UCF 201 SAR.....	72
Table 15 UCF 501 Analogs Antiplasmodial Activity	75
Table 16 UCF 501 Does not Inhibit B-Hematin Formation.	87

CHAPTER 1: INTRODUCTION

Malaria: An Introduction

Malaria, caused by the apicomplexan parasite *Plasmodium spp.*, infects over 300,000,000 people and claims the lives of over 500,000 people annually (WHO 2016). Literally meaning “bad air” the disease was originally attributed to breathing in marshland regions. In 1880, Charles Louis Alphonse Laveran first discovered the blood-borne protozoan parasite and later was awarded the Nobel Prize in 1907 for this discovery (Nobel Foundation 1907). Malaria typically presents as symptoms of fever, chills, malaise, myalgia, diarrhea, nausea, vomiting, diaphoresis and headache. More complicated severe malaria cases lead to severe anemia, hemoglobinuria, acute respiratory distress, kidney failure, cerebral malaria, seizures, coma, and death (CDC 2015). There are currently five *Plasmodium* species which can infect human: *Plasmodium falciparum*, *Plasmodium knowlesi*, *Plasmodium malariae*, *Plasmodium ovale*, and *Plasmodium vivax* (WHO 2017). While all five species are infectious, *Plasmodium falciparum* is the most deadly, comprising >90% of malaria-related deaths each year (WHO 2017).

The *Plasmodium* spp. Complicated Two-Host Life Cycle

The plasmodial life cycle consist of an asexual human liver stage, an intraerythrocytic asexual life cycle and a sexual development stage originating in human red blood cells (RBC) and further developing within the mosquito mid-gut as shown in Figure 1.

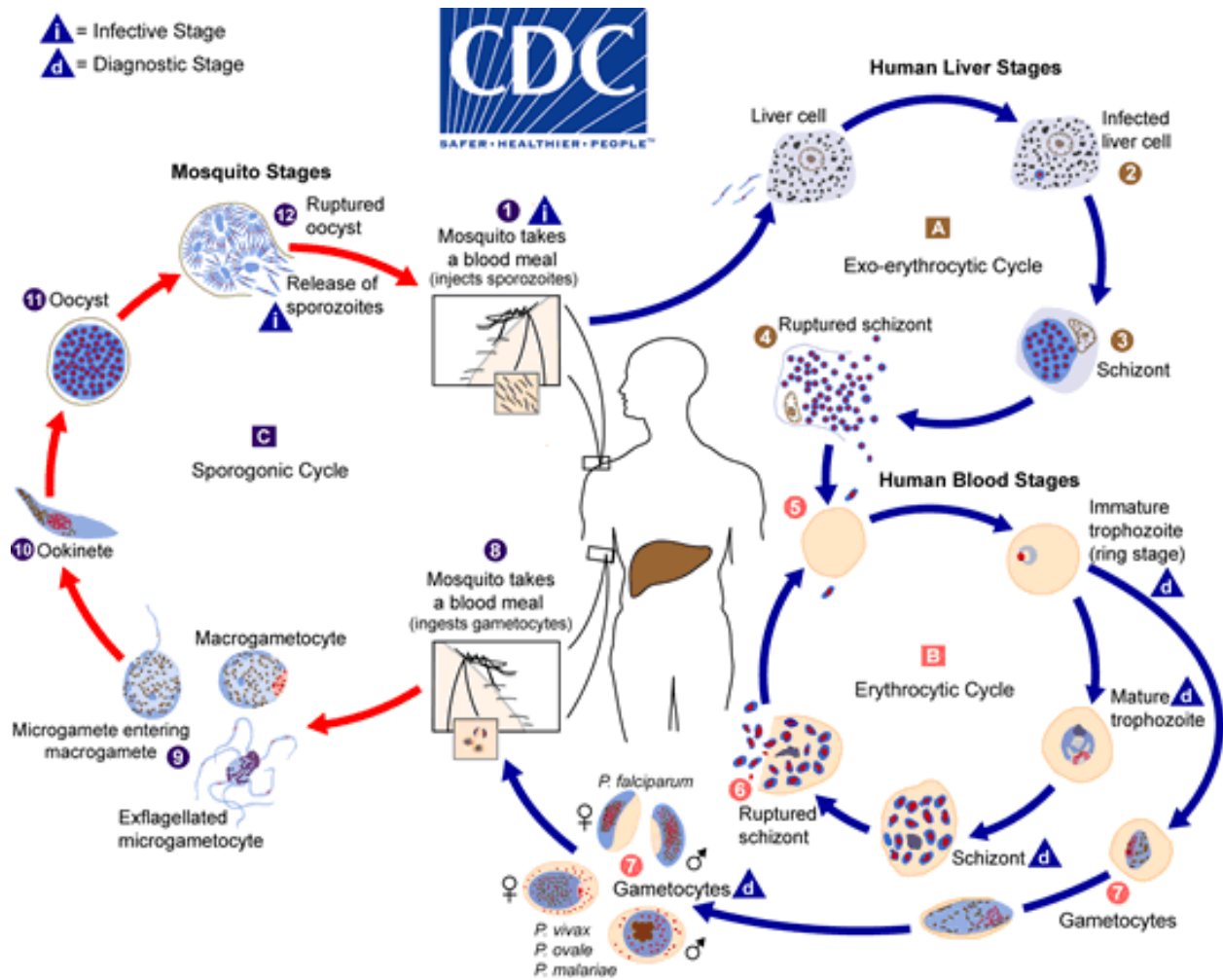


Figure 1 *Plasmodium* spp. Life Cycle

Source: Center for Disease Control and Prevention

<https://www.cdc.gov/malaria/about/biology/index.html>

Lessons From the Past

The Global History of Malaria

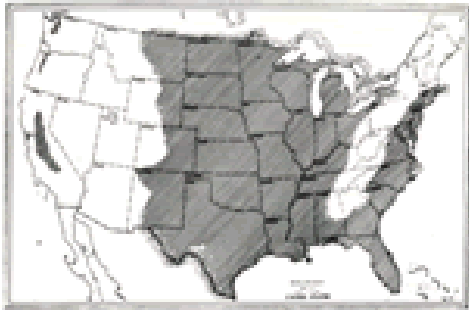
The first cases of malaria in history are documentation of malarial symptoms in the *Nei Ching* and also evidenced in Vedic prayers of India around 3000 BC (Carter and Mendis 2002). Over the next few millennia, many Sumerian, Egyptian, Greek and Roman writings detailed the effects of malaria and credit malaria with the decimation of many rural and city-state populations (Jones and Withington 1909, Celli and Celli 1933, CDC 2016). The disease is linked to the deaths of many famous and influential people throughout history, including: Pharaoh Tutankhamen “King Tut” (Hawass, Gad et al. 2010), Alexander the Great, a multitude of Popes, Oliver Cromwell, and Lord Byron. Malaria infected millions during the First and Second World War, however chemical discovery of Resochin/Chloroquine helped alleviate some of the burden.

The History of Malaria in the Americas

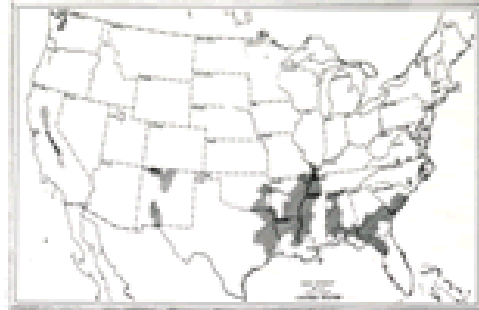
In the western hemisphere, little is recorded concerning malaria prior to the 16th century and there is considerable debate as to whether malaria was introduced by European explorers. It is possible mild malaria infections (*P. malariae*) may have already existed prior to European arrival however. During the 16th century traveling Jesuit missionaries record the Quechua, indigenous populations of South America, using *Cinchona* tree bark to cure and treat the symptoms of malaria. Early colonization of North America, and for almost the first two centuries of United States history, malaria was an ever-present threat in the lives of most communities. Thomas Bullock, a 19th century settler, records in his journal writings while settling Nauvoo, IL along the Mississippi river in

early 1840's that malaria cases were common and there were many times where almost the entire community were sick with malaria ((Bullock and Bagley 1997). Reaching its peak in the later half of the 19th century, malarial endemic regions of the United States steadily receded from over 2/3 of the country to only the Southeastern States by 1912 as shown in Figure 2.

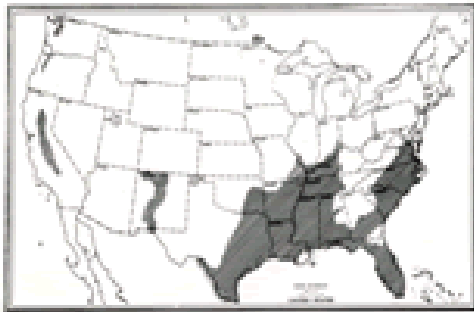
MALARIOUS AREA OF THE UNITED STATES
1882



MALARIOUS AREA OF THE UNITED STATES
1932



MALARIOUS AREA OF THE UNITED STATES
1912



MALARIOUS AREA OF THE UNITED STATES
1934-5

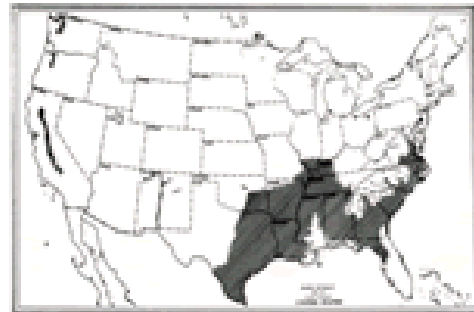


Figure 2 Distribution of Malaria in the United States, 1882-1935.

Source: Center for Disease Control and Prevention

https://www.cdc.gov/malaria/about/history/elimination_us.html

Malaria Eradication Programs

During World War II in the 1940's malaria was still endemic throughout the Southern United States and was an increasing problem to US military training and our military over seas. In efforts to curtail these threats the United States Public Health service in the early 20th century provided many resources to alleviate the growing malarial threat, including: research funding to combat malaria and insect control around active military bases in Southern United States; The support of the Tennessee Valley Authority, eliminating malaria from affecting over 30% of the regional population from 1933 to 1947; the initiation of the Malaria Control in War Areas in 1942-1945; and in the creation of the Communicable Disease Center in 1946, a center dedicated to malaria control and elimination in the US (CDC 2016). In 1947, under direction of Communicable Disease Center, the United States launched the National Malaria Eradication Program. This program primarily focused on insect control and in two and half years had sprayed over 4,650,000 homes with the insecticide Dichlorodiphenyltrichloroethane (DDT). Through these control measures the United States successfully eliminated malaria from its borders by 1949 (CDC 2016).

Hoping to build on the success of US programs, the World Health Organization (WHO) in 1955 initiated the Global Malaria Eradication Programme (GMEP). The GMEP program employed a similar course of action in adopting indoor DDT spraying. The GMEP made great strides towards elimination of malaria, particularly in eliminating malaria from Europe and North America, and parts of Asia and South America. The ultimate goal of global eradication was never achieved however, and the program was

discontinued in 1969 (Tanner and de Savigny 2008). Much of the success, or failure, of the GMEP depended on how organized and committed local governments and health care clinics were in implementing the program and it became apparent that one size truly did not fit all in malaria elimination plans. It is clear that for future programs to be successful there will need to be better engagement of local infrastructure, a more comprehensive battery of treatment and prevention methods, and improved education of affected individuals on preventative and treatment methods ((Najera, Gonzalez-Silva et al. 2011) (Russell, Beebe et al. 2013).

History of Malaria Control Measures

Insecticide Treated Bed Nets

Evidence of using bed nets can be seen as early as ancient Egypt, and there is considerable evidence that insecticide treated bed nets have proven to be the most successful preventative measure for decreasing malaria cases globally since DDT spraying (Jamet 2016). Since 2000, sub-Saharan Africa populations protected by long-lasting insecticide treated nets (LLIN) has increased from 2% to over 59% (Bradley, Ogouyemi-Hounto et al. 2017). There is, however, growing concerns that we may see a reversal of this success in the very near future primarily due to the fact that LLINs were manufactured to be protective for only 2-3 year periods and most nets in use currently are from the 2009 to 2015 influx. Another concern is the growing resistance to pyrethroids (the chemical class used in LLINs). 82% of malaria endemic countries which provide monitoring data report resistance to at least one insecticide, and 68% report resistance to two or more, with pyrethroid resistance the most commonly reported

(WHO 2016). This underscores the critical need for new insecticide or vector control method development if we hope to continue to see malaria cases on the decline.

Indoor Residual Spraying

Although historically paramount to malaria elimination programs, indoor residual spraying (IRS) among populations at risk has declined by over 45% since 2010 (WHO 2016). This drastic decline is due to increased insecticide resistance reports and also to increased prevalence of LLIN use in these populations since 2010. It is expected for IRS use to continue to decline as availability of other preventative measures steadily increase.

Vaccines

The most ideal course of action for malaria control would be the development of a malaria vaccine. Efforts towards a malaria vaccine have been actively underway since 1910 and many promising advances have occurred over the past two decades. Malaria vaccine candidates currently in preclinical or clinical trials include:

- RTS,S Vaccine- a recombinant protein vaccine targeting the immune response against circumsporozoite (CSP) protein which would prevent *Plasmodium falciparum* from ever establishing an infection. This vaccine candidate has shown some efficacy in children providing protective immunity after 3 doses up to 30% (Rts, Agnandji et al. 2012). There is another large-scale clinical trial planned in Africa in 2018.

- NYVAC-Pf7- a multi-stage targeting vaccine candidate combining sporozoite, liver stage, blood stage, and sexual stage antigens. This candidate yielded four antibody responses in *Rhesus* monkeys and had protective immunity in some human clinical trials, further development is currently underway (Tine, Lanar et al. 1996).
- In 2015 using self-assembling protein nanoparticles in mice showed protective immunity using RTS,S without required boosters/adjuvants (Burkhard and Lanar 2015).
- PfSPZ- Irradiated sporozoites vaccine has shown protective immunity for up to one year, and has been fast-tracked by the FDA for further development (Ishizuka, Lyke et al. 2016).

In spite of these successes, to date there are no fully protective or licensed vaccines against any human parasitic diseases.

Current Antimalarial Therapy

For any malaria eradication program to have any chance of success it will be required to ensure effective chemical therapeutics be given to infected populations quickly, often, and inexpensively. Since ancient times mankind has utilized plants and other chemicals to treat illness and disease, malaria included. Early use of *Artemisia annua*, or sweet wormwood, is documented in ancient Chinese herbal remedies as a cure for malaria. In the 16th century, bark from the *Cinchona* tree was widely used among Quechua tribes of South America. Quinine was later isolated as the active antimalarial component of *Cinchona* bark in 1820. Unfortunately, *Plasmodium spp.*, especially *P. falciparum*, have

shown remarkable abilities to develop drug resistance and as parasites developed resistance, the search for new chemicals were sought out. Chloroquine in the 1930's and 1940's and more recently, Artemisinin, isolated from the original sweet wormwood. Artemisinin combination therapy (ACT) is the WHO recommendation for treating uncomplicated malaria throughout the world currently (WHO 2016). There are currently seven major chemical classes of antimalarial drugs (Table 1: acid alcohols, 4- and 8-amino quinolones, antibiotics, antifolates, endoperoxides, sulfonamides). These classes act against three main plasmodial targets: the electron transport chain (Sibley, Hyde et al. 2001) (Baggish and Hill 2002), the apicoplast (Dahl and Rosenthal 2007), or the digestive vacuole (Famin and Ginsburg 2002). Alarmingly, there is well-established or emerging drug resistance to all seven chemical classes, including endoperoxides like artemisinins.

With no fully protective vaccine in sight, most LLINs past (or on the waning edge of) their viable utility, and documented cases of resistance to all current antimalarials, there is critical need for novel antimalarial compounds with unique mechanisms of action. It would also be ideal that novel compounds demonstrate transmission blocking potential.

Table 1 Antimalarial Chemical Classes and Resistance

Chemical Class	Example	Documented Resistance
Acid Alcohols	Mefloquine	Yes, 1 st case in 1982
4- Amino Quinolones	Chloroquine	Yes, 1 st case in 1957
8- Amino Quinolones	Quinine	Yes, 1 st case in 1910
Antibiotics	Clindamycin	Yes, 1 st case in 1989
Antifolates	Pyrimethamine	Yes, 1 st case in 1967
Endoperoxides	Dihydroartemisinin	Yes, 1 st case in 2011
Sulfonamides	Sulfadoxine	Yes, 1 st case in 1967

CHAPTER 2: METHODOLOGY

Drug Lead Discovery Scheme

The library screening process in this dissertation follows the described outline in Figure 3 below.

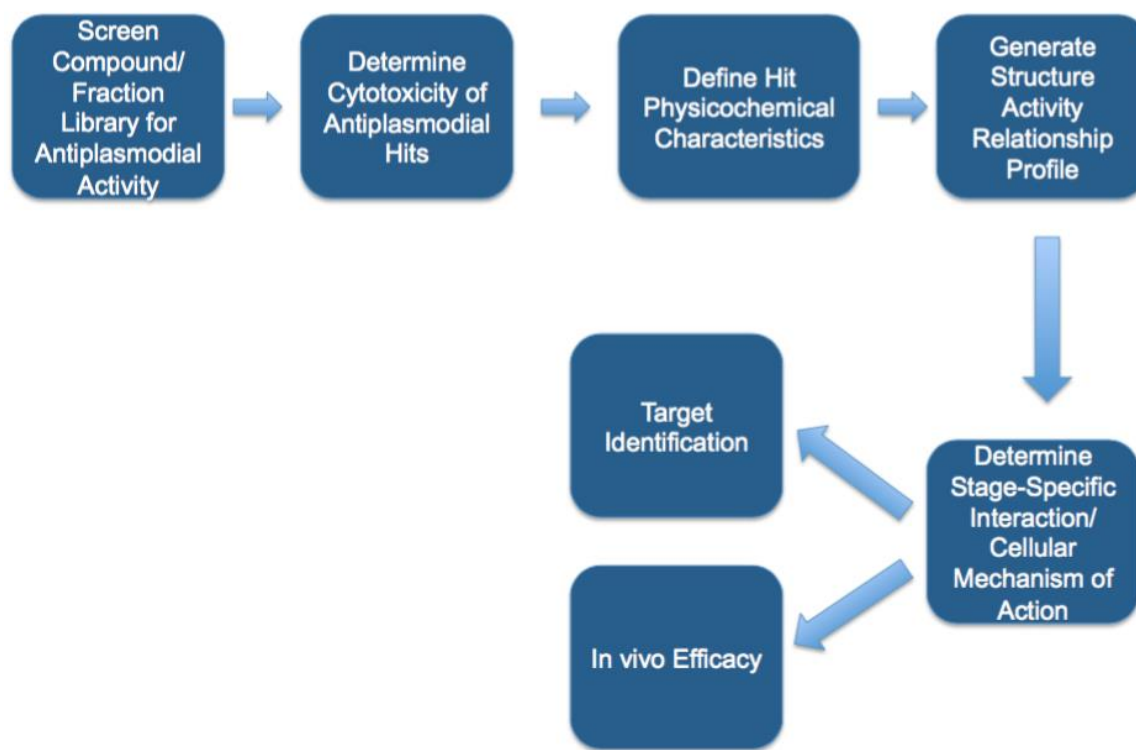


Figure 3 Drug Lead Discovery Scheme

Screening Library Selection

Compound sources for screening assays have historically come from two types of libraries: synthetic or natural product. The benefit of synthetic libraries is their clear, tractable path to acquire more compound and the generation of structure activity relationship is relatively straight forward, neither of these hold true for natural product libraries. However, limited chemical diversity within synthetic libraries typically results in

low hit rates in modern screening programs (<1%). Natural product libraries however are pre-validated by nature to be bioactive and yield hit rates of up to 3%. Unfortunately dereplication of natural product extracts is often laborious and the skill/knowledge to synthesize these dereplicated compounds and generate structure activity relationship analogues is often not available or yet unknown (Proksch, Edrada et al. 2002). In effort to create synthetically tractable compounds with the improved bioactivity of natural products, hybrid libraries were created. Hybrid libraries either highlight privilege elements of natural products combined together in known synthetic scaffolding (Vasilevich, Kombarov et al. 2012) (Rishton 2008) (Cordier, Morton et al. 2008) or they are the synthesis of non-complex, small natural product scaffolds followed by multiple rounds of small chemical additions quickly resulting in libraries of vast and diverse compounds (Tan 2005).

In this study, four different types of chemical libraries for our screening process were selected: a marine natural products library of Harbor Branch Oceanographic Institute (HBOI), a natural product based high-density combinatorial library from Torrey Pines Institute for Molecular Studies (TPIMS), Memorial Sloan Kettering Cancer Center's (MSKCC) alkaloid/terpene natural inspired library, and a privileged elements of natural product-inspired library (Asinex).

Culturing *P. falciparum*

Multi-drug resistant, Dd2, and chloroquine sensitive, 3D7, *P. falciparum* strains were cultured using a modified Trager and Jensen method (Trager and Jensen 1976) in RPMI media with L-glutamine (Invitrogen) supplemented with 25mM HEPES, 26mM

NaHCO₃, 2% dextrose, 15mg/L hypoxanthine, 25mg/L gentamycin, and 0.5% Albumax I. Culture media was changed daily and incubated at 37°C in 5% CO₂ and 95% air. Daily blood smears were taken and stained by Giemsa staining to determine parasitemia. Cultures were maintained at 4% Hematocrit and <10% parasitemia. Parasitemia above 10% was split in media and freshly diluted in 50% washed A+ RBCs from OneBlood.

SYBR Green-I Fluorescence Assay

Ten millimolar compound stocks in DMSO were diluted by 1/2, 1/5, and/or 1/10 fold dilutions in ultrapure water or RPMI 1640. Varying concentrations of compound were added to culture at a 1% parasitemia and 2% hematocrit in 96-well black plates. Assay conditions maintained maximum DMSO concentrations less than 0.125% per dilution. Positive (baseline 0% growth) controls consisted of Chloroquine at 1µM final concentration. Following 72 h incubation at 37°C in 5% CO₂, dilution plates were frozen at -80°C for a minimum of 30 minutes. Dilution plates were allowed to thaw followed by lysis treatment and SYBR Green I incorporation. DNA quantification was determined using a fluorescence reading on a Synergy H4 multimode plate reader set at 485nm excitation and 530nm emission as previously reported (Roberts, Iyamu et al. 2016). EC₅₀ was calculated from a dose response curve that was generated from a concentration range of 0–10µM using GraphPad Prism v5.0.

Different dilutions of the compound/fraction in 1µl of the culture medium were added to 99µl of *P. falciparum* culture at a 1% parasitemia and 2% hematocrit in 96-well plates.

Maximum DMSO concentration in the culture never exceeded 0.125%. Chloroquine at 1 μ M was used as a positive control to determine the baseline value. Following 72 hours incubation at 37°C, the plates were frozen at -80°C. After thawing, 100 μ L of lysis buffer (with SYBR Green I dye 1:10,000) was added to each well and plates were incubated at room temperature for 30 minutes prior to reading.

Cytotoxicity Assay

Hit compounds were evaluated for cytotoxicity using HepG2 human hepatocytes as reported (Roberts, Iyamu et al. 2016). A 384 well plate was seeded with 2,500 cells/well (total volume 25 μ L) and incubated for 24 hours. Serial dilutions of the compound were added to the plate and plates were incubated for an additional 48 hours. Ten μ L MTS [(3-(4,5-dimethylthiazol-2-yl)-5-(3-carboxymethoxyphenyl)-2-(4-sulfophenyl)-2H-tetrazolium), CellTiter 96® Aqueous non-radioactive cell proliferation assay, Promega] reagent was added to each well and the plates were incubated for an additional 3 hours. Cell viability was obtained by measuring the absorbance at 490nm and 630nm using Synergy H4 hybrid multimode plate reader (Biotek).

Physicochemical Profiling

To determine a physicochemical profile for the hit compounds we determined: cLogP, Molecular weight, Hydrogen bond donors and acceptors, and Total Polar Surface Area were all calculated using Marvin Sketch (Chemaxon); microsomal stability using mouse liver microsomes with/without Nicotinamide adenine dinucleotide phosphate (NADPH) (Janiszewski, Rogers et al. 2001); aqueous solubility

at pH 7.4 using UV-visible absorption based method (Avdeef, Strafford et al. 2001); and permeability using a gastrointestinal tract- blood stream passive transport model called in vitro double-sink parallel artificial membrane permeability assay (Kansy, Senner et al. 1998).

Sensitivity and Reliability Statistical Analysis

We employed a Z'-factor analysis on each assay to validate and verify accuracy. This assay was originally developed by Zhang et al (Zhang, Chung et al. 1999), for HTS validation. The equation is shown below. The Z-factor is a range from 0 (completely unreliable) to 1 (ideal assay conditions). A value below 0.5 is considered unreliable and perhaps requires some modifications before the assay can be re-run. A value between 0.7 and 1 is considered acceptable for hit validation in our lab.

$$Z - factor = \frac{3(\sigma_p + \sigma_n)}{|\mu_p - \mu_n|} \quad (1)$$

Where σ_p represents the standard deviation of the positive controls and σ_n is the standard deviation of negative controls. Also, μ_p represents the mean of the positive controls and μ_n represents the mean of the negative controls.

Rate of Killing and Parasitocidal/Parasitostatic Studies

To determine the speed of action asynchronous Dd2 cultures were treated with 5xIC₅₀ concentrations of test compound for 6 hours, 12 hours, 24 hours, 48 hours, and 72 hours. After incubation cultures were washed three times in PBS and then resuspended in culture media. Parasite growth was monitored every 24 hours via Giemsa smears. Cultures which were brought to <1% parasitemia within 12 hours of treatment were

considered fast acting, while those requiring longer incubation periods were slow acting. Cultures that returned to normal growth after treatment were considered parasitostatic, otherwise they were classified as parasitocidal.

Cellular Mechanism of Action

In efforts to better understand the cellular mechanism of action of top hit compounds, 5X EC₅₀ concentrations of compounds were added to tightly synchronized cultures at 6 hours post invasion, 18 hours post invasion, 30 hours post invasion, and 42 hours post invasion. At 12-hour intervals smears were made for Giemsa staining and samples were collected and fixed in 4% glutaraldehyde. After fixing, samples were permeabilized in 0.025% Triton X100 and RNase A treated. Finally, slides were stained overnight with YOYO-I, a DNA intercalating dye. Stained samples were run on flow cytometric analysis using Cytoflex S (Beckman) (488 nm Laser with 533/30 filter) or Attune NXT at a voltage of 260 with excitation wavelength of 488nm and an optical filter of 530/30. Flow results were confirmed with Giemsa stain smears.

in vivo Efficacy

To determine *in vivo* efficacy 8 weeks old female Balb/c mice were infected with 1×10^6 *P. berghei* ANKA parasitized RBC (from a donor mouse) by intraperitoneal injection. Compounds were formulated in a delivery vehicle comprised of 0.5% hydroxyethylcellulose, 0.1% Tween 80 (oral delivery only), Phosphate Buffered Saline (oral or IP), or a solution of 5% N-methyl-2-pyrrolidone, 5% Solutol HS-15, 30% PEG-400, 60% hydroxypropyl- β -cyclodextrin (20% w/v prepared in RO water) (IP). Control

groups received vehicle only. Parasitemia was monitored by microscopic evaluations of Giemsa-stained thin smears of daily superficial temporal or submandibular vein bleed samplings. All animal study protocols were approved by the Institutional Animal Care and Use Committee at the University of Central Florida.

β -Hematin Formation Assay

Inhibition of β -hematin formation was assessed for compounds using the method described in Sandlin et al (Sandlin, Carter et al. 2011). In a 384-well flat, clear bottom plate 100 mM (final concentration) of compound was added followed by the addition of 20 μ L water, 7 μ L of acetone and 5 μ L of 348mM Nonidet P-40. Finally, 25 μ L of 228 mM hematin-DMSO suspension was added to each well and the plate was incubated for 6 hours at 37 C in a shaking incubator. β -hematin formation was analyzed using pyridine ferrochrome assay (Ncokazi and Egan 2005) . After incubation, a 5% v/v final concentration of pyridine (from a solution of 20% acetone, 200mM HEPES, 50% pyridine and water) was added and the plate was incubated under the same conditions as above for an additional 10 min. Absorbance values of resulting pyridine-ferrochrome complex was measured at 405 nm using Biotek Synergy H1 multireader.

Synthesis of UCF 501

One year into the project our supply of UCF 501 was exhausted and we were required to synthesize additional compound. Following the synthetic scheme (where) preparation of 4-chloro-6-methoxy-2-methylquinoline (cmp 3) was carried out as described in (Thomas, Adhikari et al. 2010). 1g of cmp 3 was then converted to 4-chloro-6-methoxy-

2-[(E)-2-(4-nitrophenyl)ethenyl]quinoline by addition of cmp 3 and *p*-TsNH₂ at a 1:3 molar with minimal *m*-Xylene as a solvent at 140 °C overnight. This product was purified by liquid chromatography and confirmed by ¹H NMR. This product was converted to final product UCF 501 by reacting with Pd(OAc)₂, BINAP, K₃PO₄, 1,4-dioxane overnight at 85 °C. Compound was purified and treated with 3 molar equivalents phosphoric acid and lyophilized to yield 2.1g UCF 501.

Resistance Profiling

Generation of *Pf* resistant lines typically follows one of two techniques: Treating a culture with compound at IC₅₀ and incrementally increasing concentration until parasites are doubling every 48 hours under at 5-10 fold higher than IC₅₀ concentrations; A second method is to treat cultures with a very high concentration of compound (3x IC₉₀) and wait for these cultures to begin doubling every 48 hours. We began by limiting dilution cloning to create clonal populations of Dd2 and then attempted to create resistant lines by incremental increasing of concentration and also by maintaining culture at 3xIC₉₀ following a similar outline as recently published works ((McNamara, Lee et al. 2013)) Unfortunately after several attempts, neither of these methods resulted in viable parasite lines. Recently, new methods of sequencing analysis have allowed groups to generate resistance lines without the required clonal populations (Sonoiki, Palencia et al. 2016).

Additionally, pulsing compound pressure at IC₉₀ for 48 hours followed by daily replacement of normal culture media was much more effective at generating resistant parasites rather than growing under constant pressure alone. Pulsing cultures were

maintained in normal media until parasite growth showed recovery (doubling every 48 hours). Doubling cultures were either pulsed again, or split and maintained under constant IC_{50} compound pressure. Pulsing treatment of cultures at IC_{90} typically resulted in viable parasite growth within two weeks for successful resistant lines. Similar results were seen in continuous IC_{50} treatments where ultimately successful resistant lines showed parasite doubling growth within 3 weeks. Once parasite lines were continuously growing under treated media conditions, cultures were split and grown at increasing concentrations starting at $2 \times IC_{50}$, $3 \times IC_{50}$ and $5 \times IC_{50}$. Successful lines were tested for EC_{50} determination using SYBR Green I assay as described.

CHAPTER 3: DISCOVERY AND CHARACTERIZATION OF ANTIPLASMODIAL COMPOUNDS FROM HARBOR BRANCH OCEANOGRAPHIC INSTITUTE PEAK-FRACTION COLLECTION

HBOI Marine Natural Products Library

The Harbor Branch Oceanographic Institute (HBOI) collection was created with two purposes: to evaluate ecological effects on secondary metabolite production and to maximize taxonomic diversity. Most marine libraries are collections gathered from shallow dive samples up to 50 feet below sea level. At HBOI, the Johnson Sea Link manned-submersible vessel (Figure 4) is fitted to locate and collect samples at depths up to 3,000 feet below sea level. This added depth provides masses of diverse samples that are inaccessible to other marine collection programs. From their vast marine invertebrate collections, the Institute has generated a peak fraction library consisting of 2600 marine natural product fractions.

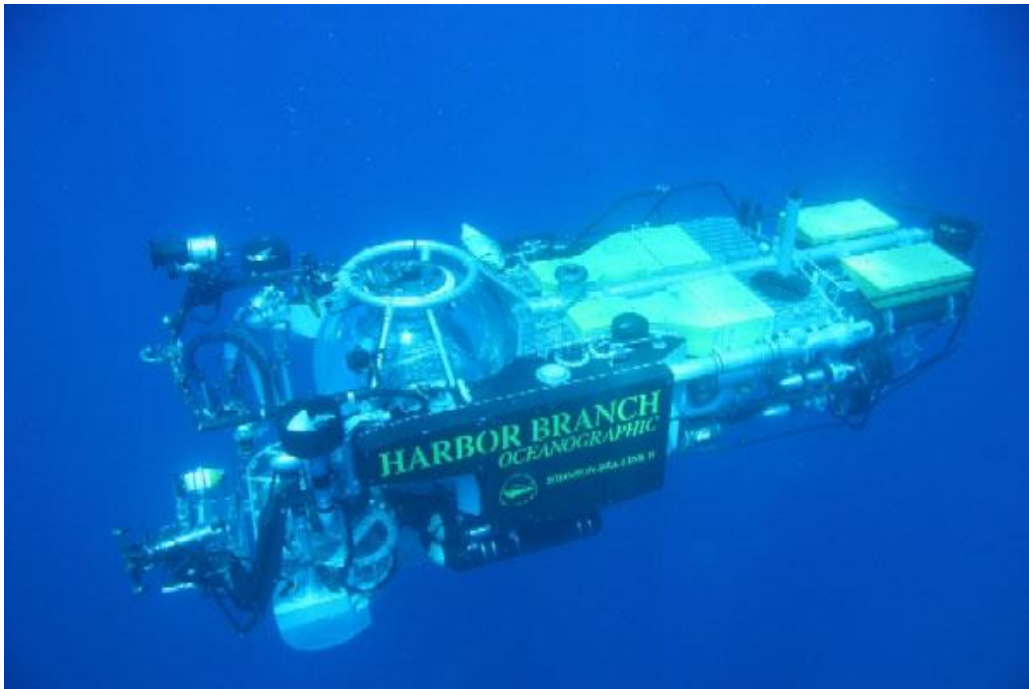


Figure 4 HBOI Johnson Sea Link Manned Submersible

Source: USGS

URL:

https://archive.usgs.gov/archive/sites/fl.biology.usgs.gov/DISCOVERE/discovere_2009/index.html

Hit Identification

Screening the peak fraction library revealed 165 fractions from 85 organisms demonstrating >70% inhibition against *P. falciparum* at 5µg/mL. In effort to eliminate chemotype redundancy, only the top few fractions per organism were selected and screened for EC₅₀ determination using SYBR Green I assay. Thirty fractions from twenty different species showed excellent potency, with EC₅₀ <1µg/mL (Table 2).

Table 2 HBOI Antiplasmodial Hit Selectivity.

Fraction	Sample ID	Field ID	Dd2 IC ₅₀ (µg/mL)	Cytotoxicity IC ₅₀ (µg/mL)	Selectivity Index
10.D08	13-VIII-99-2-004	Gastropoda, Aplysia? Sp.	0.10	31	310
18.G07	13-IV-05-1-006	Paramuricea Sp.	0.44	>50	>113
41.A09	10-V-00-1-004	Bebryce Grandis	0.47	>50	>106
27.C10	31-III-89-2-003	Amphibleptula	0.47	>50	>105
27.B10	10-VI-91-1-003	Corallistes	0.51	>50	>99
29.A07	20-VIII-01-1-012	Axinellidae	0.52	>50	>95
9.H09	15-VIII-99-2-002	Dictyoceratida	0.45	42	94
39.A06	10-V-00-3-003	Aplysina	0.60	>50	>83
32.C02	28-V-91-6-007	Halichondriidae	0.64	>50	>78
18.D08	14-IV-05-2-001	Paramuriceidae	0.73	>50	>69
41.C11	31-III-89-2-003	Amphibleptula	0.73	>50	>68
8.F01	23-XI-98-1-006	Choristida? (unusual)	0.62	42	67
39.A05	10-V-00-3-003	Aplysina	0.75	>50	>66
41.C01	10-V-00-1-004	Bebryce Grandis	0.78	>50	>64
43.A11	21-V-93-3-001	Spongosorites	0.78	49	62
41.F02	10-V-00-3-003	Aplysina Sp.	0.78	>50	>61
41.G04	11-V-00-3-009	Auletta? Sp. 2	0.83	>50	>60
39.A10	23-XI-98-1-006	Aplysina	0.85	>50	>59
41.B03	10-V-00-1-004	Bebryce Grandis	0.84	>50	>59
10.D09	13-VIII-99-2-004	Gastropoda, Aplysia? Sp.	0.50	30	59
41.G06	11-V-00-3-009	Auletta? Sp. 2	0.90	>50	>55
10.C11	7-VIII-99-1-003	Spirastrella Sp.	0.90	48	53
43.A09	21-V-93-3-001	Spongosorites	0.86	46	53
18.E03	8-IV-05-1-009	Paragorgai	0.96	>50	>52
41.C10	31-III-89-2-003	Amphibleptula	0.97	>50	>51
6.D04	11-V-00-3-009	Auletta? Sp.2	0.83	39	47
7.G11	7-VIII-90-1-106	Peysonellia	1.00	47	47
43.A07	21-V-93-3-001	Spongosorites	0.91	41	45
43.A08	21-V-93-3-001	Spongosorites	0.99	42	42
9.G07	15-VIII-99-1-006	Axinellida?	0.80	33	41

IC₅₀ values are derived from 3 independent experiments, each with 3 replicates. The Z⁰ factors of these assays were >0.8. Species identification provided by HBOI.

Consistent with typical marine natural product libraries, the majority of active fractions in our study are derived from animal, and not plant life (Table 3).

Why this trend is the case for marine natural products when the trend for terrestrial natural products is opposite is still not fully understood. There is some evidence that suggests invertebrate marine life is under tremendous pressure to create chemical metabolites in effort to bolster defense against over-grazing predators (Proksch, Edrada et al. 2002).

Table 3 Source Organisms for HBOI Antiplasmodial Hits.

	Coral	Sponge	Mollusk	Other
Number of Different Organisms with EC ₅₀ < 1µg/mL	3	13	1	3

One of our early hits was identified as the Bis(indolyl)imidazole alkaloid Nortopsentin A which we have presented on earlier (Alvarado, Roberts et al. 2013). Additional dereplication of fractions from 10 organisms has revealed 9 new scaffolds with potent antiplasmodial activity and excellent selectivity (Figure 5) along with two known antiplasmodial compounds aerophysin-1 (Gutierrez, Theoduloz et al. 2005) and oroidin (Konig, Wright et al. 1998). Six additional pure peaks are pending structure elucidation at this time.

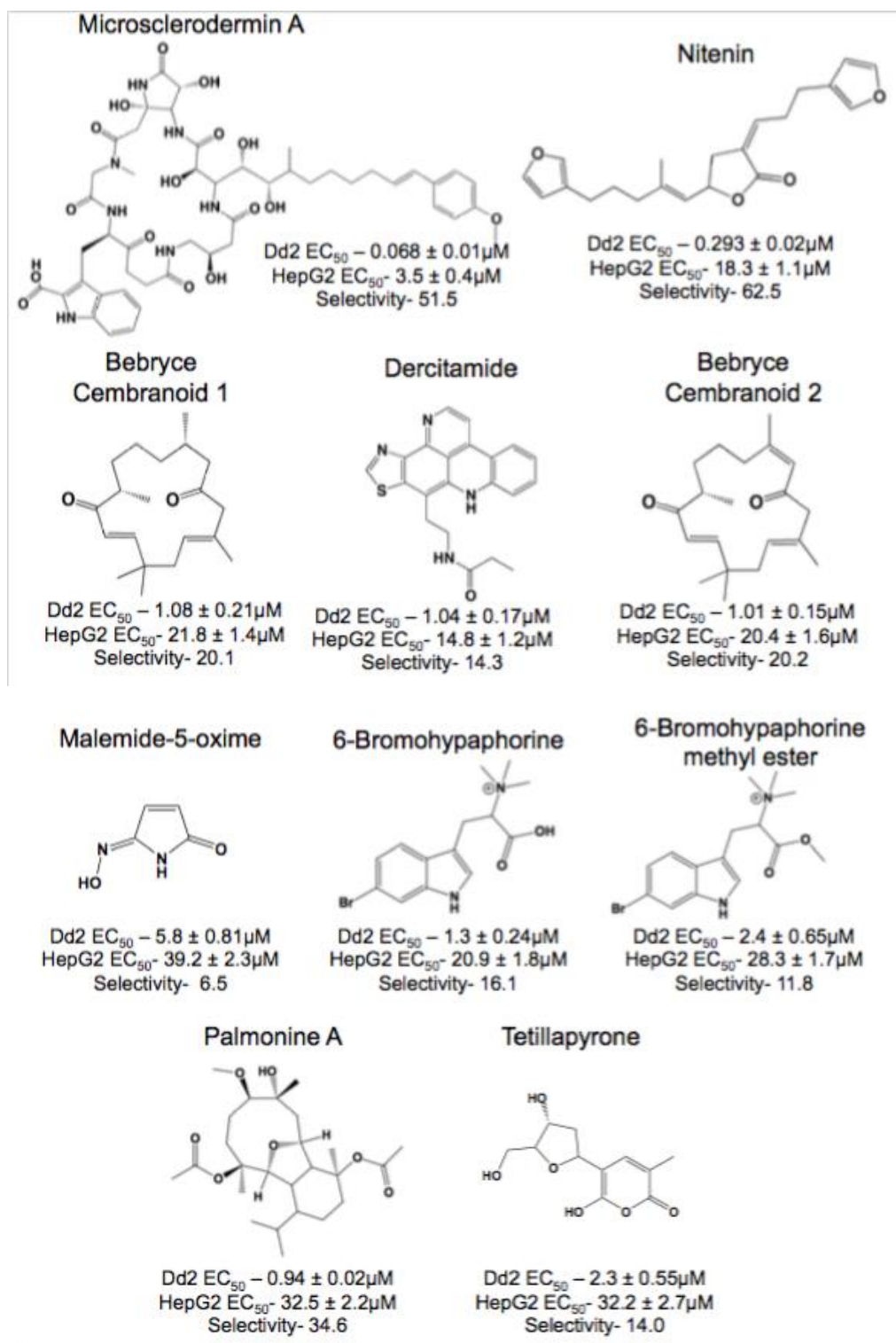


Figure 5 Selectivity of HBOI Dereplicated Hits.

EC₅₀ values (±SD) are derived from 3 independent experiments, each with 3 replicates. The Z⁰ factors of these assays were >0.8.

Physicochemical Properties of HBOI Hits

As per our Drug Lead Discovery scheme (Figure 3), to better characterize and prioritize the HBOI hit compounds we evaluated their physicochemical properties (Table 4). It is quite common for natural product compounds to expand beyond the guidelines of Lipinski's rules, and we identified compounds that spread from fully in compliance to the "drugability" guidelines proposed in Lipinski's rules (Palmonine A, Nitenin, and Dercitamide) to compounds that are completely out of compliance (Microsclerodermin A). Armed with this information, we proceeded to cellular mechanism of action studies.

Table 4 Physicochemical Properties of HBOI Hits

Compound ID	cLogP	Molecular Weight (g/mol)	H-bond Donor	H-bond Acceptor	Polar Surface Area (Å ²)
6-Bromohypaphorine	-1.26	340.24	1	1	42.09
Palmonine A	2.42	454.6	1	5	91.29
Malemide -5-oxime	-0.63	112.09	2	3	61.69
Tetillapyrone	-0.43	242.23	3	5	96.22
Nitenin	5.41	340.42	0	2	52.58
Microsclerodermin A	-2.3	994.07	13	16	366.58
Dercitamide	3.32	374.46	2	3	70.67
Bebryce Cembranoid 1	5.61	304.47	0	2	34.14
Bebryce Cembranoid 2	5.56	302.45	0	2	34.14

HBOI Hits Cellular Mechanism of Action

Understanding the cellular mechanism of action for these top HBOI hits provides insight for when these compound interact in the intraerythrocytic cycle these compounds interact. This information can be used to elucidate what pathways may be involved and lead to potential target identification. To this end, we tested the effect of these hits on intraerythrocytic cycle progression starting at early ring, late ring, trophozoites, and schizonts stages. Parasite development was measured every 12 hours by taking samples for thin blood film Giemsa smears and also by fixing samples for flow cytometry.

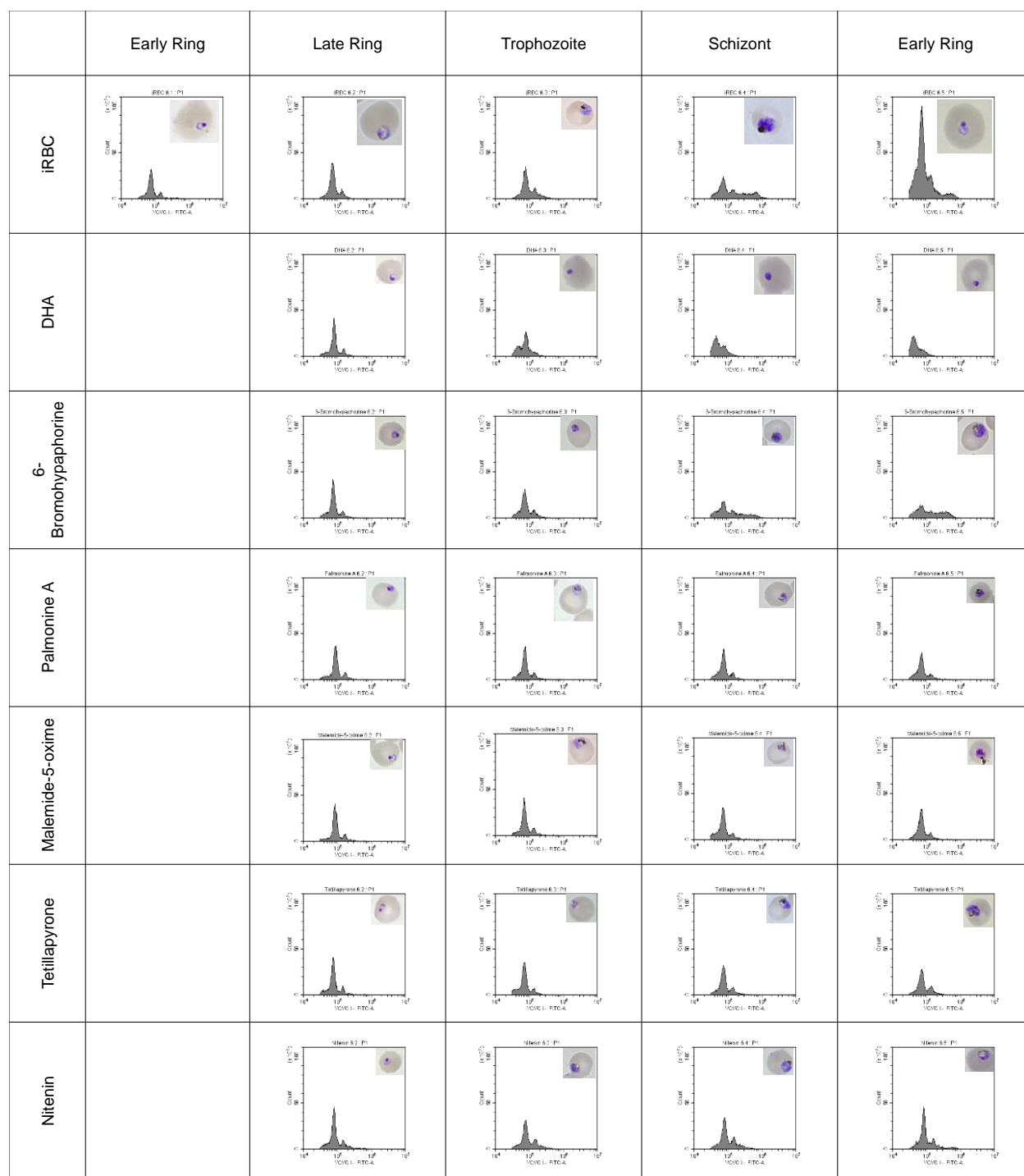


Figure 6 Stage Specific Interaction of HBOI Antiplasmodial Hits.

Synchronized culture was treated with compound at $5 \times EC_{50}$. Effect of compound on growth measured by flow cytometric analysis of YOYO-1 labeled cells. Giemsa stained thin smears were prepared every 12 h for microscopic evaluations of parasitemia to quantify parasitemia (inset). Plots represent cell count in y-axis versus FL1 channel representing DNA content.

This study identified:

- 5 compounds which inhibit at ring or ring-trophozoite transition (Palmonine A, Tetillapyrone, Malemide-5-oxime and Microsclerdermin A and Nitenin)
- 4 compounds which inhibit development beyond Schizont stages (6-Bromohypaphorine, Dercitamide, and Bebryce Cembranoid 1 and 2 (data not shown))

Many of these compounds interact with parasite stages different from most known antimalarials, especially acting early in the cycle at the ring-trophozoite transition. This experiment was repeated for Nitenin and Microsclerdermin A with similar results (Figure 7).

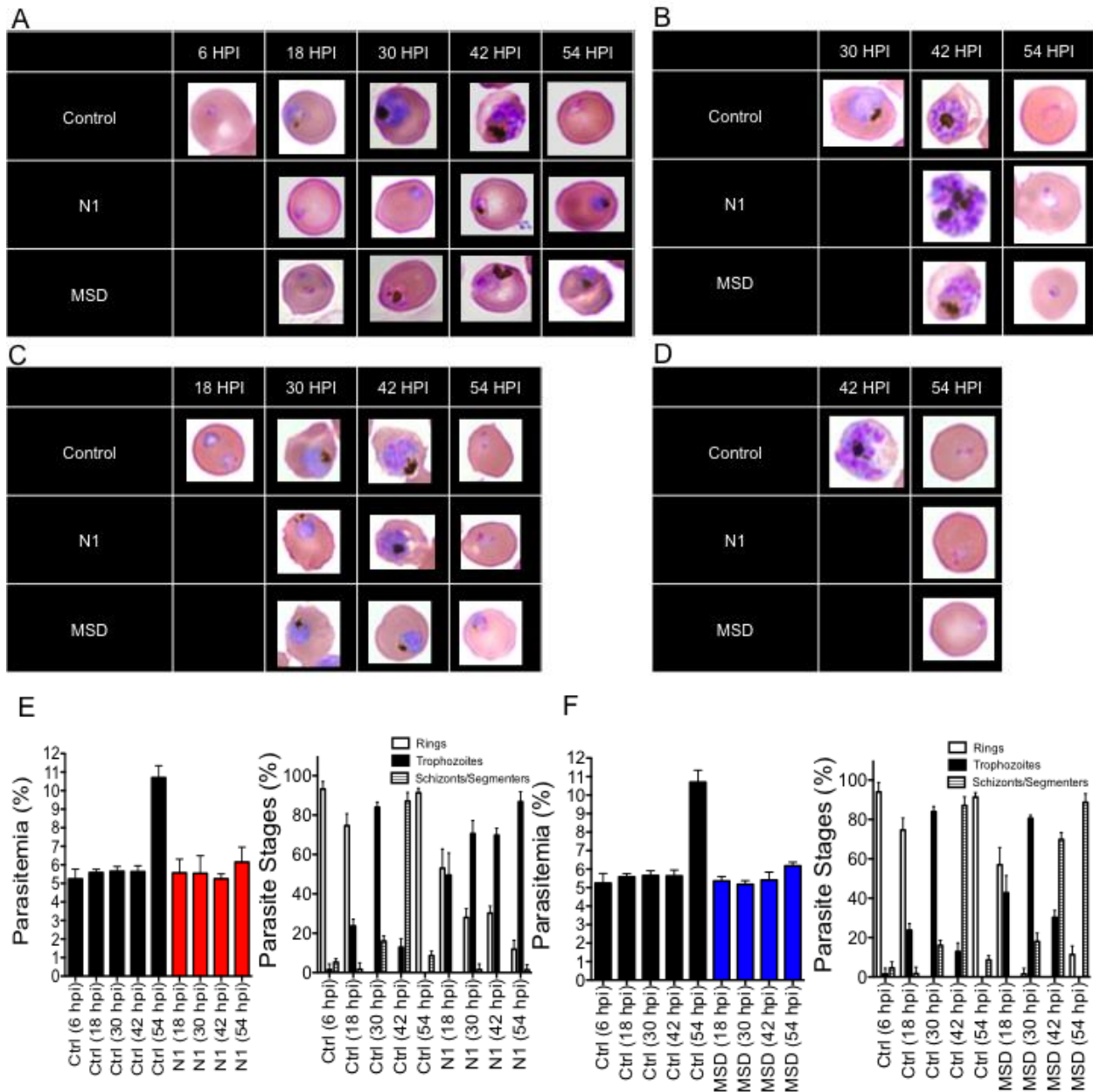


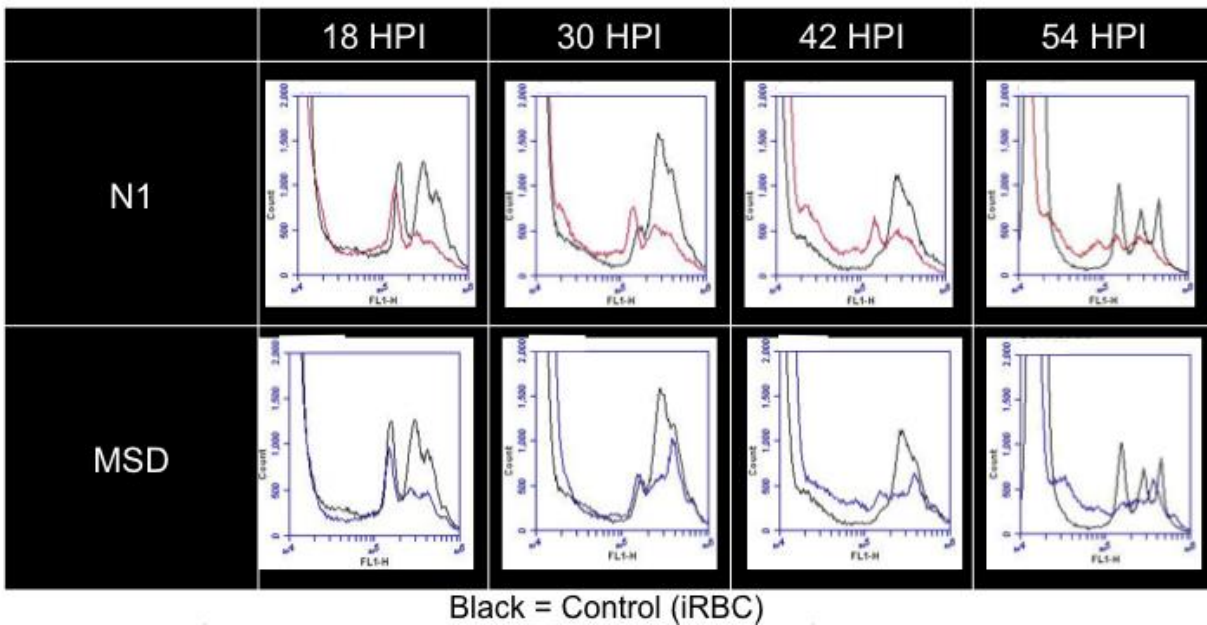
Figure 7 Nitenin and Microsclerodermin A Cellular Mechanism of Action.

Tightly synchronized parasite cultures were closely monitored until reinvasion occurred. Six hours post reinvasion (HPI) culture was plated into a 96 well plate and the antiplasmodial compounds or controls were added at 12-hour time intervals starting at 6 (A), 18 (B), 30 (C), and 42 (D) hours post invasion. At each interval slides were made and prepared for imaging using Giemsa stain. Parasitemia and stage development was observed and >1000 RBC's were counted for each compound at each time interval. Bar graph representations of parasitemia changes and stage development are also shown for N1(Nitenin) (E) and MSD (Microsclerodermin A) (F).

It appears that the HBOI compound Nitenin is fast acting and inhibits development at the ring-trophozoite transition while Microsclerodermin A, while also being slightly hemolytic, appears to stop parasite progression at ring if given at 6 or 18 hours post invasion, or beyond the schizont development when given prior to 30 hours post invasion.

These results have been shared with HBOI and we are currently awaiting additional shipments of compounds to continue *in vivo* efficacy and target identification experiments.

Table 5 Flow Cytometry Analysis of Stage-Specific Interaction of Nitenin and Microsclerodermin A.



Stage-Specific Interaction of Nitenin and Microsclerodermin.

The stage-specific study was completed as described in Figures 12. At each time interval, aliquots were taken from each well and fixed overnight. Fixed samples were permeabilized, treated with RNase and stained overnight with YoYo-1, a DNA intercalating dye. Shown above are the parasite specific peaks detected at the given time points with infected RBC's alone compared to N1 (Nitenin) treated or MSD (Microsclerodermin A) treated samples. At least 300,000 total events were plotted and analyzed above for each time interval.

CHAPTER 4: DISCOVERY AND CHARACTERIZATION OF ANTIPLASMODIAL COMPOUNDS FROM THE TORREY PINES INSTITUTE FOR MOLECULAR STUDIES HIGH-DENSITY COMBINATORIAL LIBRARY

TPIMS High-Density Combinatorial Library

The TPIMS high-density combinatorial library contains over 30 million synthetic compounds from largely underexplored regions of chemical space (Singh, Guha et al. 2009). These compounds were created and organized using scaffold ranking technologies which allow equivalent mixtures of many thousand variations of similar scaffolding to be screened in one well of a 96 well plate. Many mixture libraries can then be added to one 96 well plate and screened for activity in a scaffold ranking plate. After hit scaffold libraries are identified, compound mixtures are separated into a positional scanning layout detailed in Figure 8. Briefly, all major R substituents are mixed in multiple well formats where one R-group is constant throughout the well and the remaining are randomized. This is then repeated sequentially until the last R group is held constant and the remaining R groups are randomized.

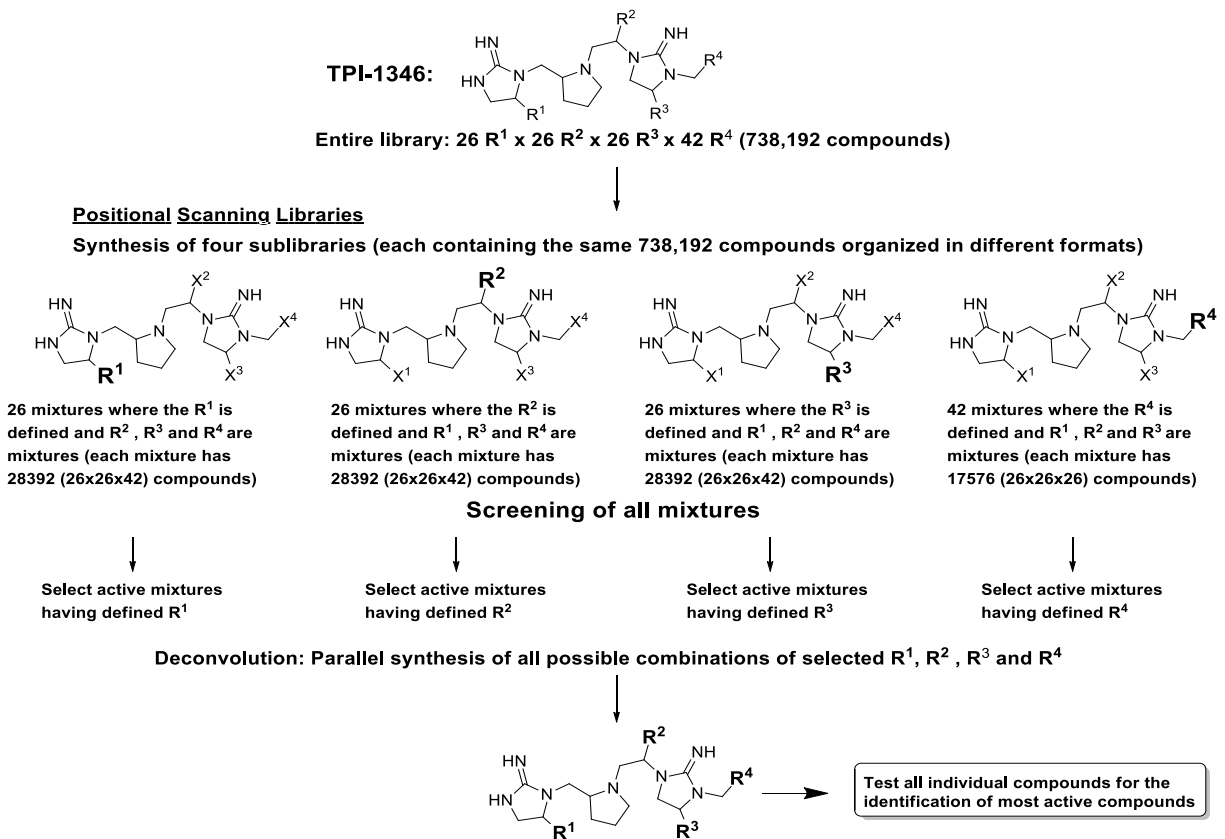


Figure 8 TPIMS Positional Scanning Library Design

This layout facilitates rapid screening of millions of compounds separated into mixtures of compounds with variations on specific “R” groups. In our preliminary screening of 56 different scaffold libraries on a scaffold ranking plate, we identified 12 libraries that exhibit >80% inhibition of Dd2 at 10µg/mL. Ten of these libraries had antiplasmodial $IC_{50} < 5\mu\text{g/mL}$ (Table 6).

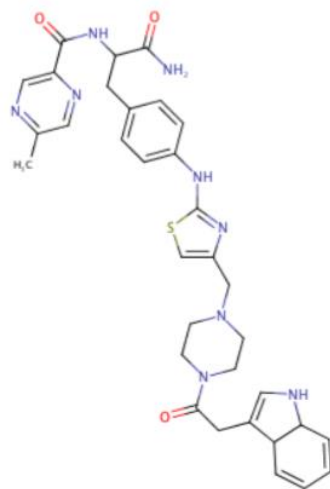
Further screening led to the discovery of a thiazole-piperazine scaffold library 2291-SB1 which has antiplasmodial EC_{50} of 102nM and a selectivity of over 140 (Figure 9).

Table 6 Antiplasmodial Activity and Selectivity of Top TPIMS Libraries

Library ID	Compound # in Library	<i>Pf</i> Dd2 IC ₅₀ (µg/mL)	HepG2 IC ₅₀ (µg/mL)	Selectivity
2275	57,868	0.65	18.9	29.1
1955	738,192	0.67	>20	>29.8
2291	4,900	0.71	>20	>28.2
2157	45,864	1.33	>20	>15.0
2159	45,864	2.71	>20	>7.4
2049	17,340	2.87	>20	>7.0
2221	2,340	3.72	>20	>5.4
2239	2,016	3.79	>20	>5.3
1319	56,610	3.89	12.4	3.2
1664	31,320	4.45	11.5	2.6

EC₅₀ values (±SD) are derived from 3 independent experiments, each with 3 replicates. The Z⁰ factors of these assays were >0.8. *P. falciparum* Dd2, chloroquine resistant.

2291-SB1



Dd2 EC₅₀ - 0.102 ± 0.02 μM
HepG2 EC₅₀ - 14.4 ± 1 μM
Selectivity- 141

Figure 9 Antiplasmodial Activity of 2291-SB1.

EC₅₀ values (±SD) are derived from 3 independent experiments, each with 3 replicates. The Z⁰ factors of these assays were >0.8. *P. falciparum* Dd2, chloroquine resistant.

Physicochemical Properties of TPIMS 2291

To better understand the potential of TPIMS 2991 we determined and evaluated 2291's physicochemical properties. We were pleased to learn that 2291 complies with all but one of Lipinski's rules (MW >500); The Physicochemical results are summarized in

Table 7. 2291-SB1 has many properties in alignment with "drugability" and shows exceptional solubility and fair microsomal stability.

Table 7 Physicochemical Properties of 2291-SB1

Compound ID	2291-SB1	
ClogP	1.84	
Molec. Weight (g/mol)	637.8	
H-bond Donor	4	
H-bond Acceptor	8	
Polar Surface Area (Å²)	162.2	
Kinetic Solubility Results in pH 1.2 SGF (µM)	133.1	
Kinetic Solubility Results in pH 6.5 50mM NaPO4 (µM)	68.8	
Kinetic Solubility Results in pH 7.4 1x PBS (µM)	60.9	
Microsomal Stability (Results in % Remaining)	T=0 min.	100.0
	T=60 min.	26.1

Structure Activity Relationship Profiling

Perhaps the greatest benefit of positional scanning libraries is that a limited structure activity relationship profiling (SAR) for the TPIMS 2291 library was completed along the way of discovering 2291-SB1. As different functional groups were screened in attempts to isolate the most potent hit, we can in general conclude that addition of the indole ring system provides some stability to the structures activity, but only when the amide bond is incorporated on the opposite end of the structure of the thiazole tethered piperazine scaffolding core (Table 8). Beyond this observation it is difficult to determine any other distinct trends and a development of a more extensive structure function relationship is needed.

Table 8 TPIMS 2291 SAR

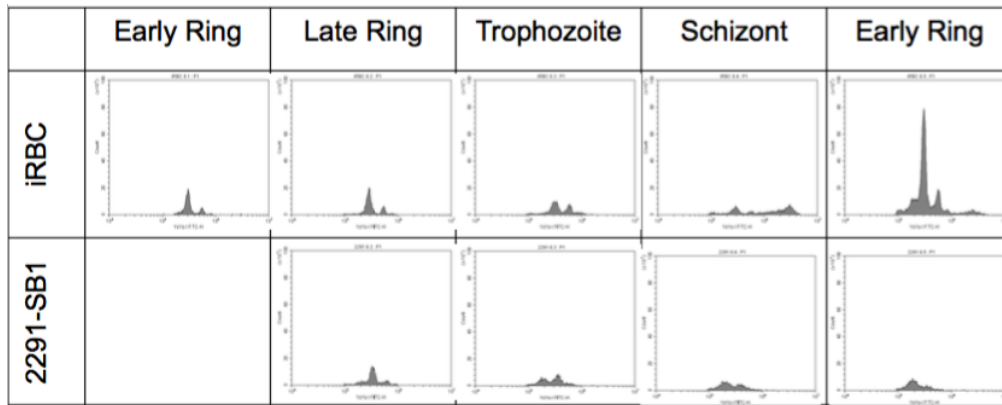
Compound ID	Structure	Dd2 EC50 (μM) n=3	Compound ID	Structure	Dd2 EC50 (μM) n=3
SB1-32, SB1-34		0.807 ± 0.07	SB1-52		0.499 ± 0.06
SB1-37		0.349 ± 0.05	SB1-53		0.684 ± 0.04
SB1-41		0.743 ± 0.09	SB1-54		0.416 ± 0.04
SB1-42		0.487 ± 0.04	SB1-55		0.555 ± 0.06
SB1-43		0.680 ± 0.07	SB1-56		0.513 ± 0.05

All values are the average of at least three independent experiments.

Cellular Mechanism of Action of TPIMS 2291

For 2291 to overcome resistance paradigms it will need to have a cellular mechanism of action distinct from known antimalarials. Therefore, to determine the stage-specific effect of 2291, we analyzed the effect of 2291 on tightly synchronized cultures. Interestingly, when 2291 is given at early ring or late ring stages, it prevents development into the trophozoites stage, however, if given at trophozoite or schizont stages it prevents schizont development (Figure 10). This demonstrates 2291 as a moderately fast acting compound that can inhibit multiple stages of development. These results also indicate 2291 as a potential inhibitor of DNA synthesis or protein transport to the RBC membrane as both of these functions are upregulated during trophozoite and schizont stages (Pease, Huttlin et al. 2013).

A)



B)

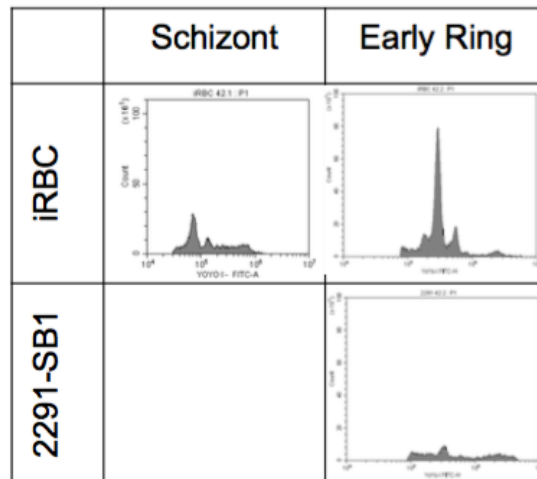


Figure 10 Stage-Specific Activity of TPIMS 2291.

Tightly synchronized cultures were treated with TPIMS 2291 at 6, 18, 30, and 42 hours post invasion. Treated cultures were monitored for parasite development by 12-hour interval sample fixation for flow cytometry staining and analysis with YOYO-I. A) Early ring treatment (6 hours post invasion) shows rapid activity of 2291 in blocking ring development. B) Treatment of 2291 on developing trophozoites and schizonts results in blocked progression beyond schizonts development.

2291-SB1 *in vivo* Efficacy

Armed with this information, we tested 2291-SB1 for *in vivo* efficacy. Swiss-webster mice were infected with 1×10^6 *P. berghei* luciferase expressing parasites. After infection was established (three days), mice were treated with 100mg/kg once daily for four days by oral gavage. On day 7, parasite load was determined by IVIS luminescence imaging. In this study however, 2291-SB1 had no effect on parasitemia (data not shown). After discussion with our chemist we determined to test 2291-SB1 a second time, but with *ip* injections rather than oral gavage. While this study is currently underway 2291-SB1 is showing promising results by inducing a delay in parasite growth and prolonging mice survival by at least 2 days.

Transmission Blocking Potential

One of the yet unaddressed needs for next generation antimalarials is the absolute necessity of the compound to have transmission blocking potential. This can be shown in sporozoite activity or in gametocyte activity. To test 2291-SB1 transmission blocking activity or collaborators screened 2291-SB1 against NF54 stage V gametocytes. This assay measures luciferase expressing gametocyte development in the presence of test compound compared to controls (untreated and puromycin). In this assay 2291-SB1 showed gametocyte inhibition activity with an IC_{50} of 240nM.

NF54 Stage V Gametocyte Activity

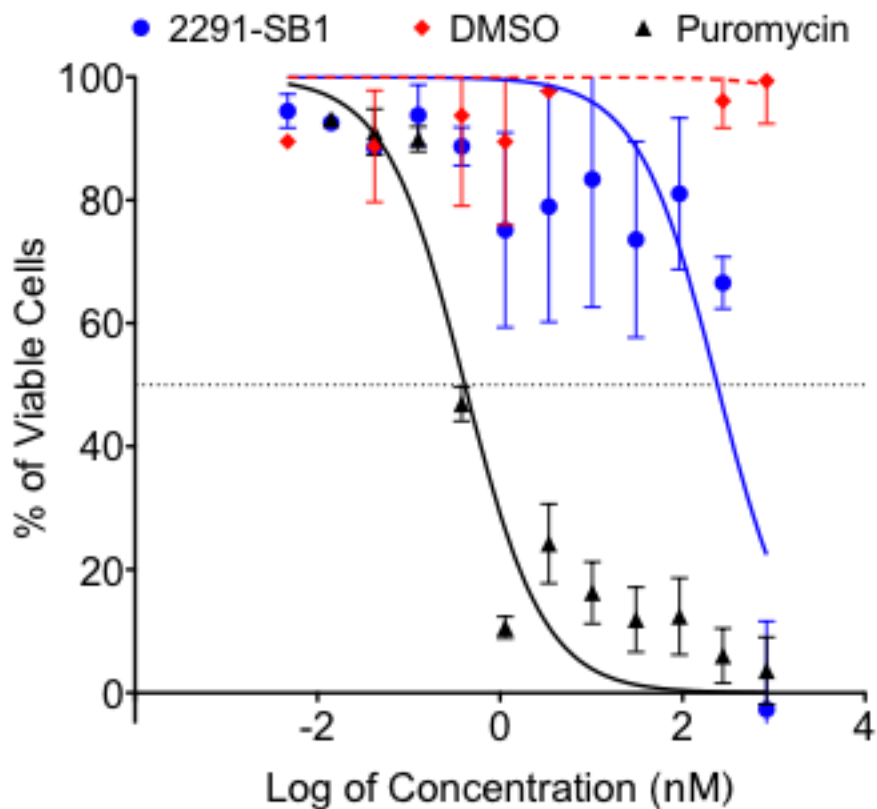


Figure 11 TPIMS 2291-SB1 Gametocyte Inhibition

Results are the average of three experiments in triplicate.

CHAPTER 5: DISCOVERY AND CHARACTERIZATION OF ANTIPLASMODIAL COMPOUNDS FROM THE MEMORIAL SLOAN KETTERING CANCER CENTER NATURAL PRODUCT BASED ALKALOID LIBRARY

MSKCC Natural-Inspired Alkaloid Library

Derek Tan at MSKCC has pioneered diversity-oriented synthesis of natural product based libraries for the past decade (Tan 2005). This technology facilitates rapidly expanding chemical diversity by reacting a starting compound with three to five different functional moieties as shown in Figure 12.

We screened 1,200 natural product-based synthetic compounds from MSKCC DOS libraries and identified 3 potent antiplasmodial scaffolds. The front-runner Alkaloid library scaffold hit, M03 has excellent potency (160nM) and selectivity (12.7 fold) and was prioritized for further development and characterization (Figure 13).

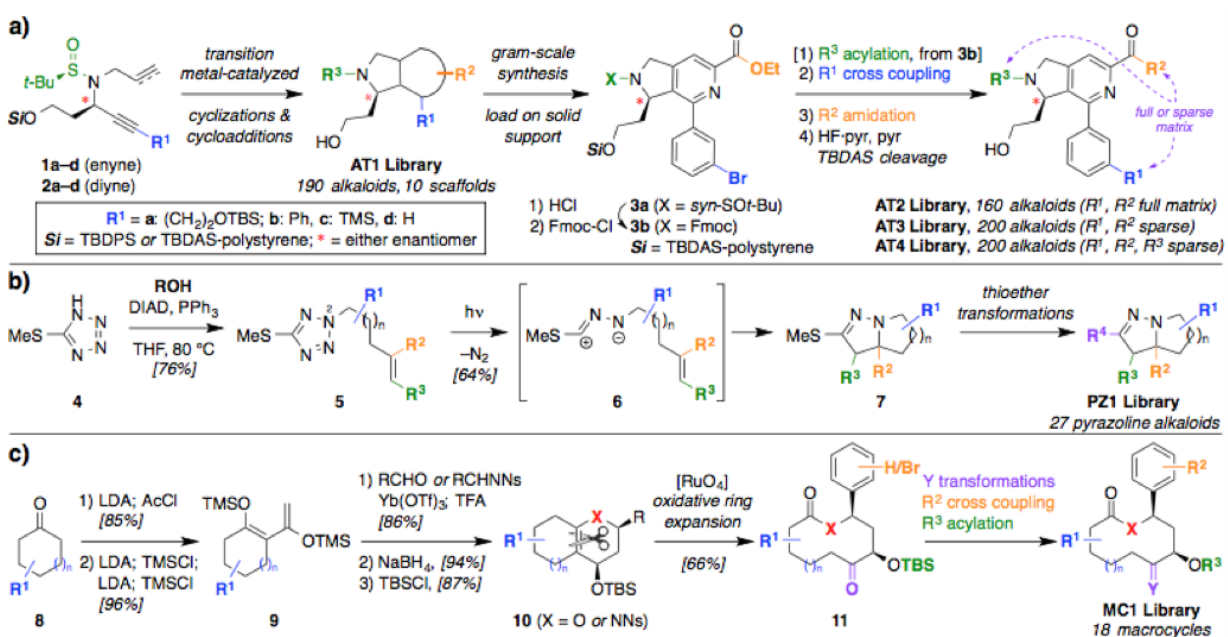


Figure 12 Diversity Oriented Synthesis

Natural product-based diversity-oriented synthetic scheme for flexible and efficient synthesis of alkaloid (a), polycyclic pyrazoline (b), and macrocyclic (c) libraries.

Source: Derek Tan

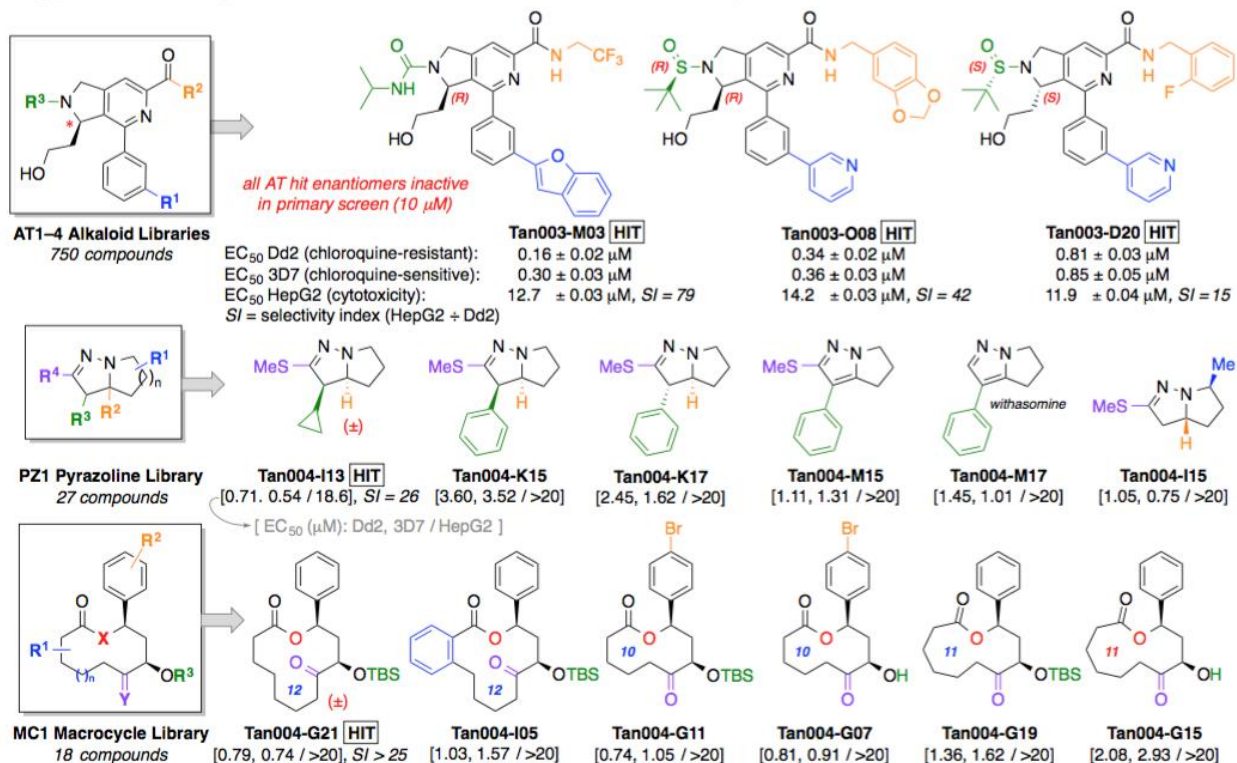


Figure 13 MSKCC Hits Antiplasmodial Activity.

EC₅₀ values (\pm SD) are derived from 3 independent experiments, each with 3 replicates. The Z⁰ factors of these assays were >0.8. *P. falciparum* Dd2, chloroquine resistant; 3D7, chloroquine sensitive.

Physicochemical Properties of MSKCC-M03

For a natural product-based compound the MSKCC-M03 alkaloid meets most of the Lipinski criteria for drugability including exceptional microsomal stability. The only concern MSKCC-M03 may have is with solubility, never able to rise above 8.4 μM without special (more toxic) solvents like DMSO.

Table 9 Physicochemical Properties of MSK-M03

Compound ID		MSK-M03
ClogP		3.88
Molec. Weight (g/mol)		568.5
H-bond Donor		3
H-bond Acceptor		5
Polar Surface Area (Å²)		103.8
Kinetic Solubility Results in pH 1.2 SGF (µM)		7.7
Kinetic Solubility Results in pH 6.5 50mM NaPO4 (µM)		6.5
Kinetic Solubility Results in pH 7.4 1x PBS (µM)		8.4
Microsomal Stability (Results in % Remaining)	T=0 min.	100.0
	T=60 min.	61.5

Pharmacokinetic Properties of MSK-M03

Pharmacokinetic studies were conducted at SAI Life Sciences, India, a contract research organization. Different formulations of vehicle were evaluated for optimal delivery, a formulation composed of 5% N-methyl-2-pyrrolidone, 5% Solutol HS-15, 30% PEG-400 in 60% hydroxypropyl- β -cyclodextrin (20%w/v) was found to be the best for maximum solubility of MSKCC-M03. As described in Table 10, the compound achieved only 57% relative abundance in pharmacokinetic studies suggesting poor stability in mouse. Interestingly, MSKCC_M03 was stable in human serum studies where MSKCC-M03 has a $t_{1/2}$ of over 2 hours (Table 11). This suggests that the rodent malaria model may not be an acceptable model for determining *in vivo* MSK-M03 antimalarial effectiveness.

Table 10 MSK-M03 *in vivo* PK (mouse)

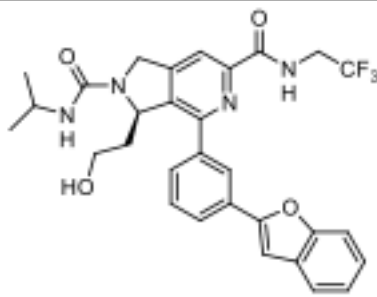
	 <p style="text-align: center;">Tan003-M03</p>
PK (<i>ip</i> , plasma/liver) $t_{1/2}$ T_{max} C_{max} AUC_{inf}	(Dose: 50mg/kg) 1.2 h / 2.2 h 1.0 h / 0.1 h 14.0 μ M / 58.6 μ M 52.7 μ M•h / 186.0 μ M•h
PK (<i>po</i> , plasma/liver) $t_{1/2}$ T_{max} C_{max} AUC_{inf}	(Dose: 50mg/kg) 8.2 h / 3.1 h 0.25 h / 0.25 h 10.9 μ M / 53.8 μ M 29.9 μ M•h / 107.9 μ M•h
F_{rel} (AUC_{inf} <i>po</i> / AUC_{inf} <i>ip</i>)	57%

Table 11 MSK-M03 *in vivo* PK (human serum)

Time (hr)	% Parent compound remaining			
	R1	R2	R3	Mean
0	100	100	100	100
0.25	110	110	92	104
0.5	117	112	110	113
1	113	105	93	103
2	76	93	86	85
$t_{1/2}$ (min)	> 120			

Human serum levels of MSKCC-M03 at 15, 30, 45, 60, and 120 minutes.

Structure Activity Relationship Profiling for MSKCC-M03

Diversity Oriented Synthesis (DOS) incorporates multistep synthesis of similar reagents repeatedly. This inherently created small scale SAR for MSKCC-M03 (Figure 14). It is clear from this SAR that the scaffold was unable to tolerate changes to its core structure without a drastic shift in potency. Deletions of the hydroxyethyl side chain, nitrogen side chain substitutions, and amide side chain derivatives all led to a loss of activity. Aromatic ring substitutions were occasionally tolerated, but still led to a drop in activity.

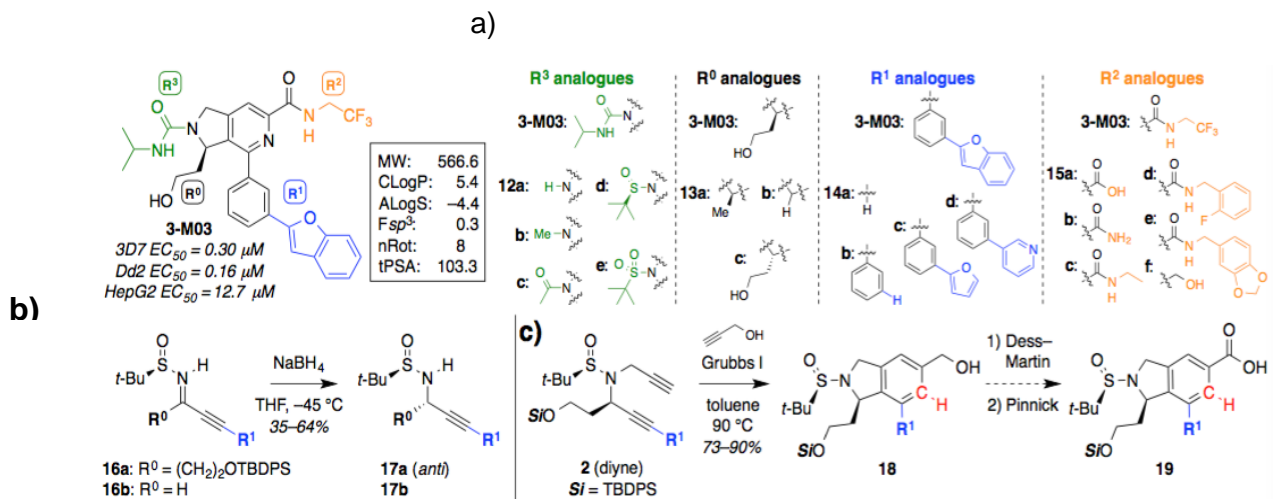


Figure 14 MSKCC-M03 SAR

Synthesis of structural analogs of MSK-M03 including deletion mutants at the four substituent positions R⁰ – R³ (a), sulfonamide diastereomers and des-hydroxyethyl R⁰ side chains (b), and establishment of deaza-scaffold synthesis and alcohol oxidation. These scaffold analogs were screened for antiplasmodial activity using the SYBR Green I assay as described above for EC₅₀ values (data not shown). The Z⁰ factors of these assays were >0.8.

Source: Derek Tan

Rate of Killing and Parasitocidal/Parasitostatic Evaluation

To evaluate the rate of killing for MSK-M03, asynchronous cultures were treated with 3x IC₅₀ and 10x IC₅₀ (MSK-M03) concentrations for 6, 12, 24, 48, and 72-hour treatments. After each treatment window, cultures were washed 3 times in RPMI and then resuspended in culture media and monitored daily for parasite growth. MSK-M03 is slow acting and parasitostatic treated for 12, and 24 hours, preventing growth while under compound pressure, but upon removal parasite growth resumes normal growth after brief recovery period. When given for longer than 48 hours MSK-M03 exhibits parasitocidal activity (Figure 15). This is harmonious with an egress inhibitor as *P. falciparum* asynchronous cultures receiving a treatment window of anything less than 48 hours will yield some parasites which have not yet progressed to the steps immediately prior to egress. Only when treating longer than 48 hours is the compound able to fully prevent all parasite growth from progressing beyond egress, as all stages of asynchronous culture will encounter an egress event within a treatment window of 48 hours or more.

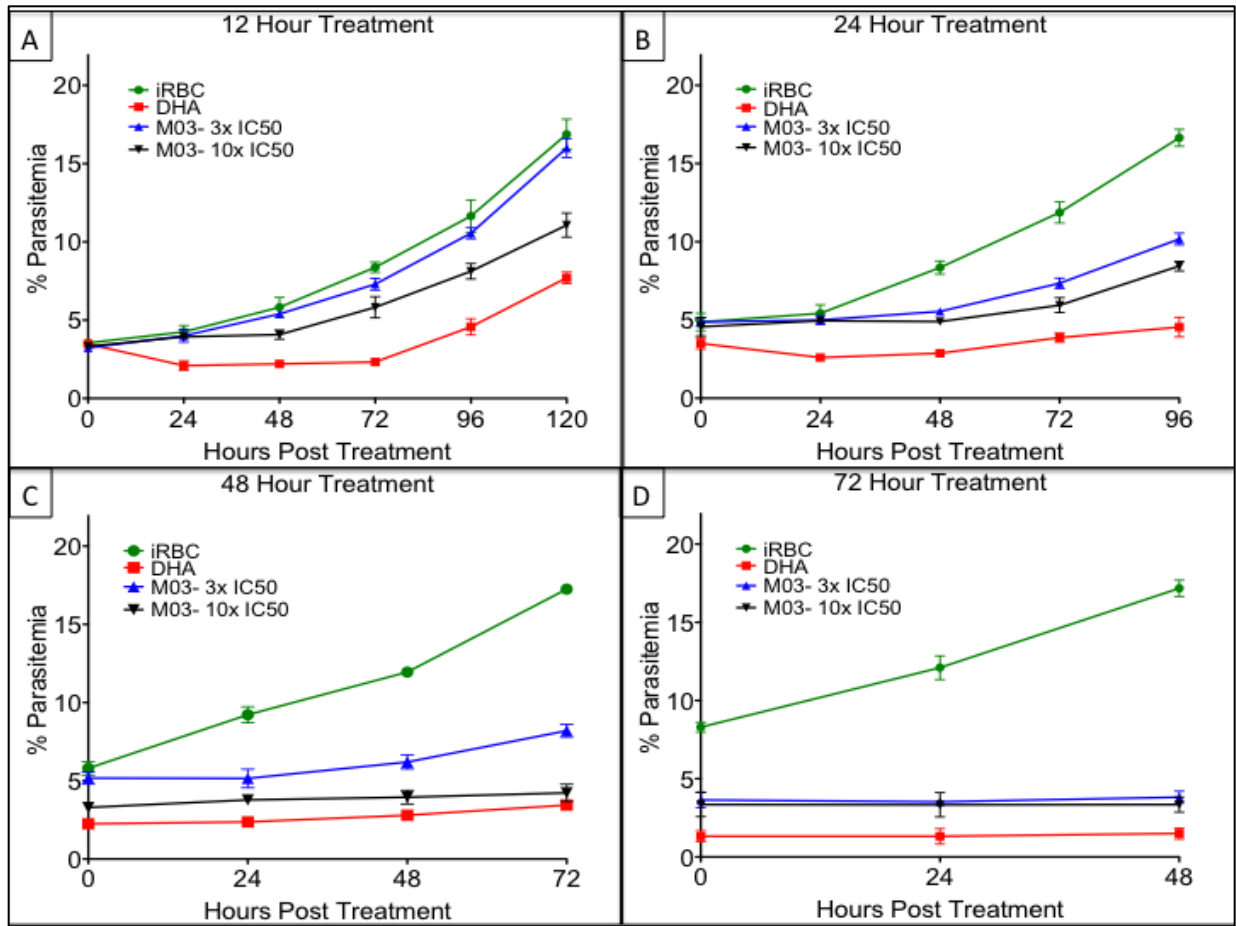


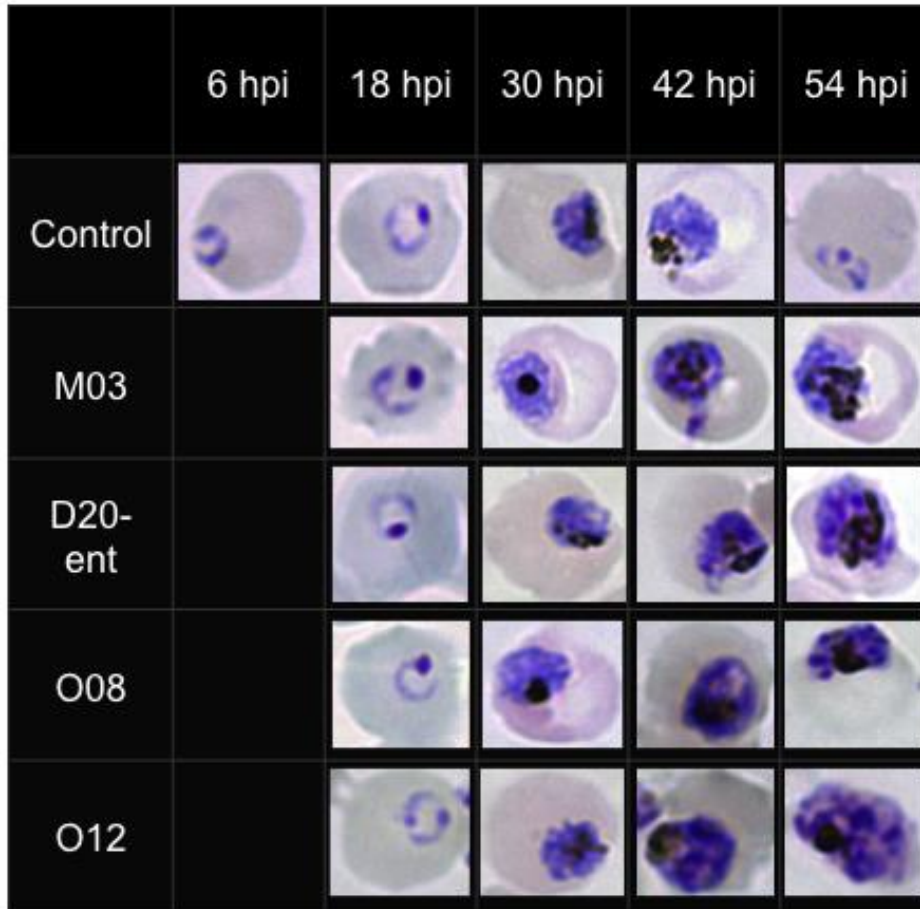
Figure 15 MSK-M03 Rate of Killing and Parasitostatic Evaluation.

3x IC₅₀ and 10x IC₅₀ concentrations of MSK-M03 were added to asynchronous parasite cultures for A (12 hour), B (24 hour), C (48 hour), and D (72 hour) treatments. After the treatment window, cultures were washed three times and resupplied with normal culture media and parasitemia was measured every 24 hours by Giemsa staining. At 48 hours treatment and beyond MSK-M03 is parasitocidal and inhibits parasite progression beyond late schizont/segmenter stage.

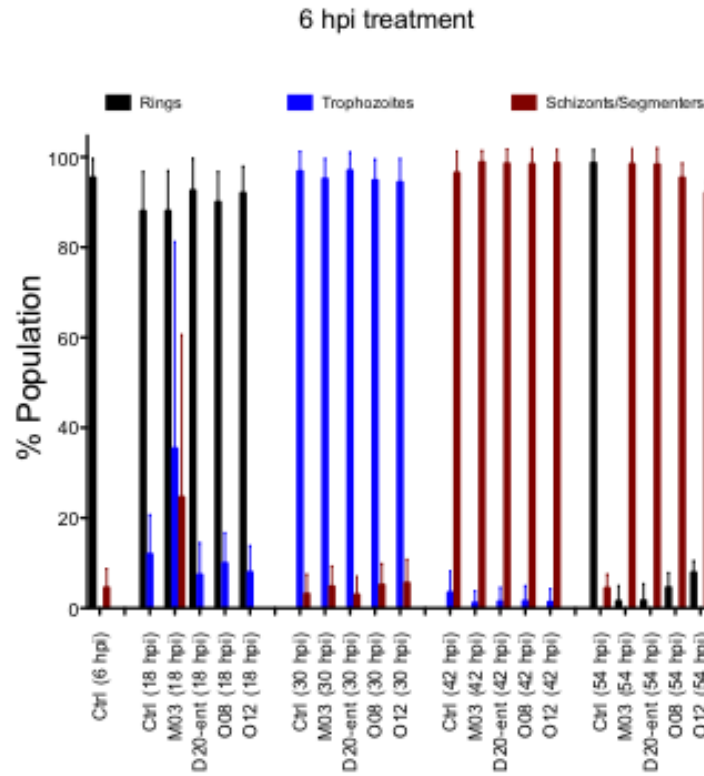
Cellular Mechanism of Action of MSKCC-M03

Similar to other stage-specific interaction studies, we set out to determine the cellular mechanism of action of MSKCC-M03 on intraerythrocytic development. As can be seen in Fig 16, regardless of development stage for onset of treatment, MSKCC-M03 inhibits egress, preventing RBC rupture leading to no release of merozoites, and no increase in parasitemia. This cellular action is reminiscent to the action of protease inhibitor E-64, a potent egress inhibitor (Salmon, Oksman et al. 2001). This result establishes MSKCC-M03 as a scaffold with a mechanism of action different from approved malaria therapeutics.

A)



B)



C)

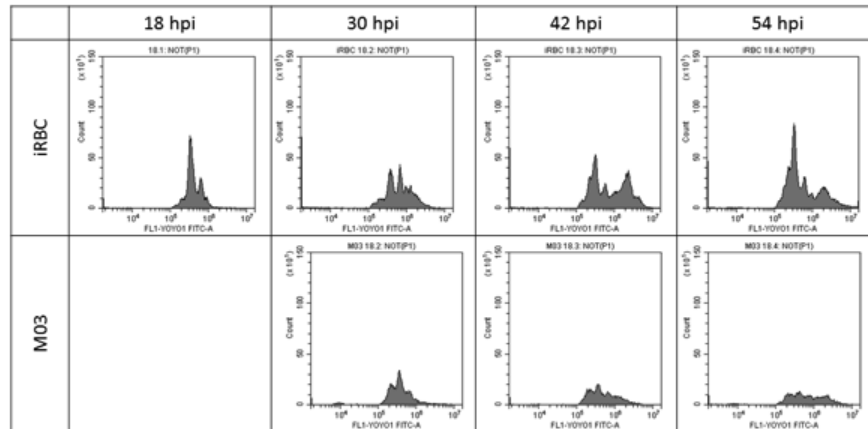


Figure 16 Stage Specific Interaction of MSK-M03.

Giemsa staining of tightly synchronized MSK-M03 treated cultures reveals MSK-M03 to inhibit parasite development beyond egress (A & B). These results were confirmed via flow cytometry (C) as described previously, and shows clear inhibition of egress as all retained parasites remain in the schizont/segmenter stage.

CHAPTER 6: DISCOVERY AND CHARACTERIZATION OF ANTIPLASMODIAL COMPOUNDS FROM NATURAL PRODUCT-INSPIRED ASINEX BIODESIGN LIBRARY

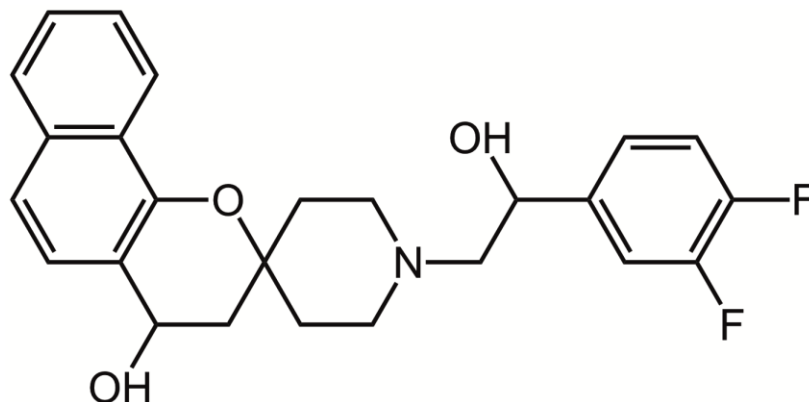
Asinex Natural Product-Inspired Library

The Asinex BioDesign library, is aimed to combine naturally occurring ring systems and functional groups into chemically tractable and diverse library sets called Biocores (Kombarov, Altieri et al. 2010). In applying a few filters (Oxygen count ≥ 3 , molecular weight < 450 , and increased saturation of ring structures, along with enrichment of privilege elements of known antimalarials (but a removal of endoperoxides), we narrowed the library of 70,000 down to 594 chemical compounds. Screening these compounds at $10\mu\text{M}$ concentration revealed 94 compounds with $\geq 70\%$ inhibition against multidrug resistant Dd2 strain in SYBR Green I unbiased assay. Subsequent screening at $1\mu\text{M}$ revealed 10 chemical scaffolds with $>50\%$ inhibition. These scaffolds were then serially diluted to generate to EC_{50} curves. Two top hit scaffolds, Spirocyclic chromanes (UCF 201) and Nitrostyryl quinolines (UCF 501) were selected for further characterization.

UCF 201 - Spirocyclic Chromane

One of the first scaffolding hits identified was a difluoro spirocyclic chromane which we assigned UCF 201. UCF 201 has an EC_{50} of 350nM and against Dd2 and boasts a selectivity of over 50 fold when tested for activity against HepG2 hepatocytes as shown in Figure 17. Furthermore, UCF 201 is more effective against the multidrug resistant

Dd2 than a chloroquine sensitive 3D7 strain indicating that UCF 201 activity is not effected by the PfCRT drug efflux pump mechanism.



UCF 201
Spirocyclic Chromane (SPC)

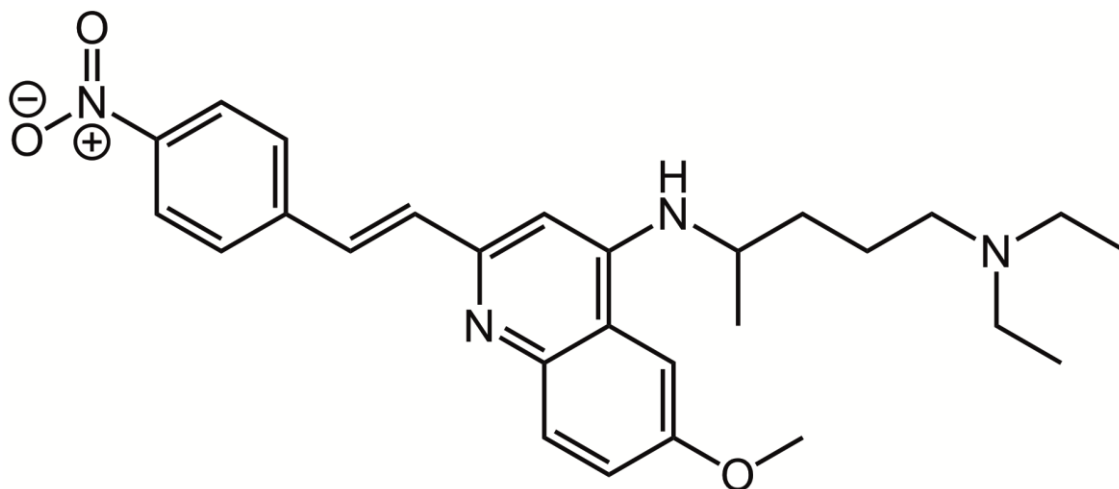
Dd2 EC₅₀ = 0.35 μM ± 0.02
3D7 EC₅₀ = 0.39 μM ± 0.03
HepG2 EC₅₀ = 19.0 μM ± 0.7

Figure 17 UCF 201 Selectivity

EC₅₀ values (±SD) are derived from 3 independent experiments, each with 3 replicates. The Z⁰ factors of these assays were >0.8. *P. falciparum* Dd2, chloroquine resistant; 3D7, chloroquine sensitive.

UCF 501 – 4-Nitrostyrylquinoline

A second compound identified in this screening process was a novel styrylquinoline that we named UCF 501. This compound had excellent antiplasmodial potency and selectivity with an EC₅₀ of 70nM against multidrug resistant Dd2 and selectivity over HepG2 of over 100 fold. Additional screening showed UCF 501 exhibits better antiplasmodial activity against chloroquine resistant Dd2 than against chloroquine sensitive 3D7, suggesting a mechanism of action distinct from chloroquine (Figure 18).



UCF 501

Dd2 EC₅₀ = 0.072 μM ± 0.02
3D7 EC₅₀ = 0.120 μM ± 0.03
HepG2 EC₅₀ = 12.9 μM ± 0.07

Figure 18 UCF 501 Antiplasmodial Activity.

EC₅₀ values (±SD) are derived from 3 independent experiments, each with 3 replicates. The Z⁰ factors of these assays were >0.8. *P. falciparum* Dd2, chloroquine resistant; 3D7, chloroquine sensitive.

Physicochemical Properties of UCF 201 and UCF 501

For further characterization of UCF 201 and UCF 501, we evaluated the Lipinski parameter compliance of UCF 201 and UCF 501 and generated *in vitro* physicochemical profiles for each compound. Both compounds are within Lipinski's suggested requirements and possess good permeability and solubility. UCF 501 also has acceptable microsomal stability while the stability of UCF 201 is somewhat lackluster.

Table 12 Physicochemical Properties of UCF 201

Compound ID		UCF 201
ClogP		3.85
Molec. Weight (g/mol)		425.5
H-bond Donor		2
H-bond Acceptor		4
Polar Surface Area (Å²)		52.9
Kinetic Solubility Results in pH 7.4 1x (µM)		24.3
Permeability Results in pH 7.4 (-logPe)		<2.9
Microsomal Stability (Results in % Remaining)	T=0 min.	100.0
	T=60 min.	15.6

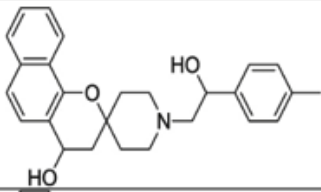
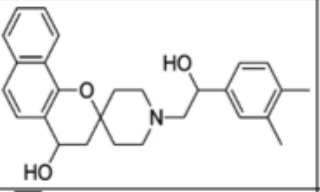
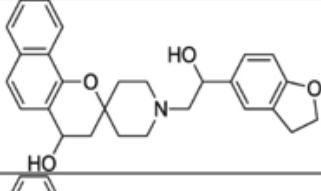
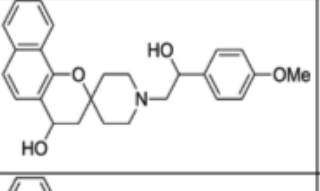
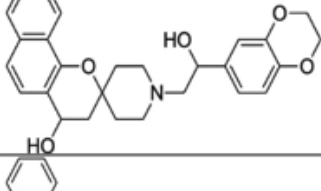
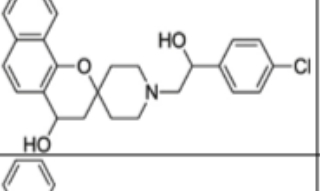
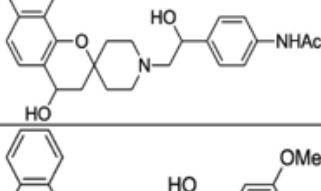
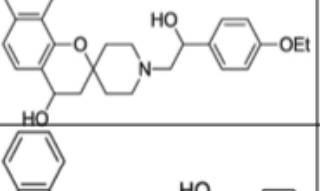
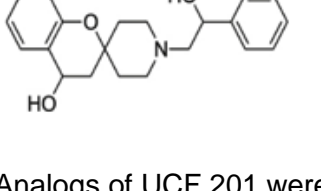
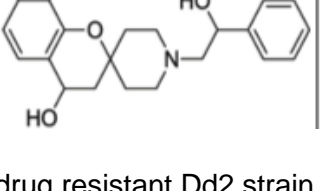
Table 13 Physicochemical Properties of UCF 501

Compound ID		UCF 501
ClogP		3.76
Molec. Weight (g/mol)		462.6
H-bond Donor		1
H-bond Acceptor		4
Polar Surface Area (Å²)		83.2
Kinetic Solubility Results in pH 7.4 1x (µM)		289.7
Permeability Results in pH 7.4 (-logPe)		2.9
Microsomal Stability (Results in % Remaining)	T=0 min.	100.0
	T=60 min.	47.8

\Structure Activity Relationship Profile for UCF 201

To better define the key structural components of spirocyclic chromane's antiparasitic activity we conducted a small-scale SAR by catalog along with 100 structural analogs synthesized in the Manetsch lab (USF/Northeastern). These compounds were screened by SYBR green I cell-based assay and cherry-picked SAR results are listed in Table 14. Unfortunately, the SAR is rather flat and further modifications including alterations to the chromane scaffolding and evaluation of piperidine nitrogen and naphthalene roles in UCF 201's activity need to be determined. It can from this study however, be declared that simple phenyl derivatives are preferred for potency to large aromatic structures and that within the phenyl group alterations to electron density had little effect on activity. It is also clear that lipophilicity, rather than electron density, has a significant impact on UCF 201 activity as increasing fluorination led to a proportional increase in potency.

Table 14 UCF 201 SAR

Structure	Dd2 EC ₅₀ (μM)	HepG2 EC ₅₀ (μM)	Structure	Dd2 EC ₅₀ (μM)	HepG2 EC ₅₀ (μM)
	0.41 ± 0.02	13.4 ± 0.3		0.85 ± 0.1	19.3 ± 1.3
	0.45 ± 0.07	17.4 ± 0.6		0.62 ± 0.08	19.1 ± 0.7
	0.51 ± 0.07	19.4 ± 1.0		0.67 ± 0.07	16.3 ± 0.7
	0.56 ± 0.08	13.3 ± 0.8		0.75 ± 0.09	13.3 ± 1.1
	0.56 ± 0.09	17.3 ± 0.8		0.87 ± 0.07	19.1 ± 1.1

Analogues of UCF 201 were screened against multidrug resistant Dd2 strain and HepG2 hepatocytes for antiplasmodial activity and selectivity determination. Values are the average of at least three independent experiments.

Determining Structure Activity Relationships for UCF 501

A small scale SAR of UCF 501 (10 additional compounds) were synthesized by our collaborator Dr. Yuan (UCF). These 10 scaffolds were created to determine: the necessity of the nitro group (which can have cytotoxicity concerns); and also to address the flexibility/requirement of the chiral center (marked with asterisk on compound 20, UCF 501 Figure 19). The synthetic steps for these compounds are detailed in (Roberts, Zheng et al. 2017). Screening these analogs against Dd2 revealed that neither the chiral center nor the nitro group is required for antiplasmodial activity, however potency significantly increases with the nitro group present (Table 15, Analog # 12 & 17).

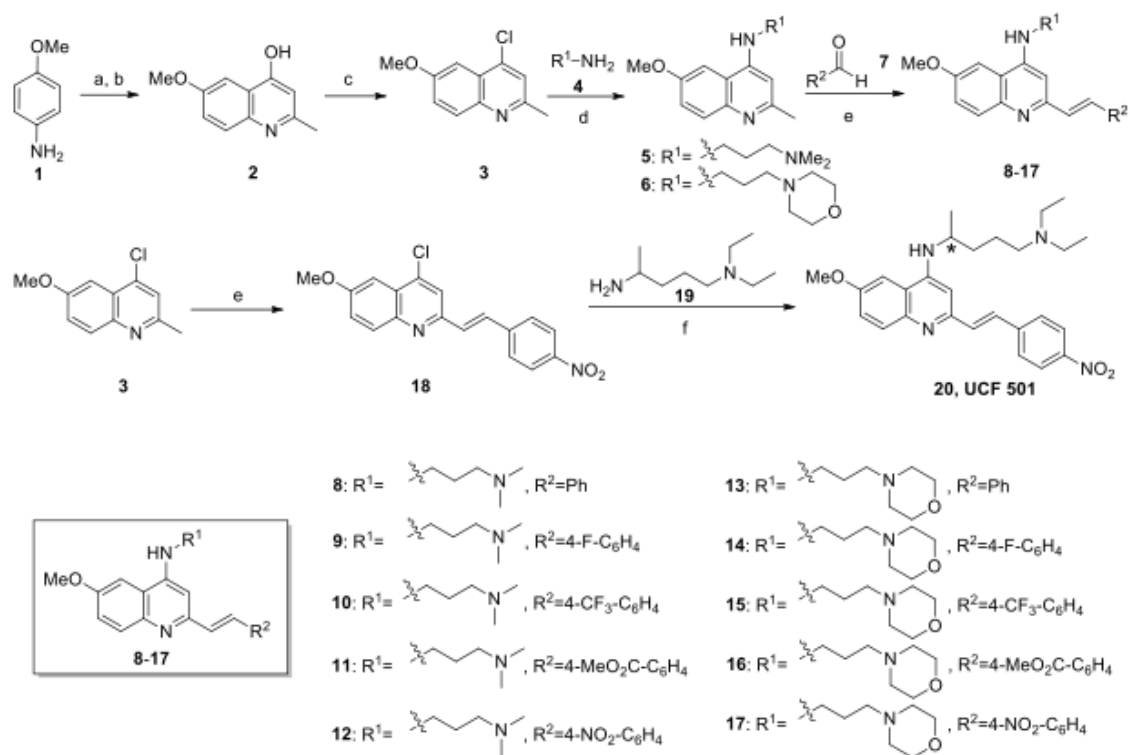


Figure 19 UCF 501 and SAR Analogs Synthetic Scheme.

(a) ethyl acetoacetate, MgSO₄, HOAc, EtOH, 90 °C; (b) Dowtherm, 270 °C; (c) POCl₃, reflux; (d) neat, pressure tube, 140 °C; (e) *m*-Xylene, *p*-TsNH₂, 140 °C; (f) Pd(OAc)₂, BINAP, K₃PO₄, 1,4-dioxane, 85 °C. * symbol indicates chiral center.

Table 15 UCF 501 Analogs Antiplasmodial Activity

Entry	SQ	Dd2 EC ₅₀ (μM)	3D7 EC ₅₀ (μM)	HepG2 EC ₅₀ (μM)
1	8	0.323 ± 0.04	0.302 ± 0.01	19.9 ± 0.4
2	9	0.137 ± 0.05	0.299 ± 0.04	12.6 ± 0.1
3	10	0.726 ± 0.04	0.605 ± 0.04	>20
4	11	0.138 ± 0.06	0.294 ± 0.06	14.9 ± 0.3
5	12	0.057 ± 0.03	0.197 ± 0.02	15.3 ± 0.5
6	13	0.303 ± 0.04	0.373 ± 0.03	18.0 ± 0.4
7	14	0.208 ± 0.04	0.310 ± 0.02	13.6 ± 0.5
8	15	0.735 ± 0.06	0.599 ± 0.03	>20
9	16	0.471 ± 0.08	0.322 ± 0.04	12.8 ± 0.2
10	17	0.123 ± 0.05	0.193 ± 0.04	15.7 ± 0.7
Chloroquine		0.172 ± 0.02	0.011 ± 0.00	>20

EC50 values are derived from 3 independent experiments, each with 3 replicates.

Synthesis of UCF 501

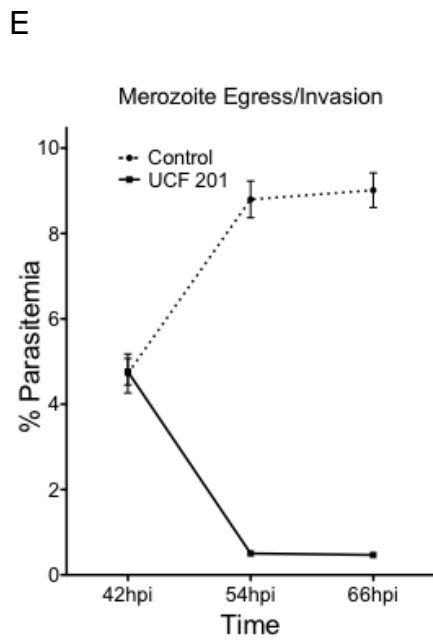
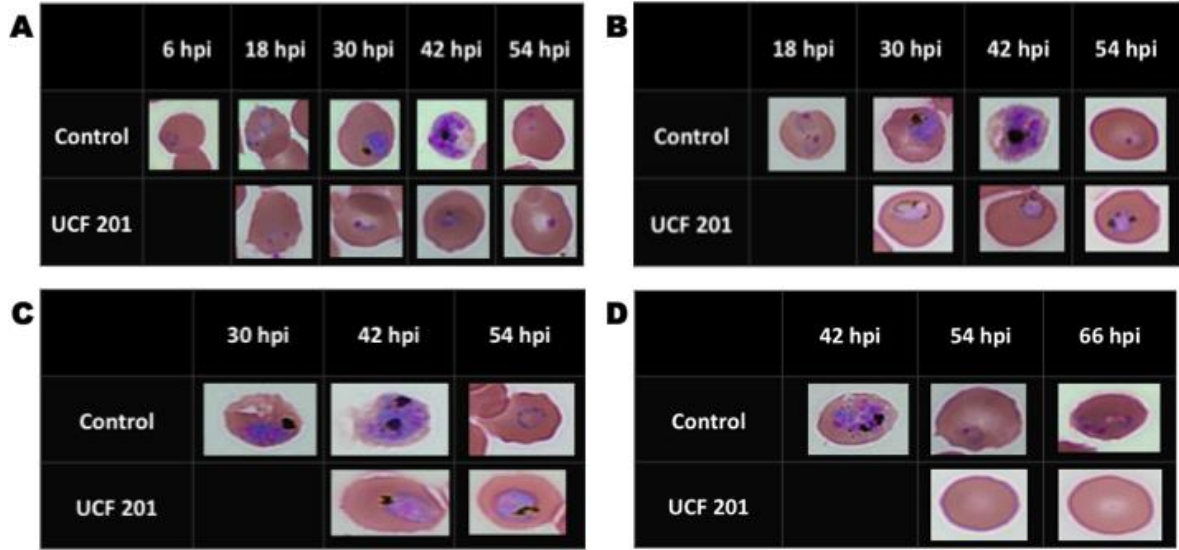
Unfortunately, at this point in our study our supply of UCF 501 was exhausted and our supplier was unable to produce more compound at a reasonable price/timeline. We decided that it would be best to synthesize UCF 501 on our own using the scheme described in Figure 19. After a few months I was able to synthesize a total weight of 2 grams of UCF 501. Resynthesized UCF 501 had an Dd2 EC₅₀ slightly less than our previous results (EC₅₀ = 50nM). With 2 grams of compound we were now able to proceed with further studies with the scaffold.

Cellular Mechanism of Action

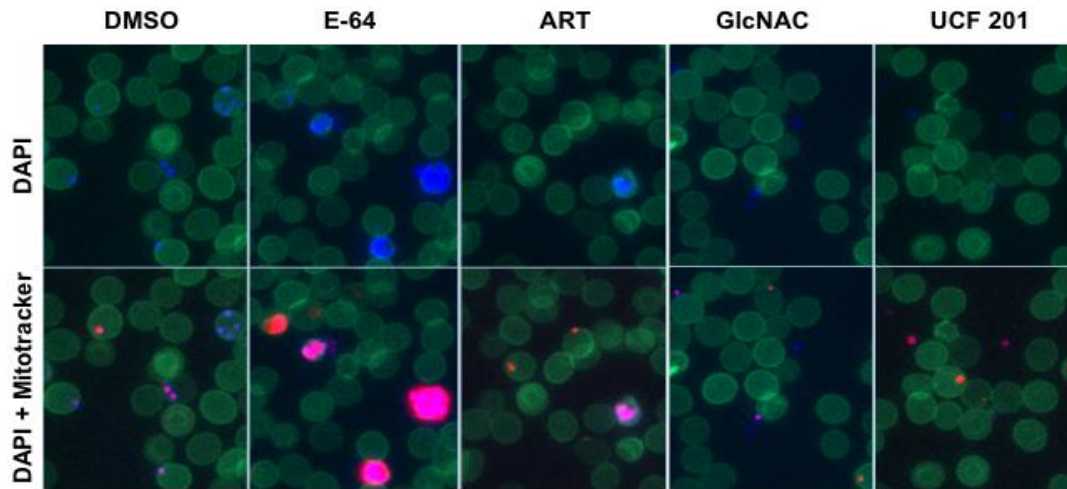
To further characterize the cellular stage-specific activity we developed an assay that provides both flow and Giemsa readout results. This assay reveals the compounds effect on: early ring development; ring to trophozoites transition; trophozoites development; schizonts development; merozoite egress; and merozoite reinvasion.

Incredibly, as can be seen from figure 19, both UCF 201 and UCF 501 treatment at 5xIC₅₀, inhibit parasite development at every stage of *P. falciparum* intraerythrocytic life cycle, including merozoite reinvasion (Figure 20). Figure 19 A-D show UCF 201's inhibition of early and late ring progression (A & B) (trophozoite development (C), and schizont progression (D). Additionally, the steep drop in overall parasitemia without accumulation of schizont/segmenters, indicates UCF 201 may play a role in merozoite deactivation or invasion inhibition (Fig. 19, E). UCF 201 treatment does not diminish the metabolic activity of merozoites (red fluorophore), but does prohibit active merozoites

from invading new RBCs (Fig. 19, F). The inhibition of early ring development is also validated by flow cytometry. In Fig. 19, G, an early ring peak slowly degrades away rather than developing into late rings, trophozoites, or schizonts.



F



G

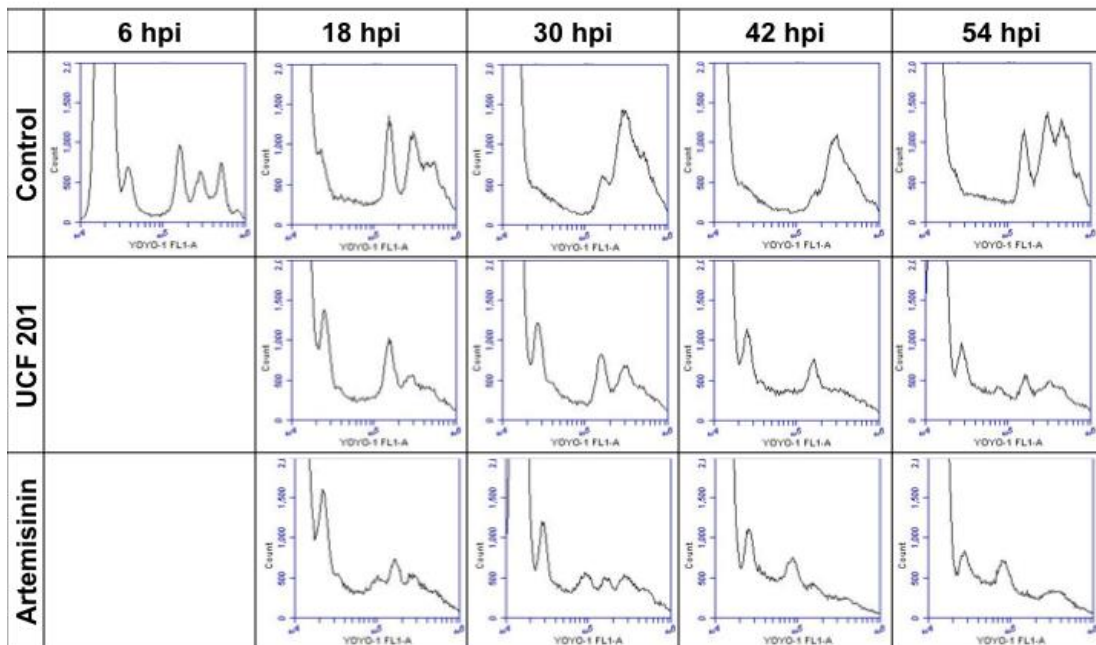
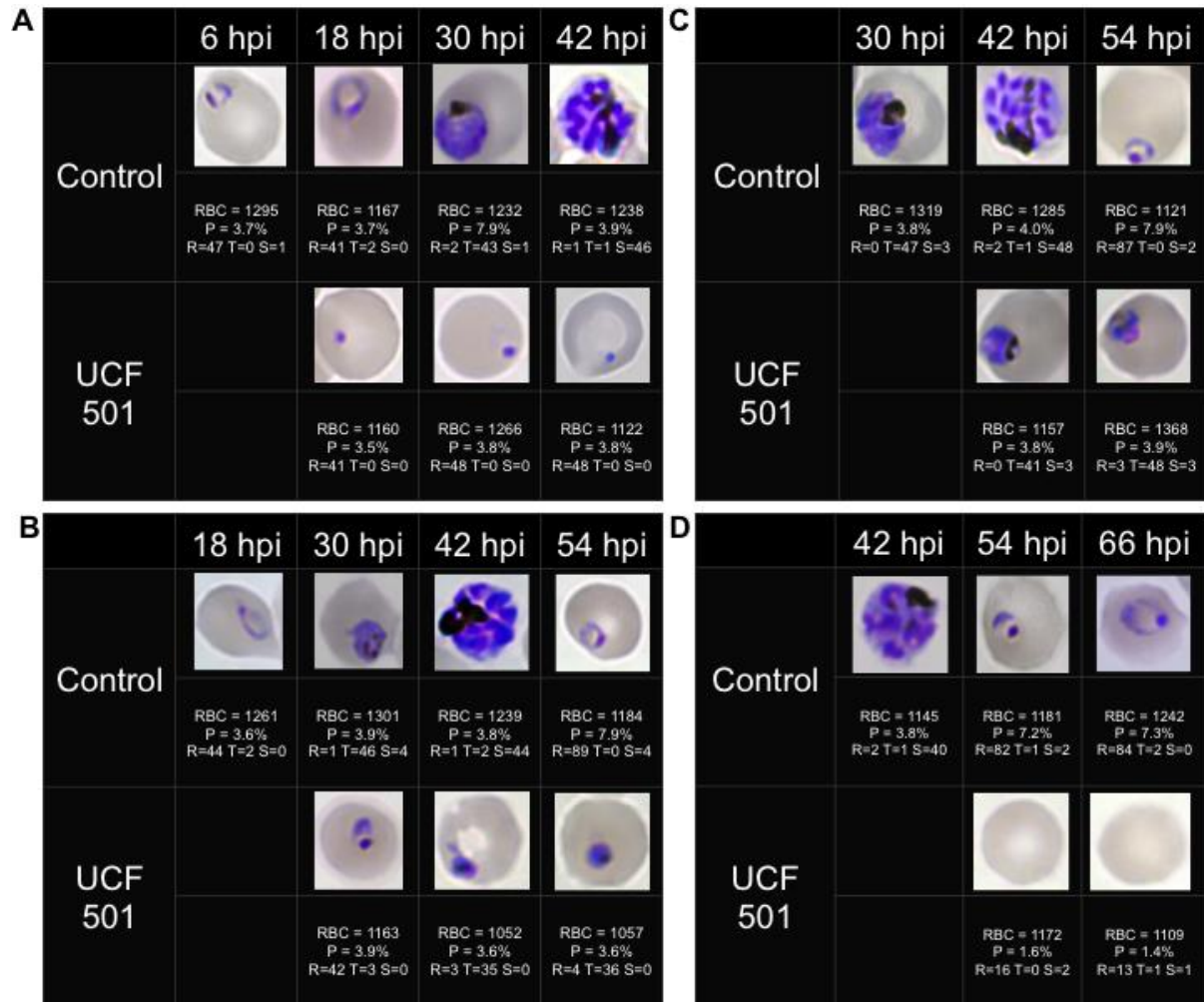


Figure 20 UCF 201 Cellular Mechanism of Action.

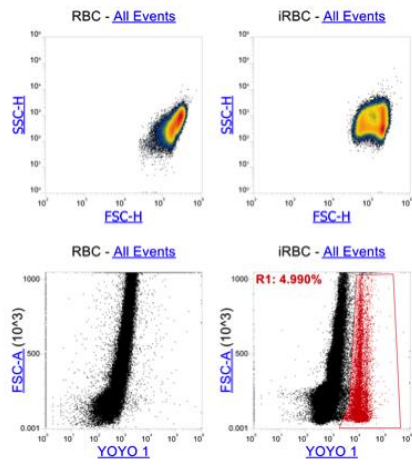
The effect of UCF 201 ($5 \times IC_{50}$) on parasite life cycle stage progression upon treatment at (A) 6 h, (B) 18 h, or (C) 30 h post-invasion time-points at $5 \times EC_{50}$ for 36 h. For the (D) 42 h post-invasion time-point the effect was followed for 24 h after compound addition. Giemsa-stained thin smears were prepared at 12 h intervals for microscopic evaluations. Microscopic images represent parasite stages after evaluating 1000 infected RBC. E-G Synchronized culture at 42 h post invasion was treated with $5 \times EC_{50}$ of the compound. Giemsa stained thin smears were prepared every 12 h for microscopic evaluations of parasitemia to quantify parasitemia. (F) Confocal plate micrograph of parasite phenotype following 24 h exposure at 42 hpi. Synchronized cultures were exposed to UCF 201 or reference compounds E-64, GlcNac, or artemisinin at 10 μ M concentration. (G) Effect of UCF 201 on *P. falciparum* growth by flow cytometric analysis of YOYO-1 labeled cells. The synchronized culture was exposed to UCF 201 at 6 hpi with $5 \times EC_{50}$ of UCF 201. Plots represent cell count in y-axis versus FL1 channel representing DNA content.

To further understand UCF 501's unique mechanism of action we next set out to determine the stage specific activity of UCF 501. UCF 501 clearly inhibits cellular progression at every stage of development. These results are shown in Figure 20. In Fig 20, A-D Giemsa staining of tightly synchronized cultures were treated at early ring (A), late ring (B), trophozoite (C), or schizont (D) stages and monitored for phenotypic cell cycle development. UCF 501 treatment inhibited early ring progression Fig 20 A, late ring progression Fig 20 B, and trophozoite progression, Fig 20 C. Most excitingly, UCF 501 inhibits merozoite invasion in Giemsa stained phenotypic studies (Figure 21 D and H), and high-content confocal imaging in Fig 20 G. These data were confirmed via flow cytometry as seen in Fig 20 E and F.

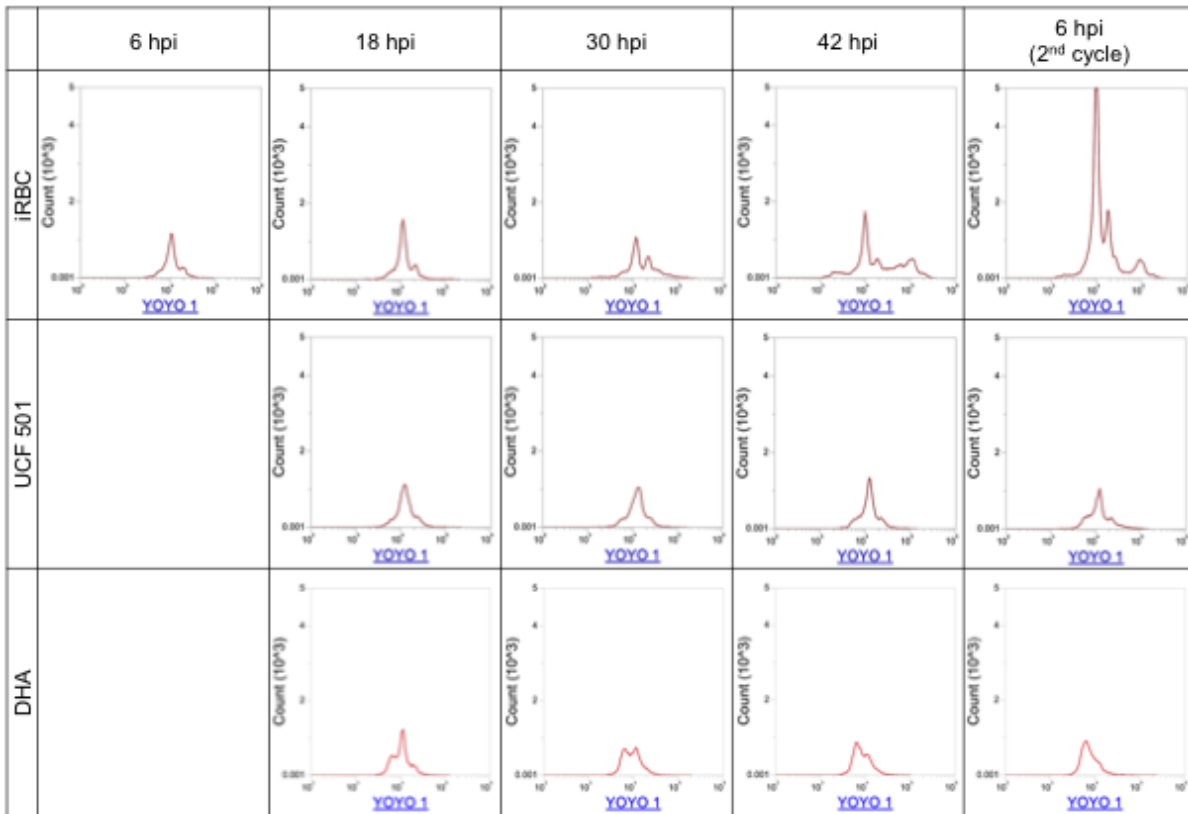
The ability of UCF 201 and UCF 501 to inhibit all stages of intraerythrocytic development and also the inhibition of merozoite invasion, a trait that is not shared with any previous antimalarial drug, warrants further characterization of these scaffolds.



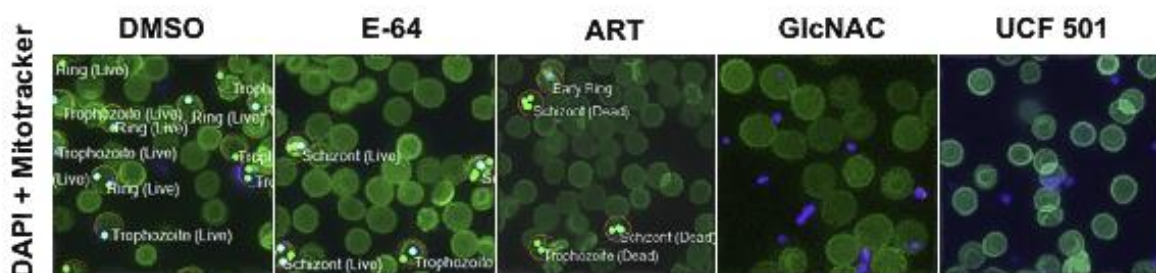
E



F



G



H

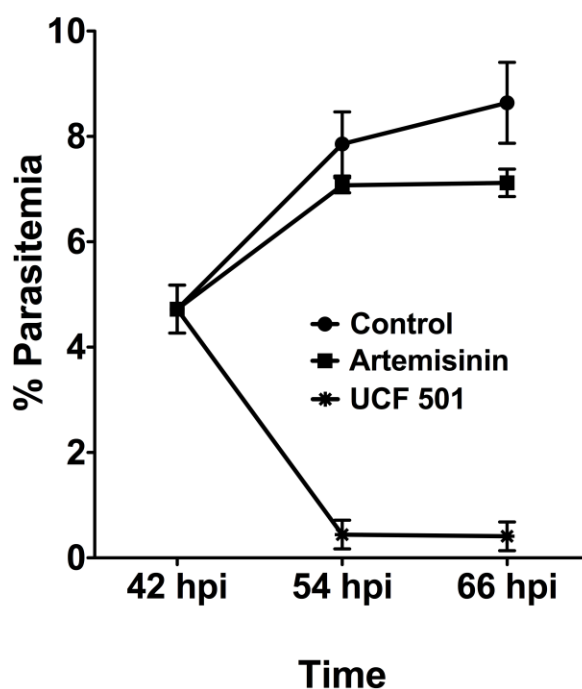


Figure 21 UCF 501 Cellular Mechanism of Action.

UCF 501 (5xIC₅₀) was added to tightly synchronized parasite cultures at (A) 6 h, (B) 18 h, (C) 30 h, and (D) 42 h post invasion and then incubated for at least 24 h. At 12-h increments treated cultures were fixed, permeabilized and stained with YOYO-1 for flow cytometry along with blood smears for Giemsa staining. YOYO-1 treated samples were read on Attune NXT flow cytometer at a voltage of 260 with excitation wavelength of 488 nM and an optical filter of 530/30. Side scatter (SSC) log/Forward scatter (FSC) log density plots (E, Top) and FSC log/YOYO-1 scatter plots (E, bottom) show distinct RBC and iRBC populations. (F) UCF 501 Inhibits Plasmodium

falciparum early in the intraerythrocytic cell cycle. Plots represent cell count in y-axis versus FL1 channel (488 nm Laser with 533/30 filter) representing DNA content. iRBC, infected red blood cells. (G) Confocal plate micrograph showing parasite phenotype following 24 h compound exposure at 42 hpi (schizont stage). Sorbitol-synchronized cultures were treated at 1 mM concentration of UCF 501 or the reference compounds E-64 (protease inhibitor blocking egress), GlcNAc (N-acetylglucosamine, invasion inhibitor), or artemisinin at 42 hpi for 24 h. Cultures were then stained in a solution containing 1nM each of wheat germ agglutinin-Alexa Fluor 488 conjugate and Mitotracker Red CMXRos followed by treatment with 4% paraformaldehyde and 5 mg/ml DAPI (2-(4-Amidinophenyl)-6-indolecarbamide dihydrochloride, 4',6-Diamidino-2-phenylindole dihydrochloride). Fluorescence imaging and automated detection of parasitized erythrocytes was done in an Operetta 2.0 system. Sample micrographs showing accumulation of extracellular merozoites in UCF 501 or GlcNAc- treated cultures compared to late rings ("Ring") in the solvent control wells, or schizonts in the E-64 and artemisinin-treated wells. The mitotracker-positive infected erythrocytes are indicated as "Live" whereas mitotracker-negative cells are labeled as "Dead". (H) Effect of UCF 501 on parasitemia when treated at the late schizont/segmenter stage. Cultures at 42 h post-invasion was exposed to UCF 501 or artemisinin at 5x EC₅₀.

UCF 501 Inhibition of β -Hematin Formation

Given the 4-amino quinoline base in UCF 501's structure, our next course of action was to determine if UCF 501 behaves similar to other quinolone compounds by inhibiting β -hematin formation. Differing from the gold standard quinoline i.e., Chloroquine, which completely inhibits β -hematin formation, UCF 501 had no effect on β -hematin formation (Table 16). This suggests UCF 501 inhibits parasite growth in a different manner than other quinoline compounds.

Table 16 UCF 501 Does not Inhibit B-Hematin Formation.

NP-40 based β -hematin Formation Assay	
Drug/Compound	% Inhibition
Chloroquine	100 \pm 1.78
8-Hydroxyquinoline	6 \pm 0.42
UCF 501	0 \pm 0.07
Compounds were tested at 100 μ M.	

Chloroquine, a known inhibitor of b-hematin formation, along with 8- Hydroxyquinoline, a non-inhibitor, and UCF 501 were tested at a concentration of 100mM for β -hematin formation inhibition using the NP-40 assay. These results are the average of two separate experiments. Compounds were tested at 100mM.

Rate of Killing and Parasitocidal/Parasitostatic Evaluation

Given UCF 501's potency, selectivity and unique cellular mechanism of action, this scaffold shows great promise as a possible candidate for Medicines for Malaria Ventures antimalarial pipeline. To further qualify for this status, it is required to determine the rate of killing and to establish the compound has a parasitocidal effect (Burrows, Duparc et al. 2017). To establish a rate of killing and determine the parasitocidal or parasitostatic effect for UCF 501, asynchronous cultures were treated with 3x IC₅₀ (UCF 501) concentrations for 6, 12, 24, 48, and 72-hour treatments. After each treatment window, cultures were washed 3 times in RPMI and then resuspended in culture media and monitored daily for parasite growth. UCF 501 is fast acting and parasitocidal, greatly reducing parasitemia with only 6 hours of treatment and completely clearing parasitemia with any exposure time of 12 or greater (Figure 22).

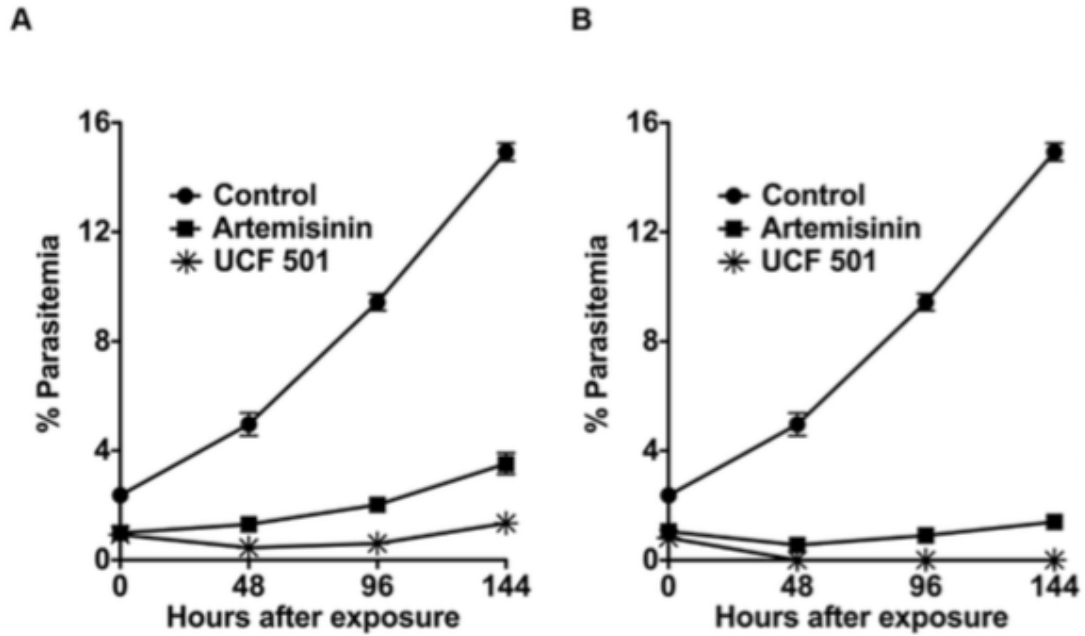


Figure 22 UCF 501 Rate of Killing and Parasitocidal Evaluation.

UCF 501 is fast acting and parasitocidal. Asynchronous cultures were exposed to 3 EC₅₀ of UCF 501 (200nM) or artemisinin (45nM) for (A) 6 h, and (B) 12 h followed by washing and growing in the absence of the inhibitors.

in vivo Efficacy

UCF 201 and UCF 501's potent activity and admirable physicochemical properties advanced the compound to testing in the rigorous rodent malaria model for *in vivo* efficacy. Adopting a modified Peter's test (Peters and Robinson 1988), We passed *Plasmodium berghei* (ANKA) from an injected donor mouse to 10 female balb/c mice at 2×10^6 parasites. Infected mice were then split into UCF 201 treated group (100mg/kg twice daily ip) and a control group (vector only). Parasite load was monitored by daily blood smears and animals were sacrificed once parasite load became greater than 40%. Figure 23 below shows UCF 201 delays parasitemia and prolongs life for an extra 7 days over control mice.

UCF 501 *in vivo* activity was tested under the same conditions as UCF 201 although under UCF 501 treatment parasitemia dropped below detectable limits and, with the exception of 1 mouse, remained below detectable limits throughout the 30-day study (Figure 24). Whereas the fully preventative effect of UCF 501 was determined in the previous experiment, an evaluation into the ability of UCF 501 to clear an established infection *in vivo* was also tested against a luciferase expressing *P. berghei* line. In this study mice were infected with *P. berghei* and allowed to establish an infection over the course of three days. After infection was established, mice were treated with vehicle control, Chloroquine, or UCF 501. In this study UCF 501 showed similar curative results (Figure 25).

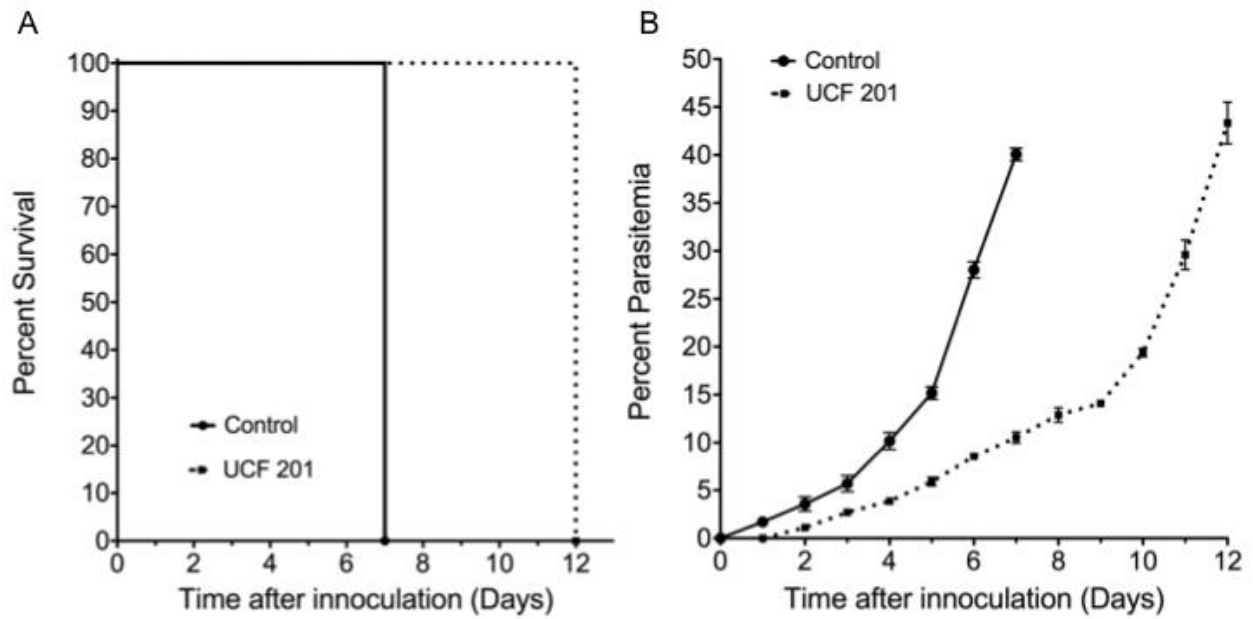


Figure 23 *in vivo* efficacy of UCF 201

Effect of UCF 201 on the survivability of *P. berghei* ANKA infected Balb/c mice was evaluated. Mice were treated orally with UCF 201 twice daily at 100 mg/kg at the time of infection.

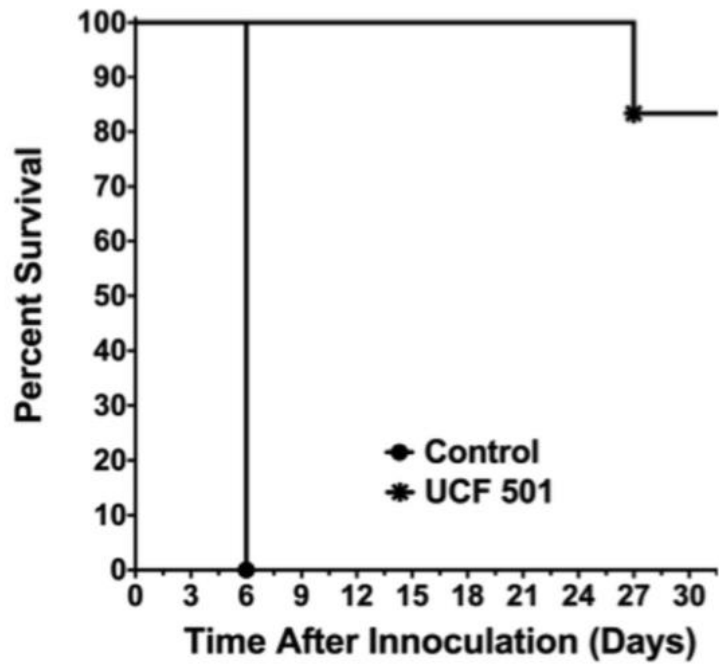
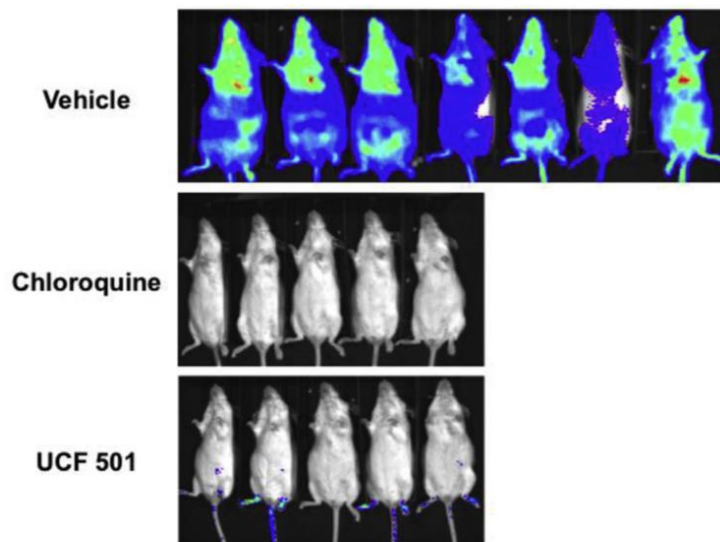


Figure 24 UCF 501 *in vivo* Efficacy.

Effect of UCF 501 on the survivability of *P. berghei* ANKA infected Balb/c mice was evaluated. Mice were treated orally with UCF 501 twice daily at 100 mg/kg at the time of infection.

A)



B)

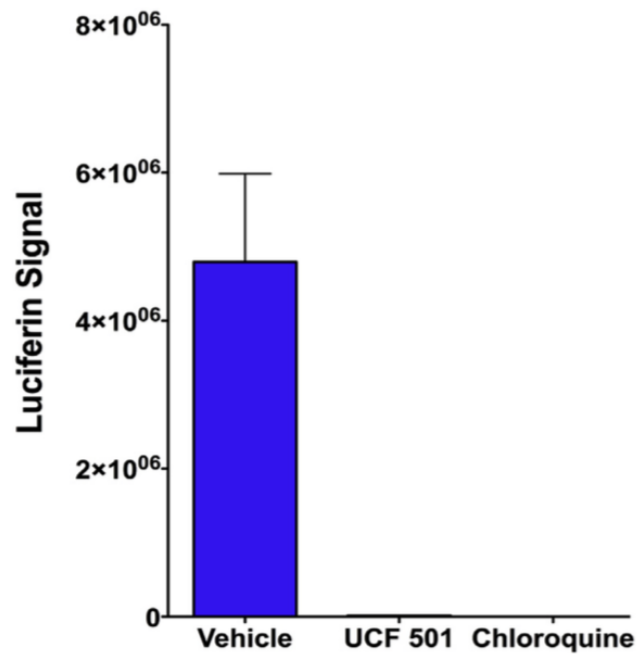


Figure 25 UCF 501 *in vivo* Efficacy *P. berghei* luciferase.

Swiss Webster mice were infected with *P. berghei* ANKA expressing luciferase, treated with 100 mg/kg orally once daily 72 h post-infection, and the luciferin signal was detected (A) and quantified (B) with an *in vivo* imaging system (IVIS).

Transmission Blocking Potential

Beyond a cure, UCF 501 needs to also have transmission blocking potential to truly become a next generation antimalarial compound as this is one of the major criticisms of current antimalarial therapy and is a requirement of malaria eradication (rather than just elimination). For this purpose, we sought to determine the effect UCF 501 has on stage V gametocyte development. To test UCF 501 transmission blocking activity, our collaborators screened UCF 501 against NF54 stage V gametocytes. In this assay UCF 501 showed gametocyte inhibition activity with an IC_{50} of 245nM (Figure 26). This finding promotes UCF 501 to early lead status, as it is both curative and transmission blocking, and brings UCF 501 into a very competitive compound for development in the Medicines for Malaria Venture (MMV) antimalarial pipeline.

NF54 Stage V Gametocyte Activity

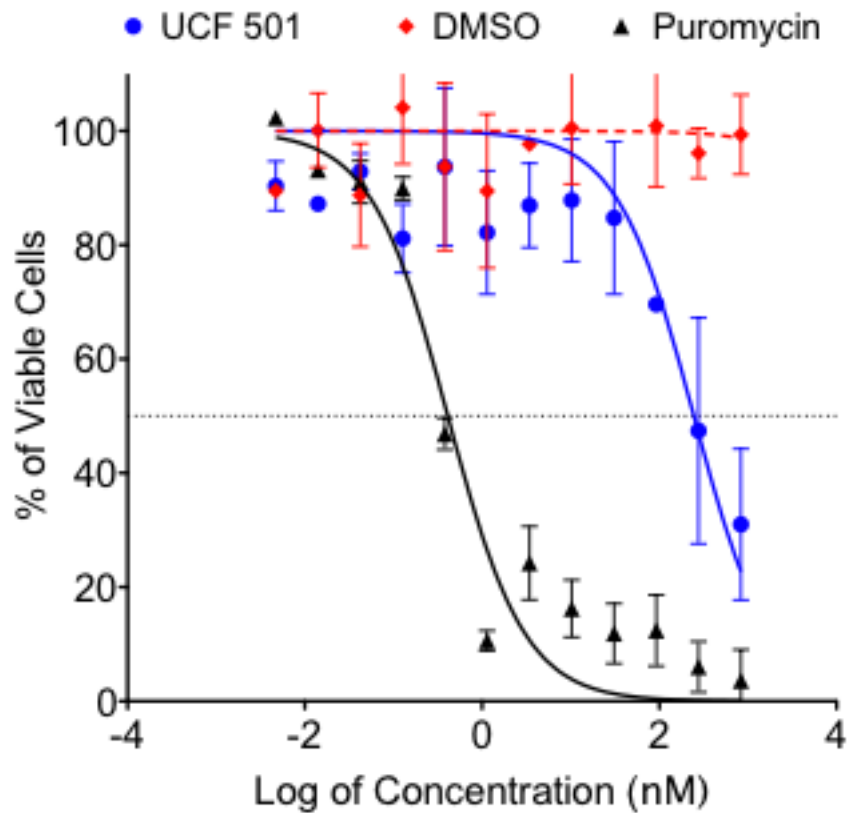


Figure 26 UCF 501 Gametocyte Inhibition

Activity of UCF 501 was screened against NF54 stage V gametocytes. Results are the average of 3 experiments in triplicate.

CHAPTER 7: TARGET IDENTIFICATION OF ANTIPLASMODIAL HITS

Necessity of Target ID

All the compounds discussed in this dissertation exhibit antiplasmodial potency, selectivity, and unique cellular mechanisms of action. These studies along with fast-acting (UCF 201, UCF 501), parasitocidal activity (all compounds discussed) and/or rodent model activity (UCF 201 and UCF 501) are sufficient to advance these compounds for early lead optimization. However, to best improve molecular potency and better understand the dynamic effect of these compounds it is necessary to determine their respective molecular targets. This can be achieved by whole genome sequencing analysis of parental and lab-generated resistance lines, screening for activity against targets involved in stage-specific interaction profile, or through probe-labeling of the compound for affinity pull-down.

Resistance Line Generation

Generating resistance lines against a pharmacophore and comparing the resistant line whole genome sequence against a parent line can be an effective way of target determination. Generation of *Pf* resistant lines typically follows one of two techniques: Treating a culture with compound at IC_{50} and incrementally increasing concentration until parasites are doubling every 48 hours under at 5-10 fold higher than IC_{50} concentrations;

A second method is to treat cultures with a very high concentration of compound ($3x IC_{90}$) and wait for these cultures to begin doubling every 48 hours. We began by limiting

dilution cloning to create clonal populations of Dd2 and then attempted to create resistant lines by incremental increasing of concentration and also by maintaining culture at $3 \times IC_{90}$ following a similar outline as recently published works ((McNamara, Lee et al. 2013))

Unfortunately after several attempts, neither method resulted in viable parasite lines. Recently, new methods of sequencing analysis have allowed groups to generate resistance lines without the required clonal populations (Sonoiki, Palencia et al. 2016). Starting with Dd2 cultures we were able to cultivate UCF 201 resistance lines using a combination of IC_{90} pulse treatments and incremental increasing of IC_{50} continuous culture treatments. Interestingly the initial IC_{50} cultures did not result in resistant parasite, but the IC_{90} pulse did on day 14 after initial treatment. Using this successful IC_{90} pulse culture we split off some culture and started treating at $1 \times IC_{50}$, this culture continued doubling every 48 hours. Cultures were split into three groups on day 22, $1 \times IC_{50}$, $2 \times IC_{50}$ and $3 \times IC_{50}$ treatment groups, all of which grew normally after a few days of treatment. The $3 \times IC_{50}$ treatment group was split and tested for EC_{50} determination and also maintained at $3 \times IC_{50}$ or increased to $5 \times IC_{50}$ on day 36. This $5 \times IC_{50}$ culture began doubling normally after 8 days of treatment. A culture was split and started at $6 \times IC_{50}$ on day 42 and has not shown any parasitemia up to day 60.

EC_{50} determination of Dd2 wt and $3 \times IC_{50}$ treated cultures revealed a decreased sensitivity to UCF 201 in the resistant line, requiring almost twice the compound concentration (355nM to 756nM). These results are shown below in Figure 27. Similar efforts were used to generate resistance against MSK-M03 and screening of MSK-M03 against a culture growing steadily under $3 \times IC_{50}$ compound pressure resulted in a shift

from 150nM to 535nM, nearly a 4-fold increase Figure 28. In effort to further clarify the target of UCF 501 and TPIMS 2291-SB1, we designed several rounds of experiments to generate resistant lines. To date we have been unsuccessful in any of these experiments regardless of methodology employed (IC_{50} incremental increase, IC_{50} or IC_{90} pulsing, or $3xIC_{50}$ constant pressure treatments), though current attempts are still underway.

These results are very promising, however, it is possible that this method will only reveal the mechanism of resistance (ex. increased expression/modulation of efflux pump). In these instances, and in those for which resistance generation cannot be obtained (UCF 501/2291-SB1), other target identification avenues must be pursued.

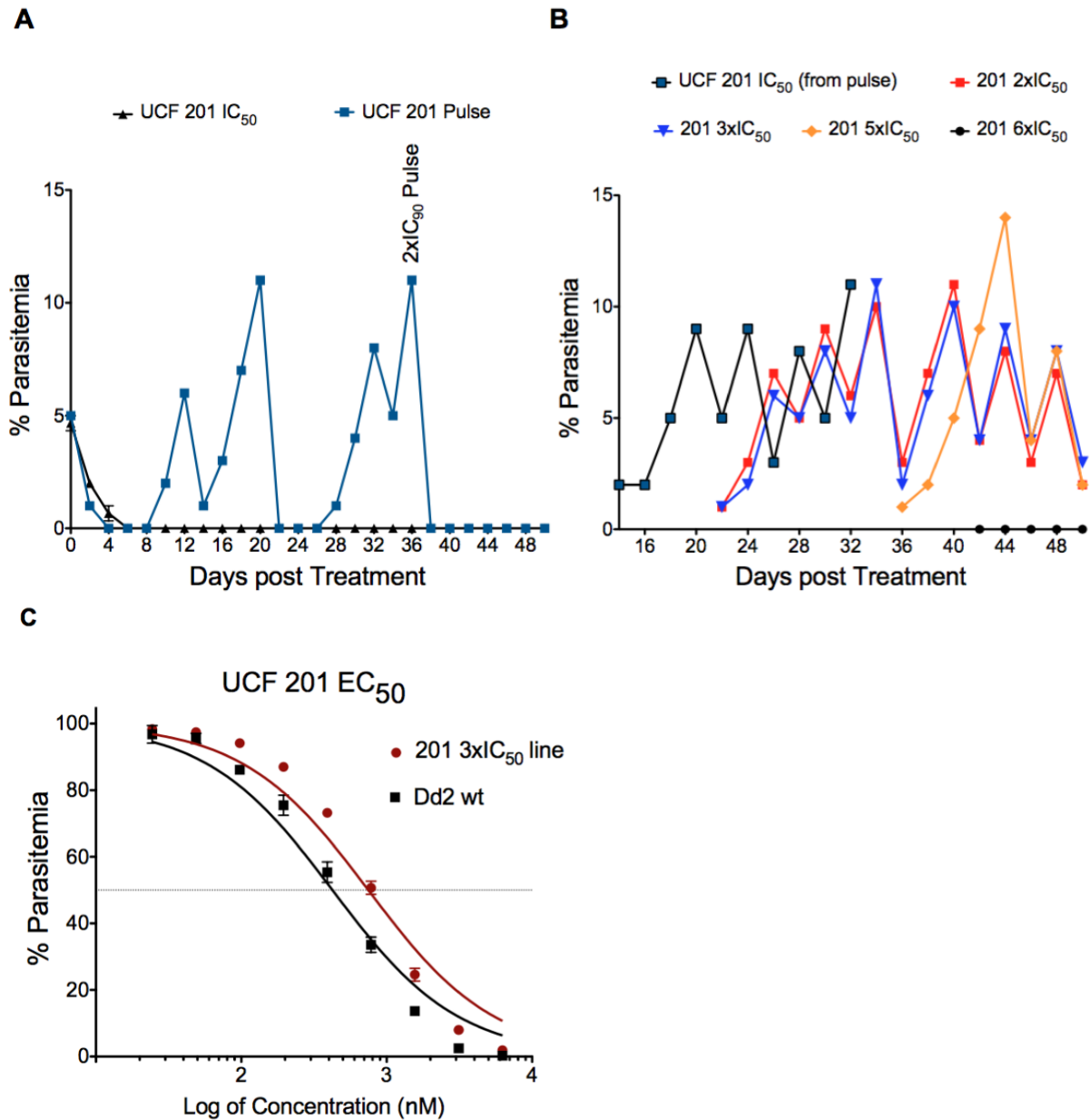


Figure 27 UCF 201 Resistance Lines and Activity.

A) Resistant lines were generated by IC_{90} pulse treatments or continuous IC_{50} culture treatment.
 B) Stably growing parasite cultures were subjected to increased concentrations of UCF 201. Once 3x IC_{50} cultures were steadily growing under compound pressure, repeat UCF 201 EC_{50} screening revealed almost a 2-fold shift in EC_{50} .

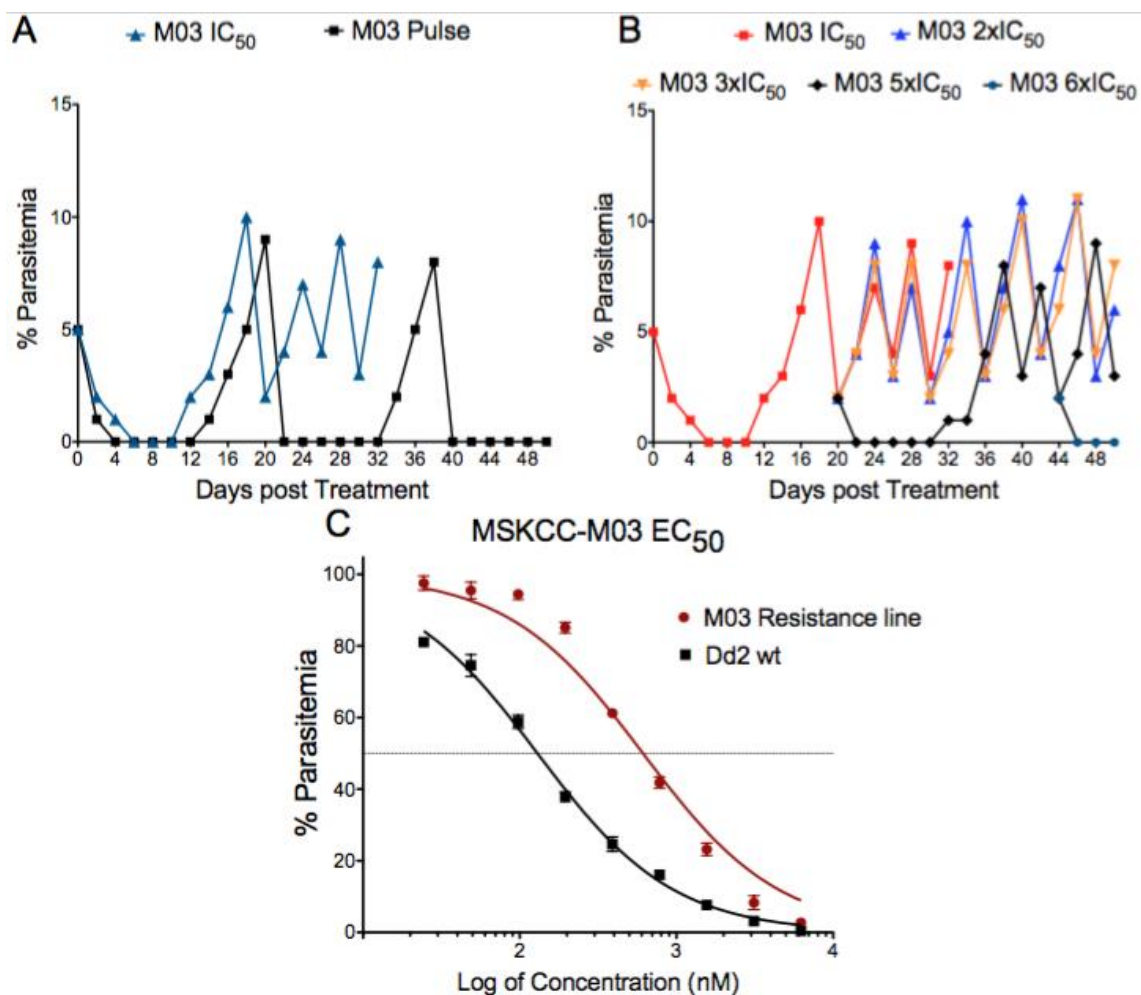


Figure 28 MSK-M03 Resistant Lines and Activity.

A) Resistant lines were generated by IC₉₀ pulse treatments or continuous IC₅₀ culture treatment.
 b) Stably growing parasite cultures were subjected to increased concentrations of MSK-M03. Once 3xIC₅₀ cultures were steadily growing under compound pressure, repeat MSK-M03 screening revealed almost a two-fold shift in EC₅₀.

Screening for Activity Against Targets Involved in Stage-Specific Interaction Profile

One of the benefits of running stage-specific interaction studies is that it can help narrow the field of possible targets. MSK-M03 for example inhibits some part of the merozoite egress signal cascade. As many of the kinases involved in this cascade are known, it could be possible to express those kinases and test for MSK-M03 activity. Two of the key regulatory kinases involved in egress are PKG and CDPK5 (Dvorin, Martyn et al. 2010) (Collins, Hackett et al. 2013). PKG is typically inactive, however if cGMP levels increase beyond minimal threshold levels (induced chemically or exogenously) PKG is then activated and will phosphorylate several downstream substrates. One effect of PKG activation is a rise in intracellular calcium. This calcium will stimulate the release of Sub1 and AMA1, which induce parasitophorous vacuole rupture. The influx of calcium may also stimulate CDPK5. CDPK5 will activate downstream effectors that trigger egress (Collins, Hackett et al. 2013). Recently PKG has also been shown to play a role in merozoite invasion as well (Alam, Solyakov et al. 2015).

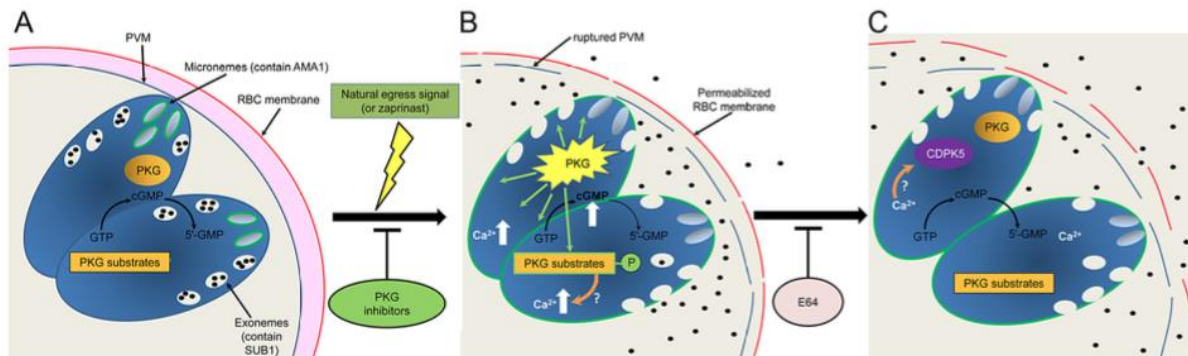


Figure 29 PfPKG and PfCDPK5 Activation Triggers Parasite Egress

Source: (Collins, Hackett et al. 2013)

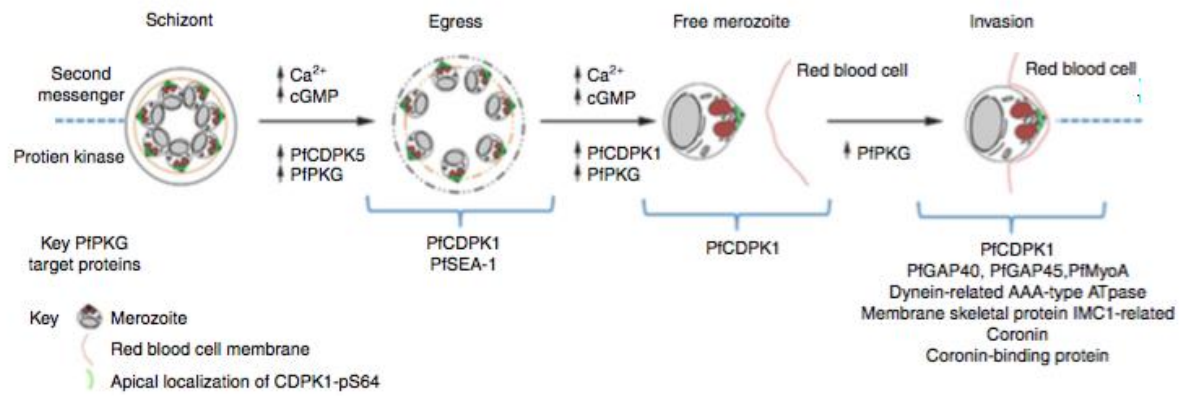


Figure 30 Plasmodium Egress and Invasion

Source: (Alam, Solyakov et al. 2015)

In effort to determine MSKCC-M03, UCF 201, or UCF 501's possible role in egress or invasion inhibition we began the process of expressing *PfCDPK5* and *PfPKG*. After designing primers, both *PfPKG* and *PfCDPK5* were PCR amplified using pfu Ultra II HS DNA polymerase (NEB). Confirmed amplifications were cut and cloned into pGex-6p-1 vector. XL-10 gold ultra-competent *E. coli* cells were transformed with either *PfPKG* or *PfCDPK5*, plated onto Ampicillin plates, and incubated overnight. *PfCDPK5* and *PfPKG* plates had many colonies the next morning and 14 colonies were selected from each for overnight culturing. Plasmids were isolated from overnight cultures using boiling miniprep or plasmid miniprep kit (Promega) and digested prior to running on 7% agarose gel with ethidium bromide. Many of the *PfCDPK5* samples contained inserts of appropriate size and these were sent off for sequencing (Figure 31). Unfortunately, none of the *PfPKG* samples had bands of appropriate sizes unfortunately. Upon a more fervent review of the literature, we found no history of success in expressing active full-length *PfPKG*. However, there was a case where a slightly truncated *PfPKG* was expressed and retained kinase activity (Deng and Baker 2002). Following this protocol we amplified the truncated *PfPKG* (*PKG₁*) and inserted amplified product into the PET 29B+ vector. Vector + insert was transformed into XL10 gold competent cells and plated on Kanamycin plates overnight. Growth colonies were screened for insert and 7 colonies were identified with inserts of the correct size (Figure 32). Sequencing was confirmed for both *PfCDPK5* (1 silent mutation) and later for *PfPKG* (100% sequenced). *PfCDPK5*-pGex-6p1 was transformed into Rosetta Blue DE3 cells and plated overnight. Growth colonies were then cultured overnight in 5mL tube that was used to inoculate a 250mL culture. Once OD₆₀₀ reached >400 Culture was induced with .1mM IPTG for 1

hour at 37C and then overnight at 20C. Induced cultures were collected the next morning, lysed by French press and sonication and frozen in MK buffer with 1x halt protease inhibitor. Samples were thawed and protein was purified by GST-affinity resin. We confirmed PfCDPK5 expression on a SDS PAGE protein gel (Figure 33). PfPKG expression is currently in progress.

After expression, these proteins will be screened for activity in a standard kinase luminescent assay. Upon activity confirmation we will commence screening of our egress and invasion inhibiting compounds like MSK-M03, UCF 201, and UCF 501.

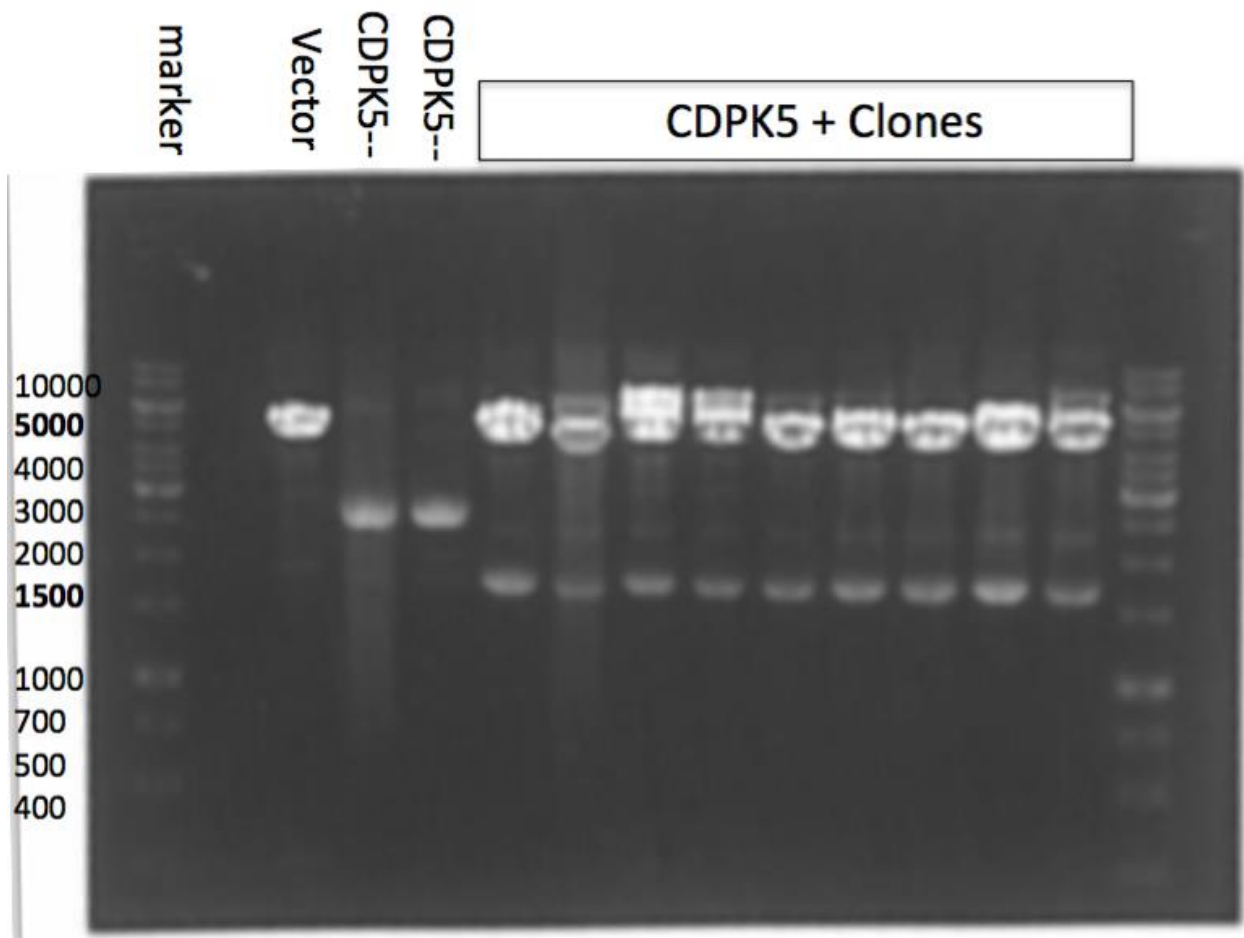


Figure 31 *Pf*CDPK5 Cloning

Plasmid DNA from pGex6pi-pfCDPK5 transformed XL-10 Gold colonies were screened for pfCDPK5 insert on 0.7% agarose gel. Track-it® 1KB ladder was used in marker lanes. PfCDPK5 is 1,707 bp. (Left to right) Vector is undigested pGex6pi. There are two lanes of plasmid DNA from colonies that did not contain PfCDPK5 followed by nine columns of colonies with plasmids containing PfCDPK5.

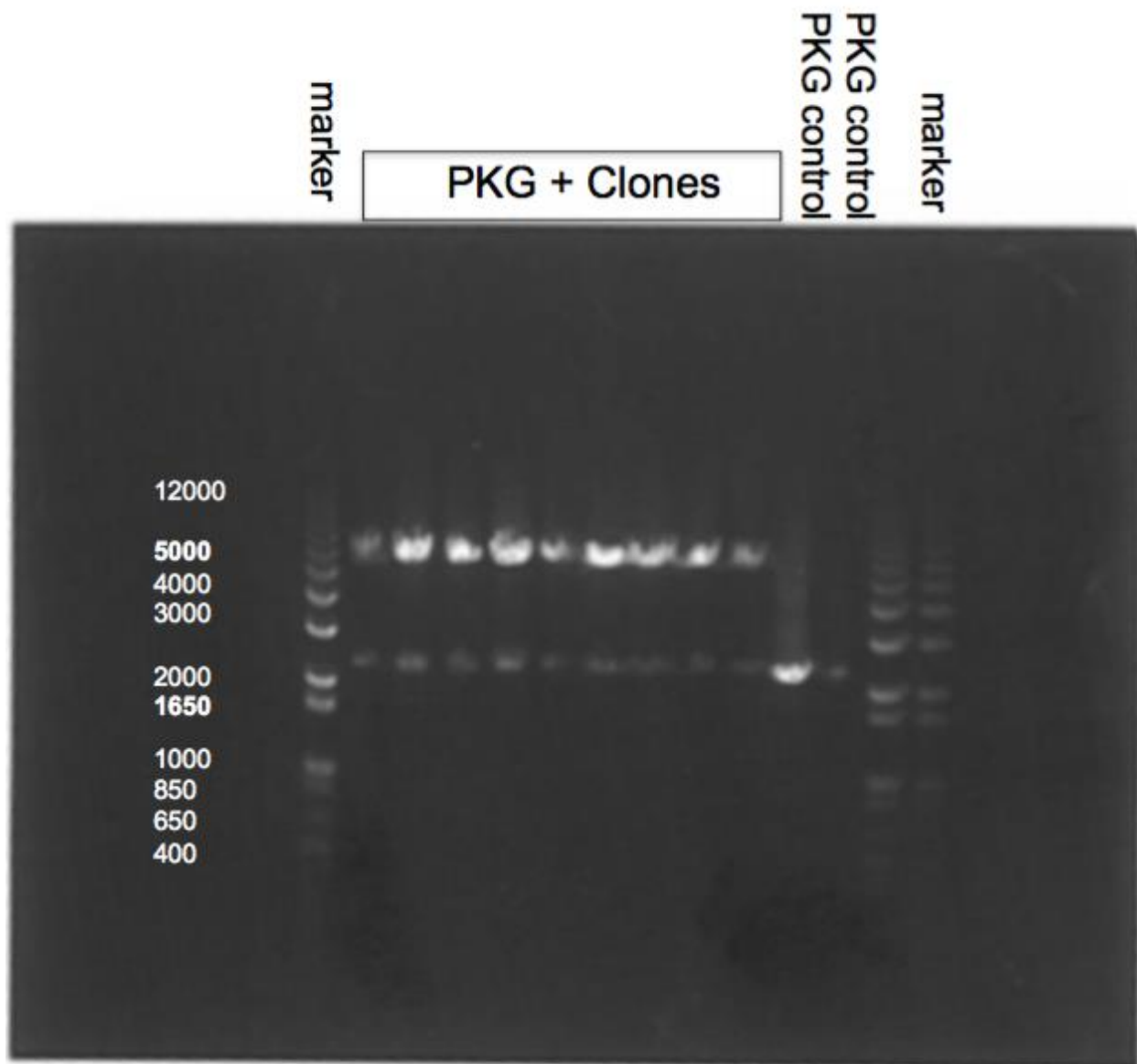


Figure 32 *PfPKG* Cloning

Plasmid DNA from pet29B+-*PfPKG* transformed XL-10 Gold colonies were screened for *PfPKG* insert on 0.7% agarose gel. Track-it® 1KB ladder was used in marker lanes. *PfPKG* is 2,282 bp. (Left to right) There are nine columns of colonies with *PfPKG* containing plasmids followed by two columns of *PfPKG* alone (PCR product).

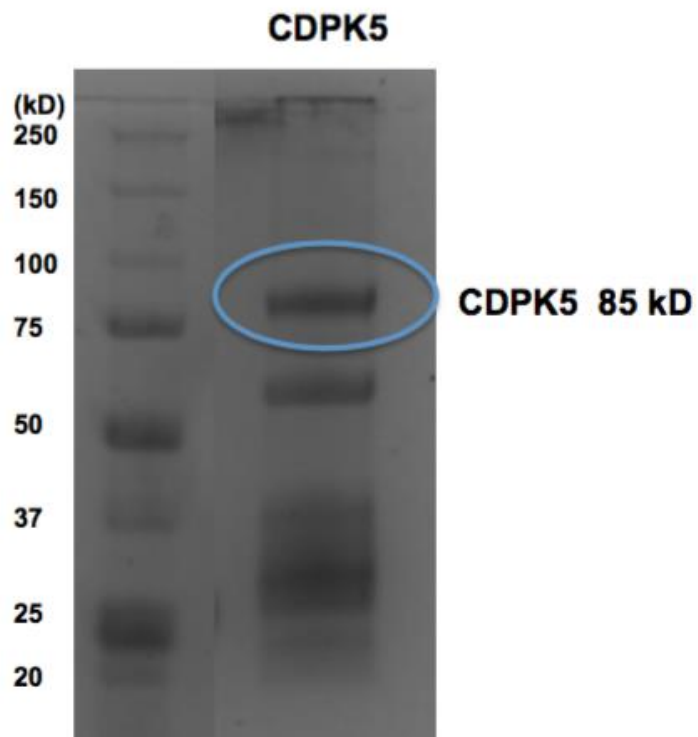


Figure 33 PfCDPK5 Expression

Expression of pGex6pi-PfCDPK5 from transformed Rosetta cells that were induced overnight at 18°C at 0.1mM IPTG. Lysates were run on SDS-PAGE gel.

Affinity Pull-Down

A third option for target identification not discussed in the previous section includes photo probe or affinity labeling. This is done through chemical modification and coupling of compounds through click-chemistry and can be used for covalent and non-covalent binding compounds (Leslie and Hergenrother 2008) and can be used for target validation as well. Labeled compounds can be used in pull-down assays similar to co-immunoprecipitation or these labeled compounds can also be used as probes in cellular lysate drug western assays.

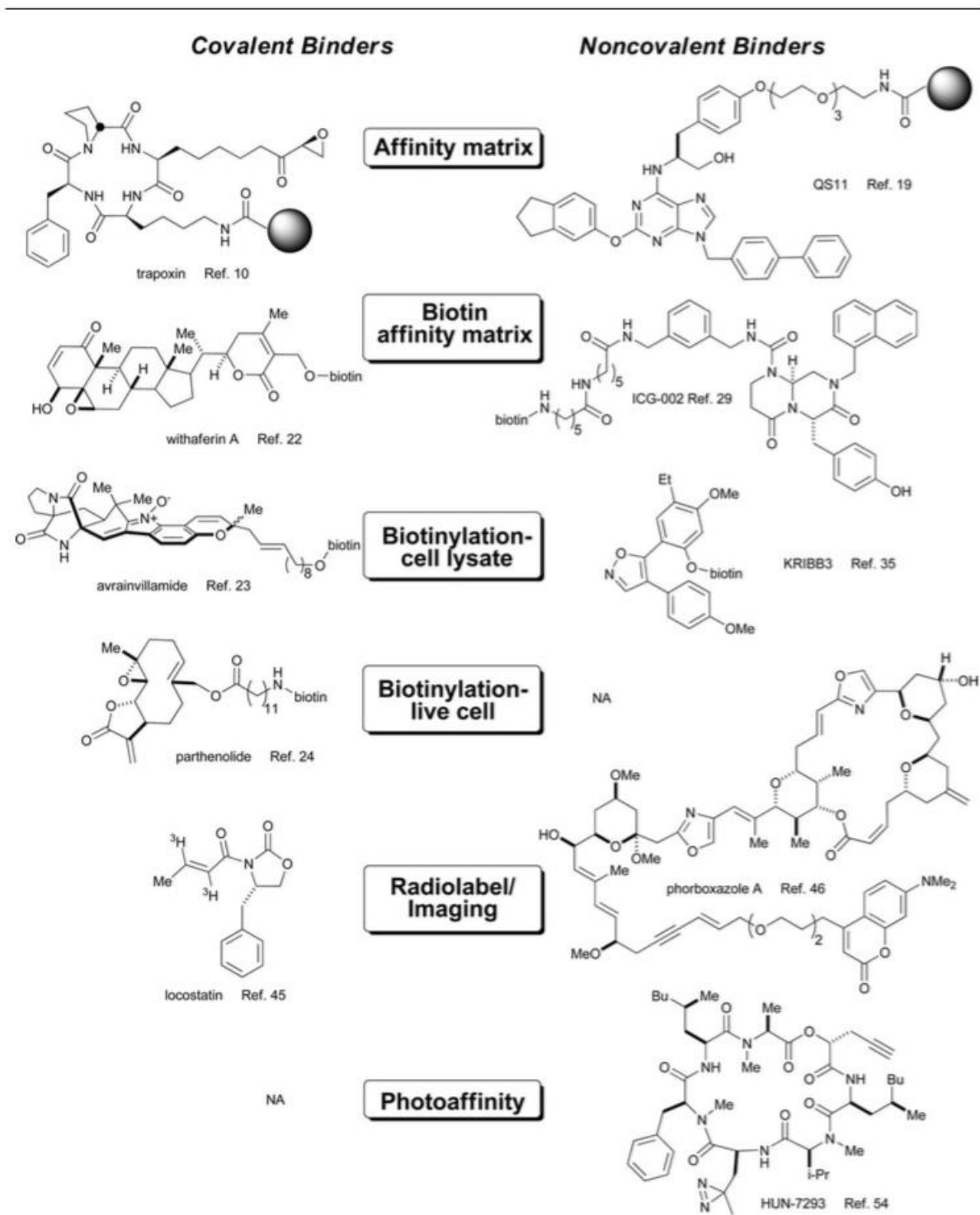


Figure 34 Affinity Probe Labeling Strategies for Target Identification

Source: (Leslie and Hergenrother 2008)

Creating the labeled compounds requires intensive chemistry that is beyond my expertise however we are exploring options for affinity labeling at MSKCC for M03.

Given that we do not know the exact nature of how any of these hit compounds are interacting with their respective target (covalently or non-covalently) our labeling strategies should focus primarily on on affinity matrix probes.

For the affinity matrix design it is most common to link your compound to an agarose or sepharose resin. These resins come with reactive functional groups (amines, thiols or carboxylic acids) that can be activated and react with amino or hydroxyl groups on the compound of interest. The point of this attachment must reside in a region that does not interact (or sterically hinder interaction) with the target substrate. Therein lies the rub, how can we determine where to establish the resin link if we do not know the compound/target interaction site? Our best approach could be to draw conclusions from the structure-activity relationship profiles for individual compounds and identify regions of minimal or no effective change on the compounds efficacy. It stands to reason that if chemical modifications have minimal impact on activity that these same sites could tolerate a linking site. Compound can also be tethered to the resin via a polyethylene glycol tail, rather than directly bound. This diminishes the potential for steric hindrance as it allows the compound to more freely interact with cellular lysate proteins.

With these points in mind we can propose a course of action to link our compounds to a resin at a site of minimal impact as shown in Figure 35.

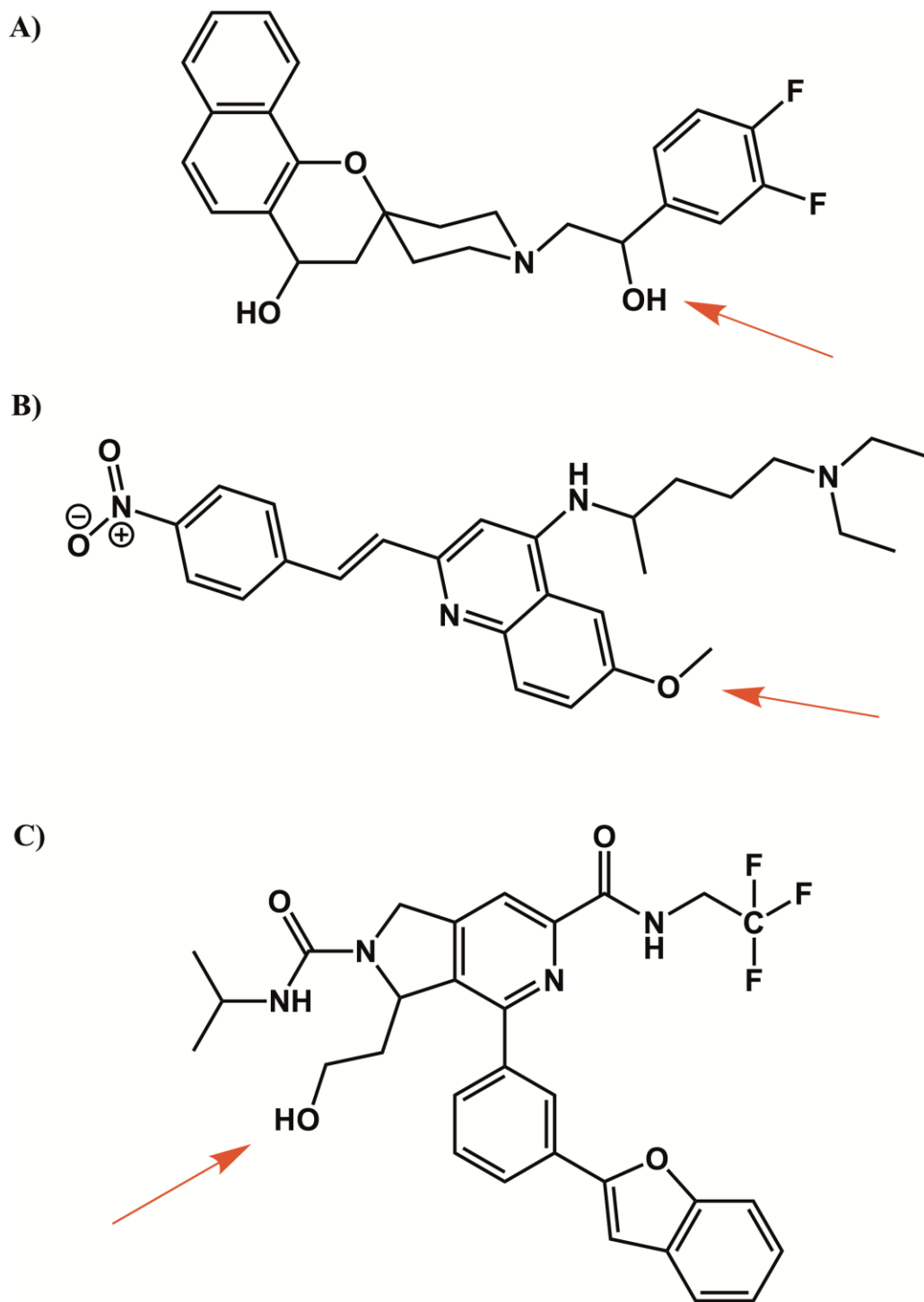


Figure 35 Likely Tolerable Affinity Probe Linker Site

Proposed linker site for affinity probe attachment based on SAR profiles for the three scaffolds UCF-201 (A), UCF-501 (B), and MSK-M03 (C).

It is expected from review of the SAR profiling that these proposed linkage sites will not interfere with these hit compounds and their targets. Interacting targets identified through an affinity pull-down assay. Our collaborator at MSKCC has recently hired a post-doc that will primarily focus on probe/affinity labeling MSK-M03. Improving and outfitting UCF 501 and UCF 201 scaffolds for affinity probe labeling will commence shortly by our collaborator Dr. Yu Yuan at UCF.

CHAPTER 8: DISCUSSION

With over half of the global population at risk of malaria infection each year it is critical that viable prophylactic and therapeutic treatment options are in place. For the past decade the constant threat of infection was held at bay through large-scale distribution of insecticide treated bed nets and Artemisinin combination therapies (ACTs). The expiration of these bed nets, and the increasing prevalence of drug resistance against all known antimalarial drugs, including artemisinin resistance, underscores the desperate situation we now find ourselves in. Typically, the call for new therapeutics has been answered by natural products as these chemicals are inherently pre-validated by nature to be bioactive (Rodrigues, Reker et al. 2016). However, access to the chemical sources and synthetic challenges for wide-scale distribution can limit the impact of natural products. This has led to a rise in synthetic chemical library screening. While this option circumvents and potential synthetic challenges, the limited chemical diversity of these libraries often leads to low total hit rates and frequent hit redundancy.

The Search for New Libraries

In this study using the Harbor Branch Oceanographic Institute's peak fraction library we identified thirteen novel potent and selective natural product antiplasmodial hits. These hits source from several different species of sponge, coral, mollusk, and algae and

include early acting ring inhibiting compounds like Palmonine A, Tetillapyrone, and Malemide-5-oxime. We also identified Bebryce cembranoid compounds which inhibit merozoite egress. The most potent of these compounds is a cyclic peptide microsclerdermin A isolated from marine sponge *Amphibleptula*. Microsclerdermin has been shown to exhibit antifungal and antiproliferative activities against pancreatic cancer cells through nuclear factor kappa B (NFkB) inhibition (Guzman, Maers et al. 2015). Prior to this study no antiplasmodial has not been reported for Microsclerdermin A. Another potent compound isolated from Spongiidae with no prior record of antiplasmodial activity is nitenin. Both microsclerdermin and nitenin demonstrated a selective index of >50 and block during ring to trophozoite transition suggesting their utility as a novel scaffold to develop next generation of malaria therapy.

Although structural scaffolds identified through our screen of HBOI peak fraction library are interesting and unique, we, along with HBOI, encountered issues with synthetically tractability. Therefore, we focused our attention on more synthetically tractable commercial libraries. However, these libraries, due to scaffold redundancy and limited chemical diversity, typically provide miniscule return on investment, providing hit rates <0.1%. Recent screening efforts of GlaxoSmithKline and Novartis libraries identified a only a few hundred antiplasmodial scaffolds from over 3.5 million compounds, and within their hits were rediscovered almost all known antimalarial scaffolds (Gamo, Sanz et al. 2010) (Guiguemde, Shelat et al. 2010). Clearly, this lack of chemical diversity leads to antiplasmodial scaffold redundancy.

Fortunately, recent efforts have sought to improve the chemical diversity of these synthetic libraries through generation of natural product-based or natural product inspired synthetic compounds libraries. Three of these improved libraries were selected in this study. Derek Tan's diversity oriented synthesis (DOS) alkaloid library from MSKCC, TPIMS positional scanning library, and Asinex BioDesign library all combine natural product substructures or natural product privilege elements into their synthetic schemes. Dr. Tan's alkaloid library was highlighted for its expansion of synthetic libraries into novel regions of chemical space (Moura-Letts, Diblasi et al. 2011). Figure 36 depicts a principal component analysis used to compare 20 different physicochemical descriptors of natural products, well characterized synthetic libraries (Chembridge, Chemdiv, etc), and natural product-based DOS alkaloids. This exemplifies the potential of natural product inspired libraries and their unique ability to incorporate larger regions of bioactive chemical space than typical synthetic libraries. From the increased chemical diversity within these libraries we were able to identify several potent antiplasmodial compounds that have cellular mechanisms of action distinct from known antimalarials. It is therefore likely that they will have novel molecular targets.

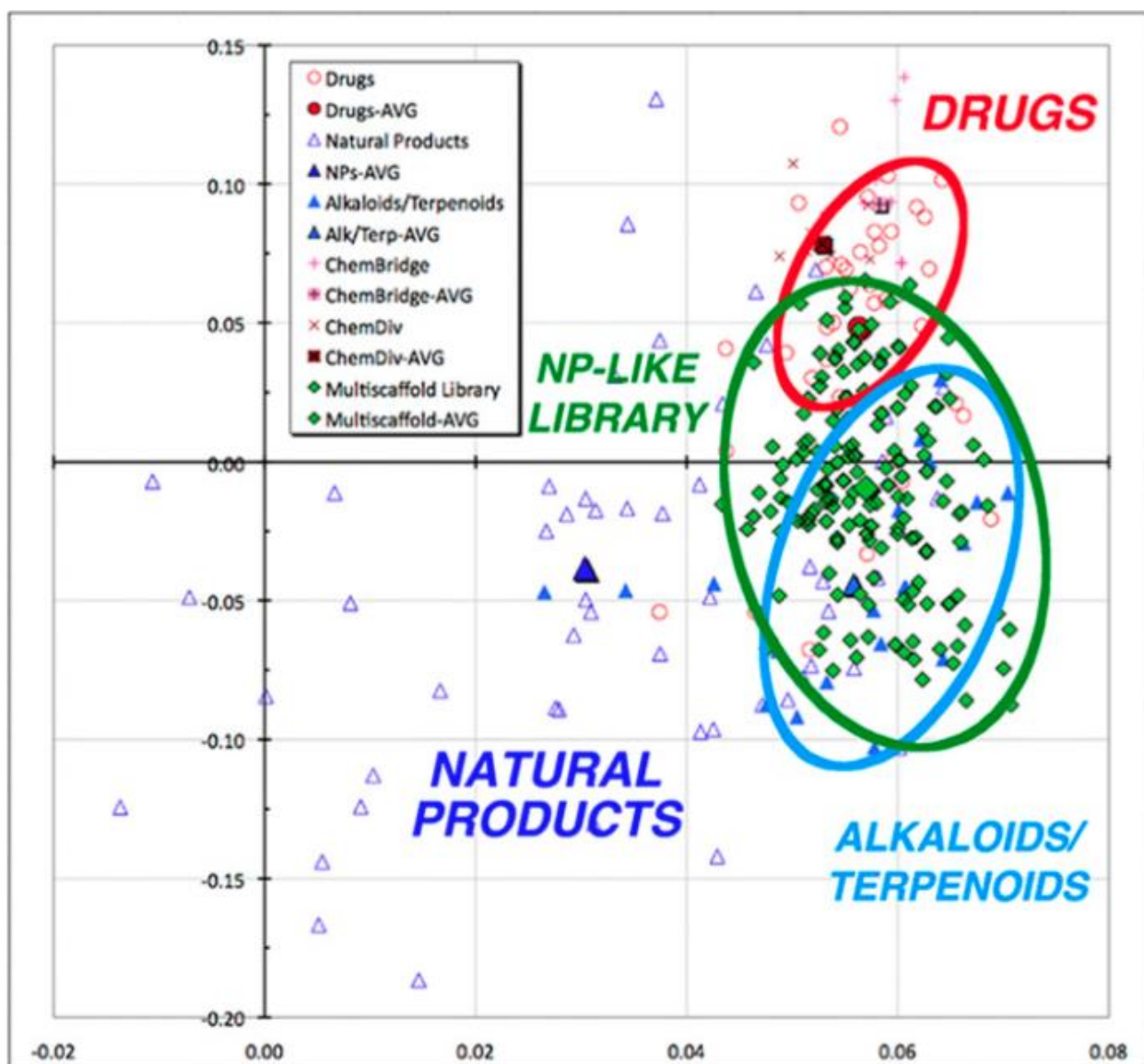


Figure 36 Natural Product-Based Synthetic Libraries Occupy Unique Regions of Chemical Space

Principal component analysis of 20 structural and physicochemical descriptors of the 40 top-selling drugs (red circles), 60 diverse natural products (open blue triangles), 20 polycyclic alkaloids and terpenoids (filled blue triangles), 20 ChemBridge and ChemDiv library members (crosses), and 190 multi-scaffold library members (green diamonds).

Source: (Moura-Letts, Diblasi et al. 2011)

Characteristics of Our Novel Antiplasmodial Hits

In screening these enriched libraries we have identified three antiplasmodial scaffolds that have nanomolar potency and excellent selectivity. In addition to this, these compounds also demonstrate *in vivo* efficacy, delaying parasitemia terminal growth for 24 hours (MSK-M03), 72 hours (2291-SB1), up to 6 days (UCF 201), or indefinitely, as a fully curative agent (UCF 501). Most exciting is the unique cellular mechanisms of action of MSK-M03, UCF 201, and UCF 501.

MSK-M03

The inhibition of merozoite egress that is seen with addition of MSK-M03 suggests a new mechanism of action for this antimalarial compounds. And while the resistance line generation is currently underway for MSK-M03 we are also exploring target identification through screening MSK-M03 activity against known regulators of merozoite egress. Egress is a complicated and carefully executed process in which individual merozoites are released from the red blood cell. This first requires a rupturing of the plasmodial membrane, followed by destruction of the red blood cell membrane. The coordinated rupturing of these two membranes is not fully understood however it is clear that an increase in cyclic GMP levels will lead to activation of PfPKG. Activated PfPKG will then phosphorylate downstream substrates leading to an increase in cytosolic Ca^{2+} (Collins, Hackett et al. 2013). This calcium flux will activate a subtilisin-like serine protease called Sub1 and PfCDPK5. SUB1 migrates to the parasite membrane and induces membrane rupture and further activates papain-like proteases called SERA (Blackman 2008). PfCDPK5 will then pursue a role in egress leading to rupture of the

RBC membrane after maturation of active merozoites. While the exact role of SERA proteins in egress (and possibly invasion) is still under intense debate and investigation (Blackman 2008).

The phenotypic inhibition of egress seen in MSK-M03 appears similar to both the E-64 induced egress inhibition ((Salmon, Oksman et al. 2001)) and “compound 1” induced egress inhibition through deactivation of PKG ((Collins, Hackett et al. 2013)). Future studies will therefore evaluate the effect MSK-M03 has on PfPKG and PfCDPK5. It has not escaped our attention that MSK – M03 could be inhibiting egress at or downstream of PfCDPK5 activation but prior to proteolysis of the RBC membrane. This would result in fully active merozoites that are stuck within the RBC membrane. The already high osmotic fragility of RBC membrane will likely be increased by the multitude of *Plasmodium* induced membrane modifications that occur during the progressing parasite lifecycle. Any mechanical disruption of the RBC membrane *in vivo* through sheering or external pressure within the mouse heart or circulatory system would result in release of active free merozoites that would invade nearby red blood cells and lead to a reinvasion event despite MSK-M03 treatment. This would then explain the poor protection seen in the rodent malaria model.

It is also plausible that the low protective effect of MSK-M03 is possibly due to cleavage of the compound by elevated esterase levels in mouse serum compared to human. If this is the case it suggests that the rodent malarial model is a poor model for MSK-M03's antiplasmodial activity. Since the human serum stability is significantly higher ($T_{1/2} > 2$ hours) it may be a better fit to have MSK-M03 *in vivo* efficacy screened against *P. falciparum* infected humanized mice We are currently in discussion with a

collaborating facility specializing in humanized mouse malaria studies for this purpose. These humanized mice are infected with *P. falciparum* and it is expected that MSK-M03 treatment using these humanized mouse models will better correlate the *in vitro* activity of MSK-M03.

Of significant interest to us is the apparent protective effect of the MSK-M03 analog, MSK-O08, at 100mg/kg ip in the rodent malarial model. After the initial two doses there was some adverse reaction in two of the mice causing us to terminate treatment for the entire group after two doses. However, the remaining three mice had decreased parasitemia levels and delayed parasitemia terminal growth for seven days. When comparing the two structures, MSK-O08 has a t-butyl sulfonyl substitution at the pyrrolo(3,4-B)pyridine 4-N atom and a pyridine substitution instead of the benzofuran substituent of MSK-M03. How these substitutions interact with the antiplasmodial molecular targets is under study, there is some evidence suggesting MSK – O08 and MSK – M03 could have distinct molecular targets. An assay is currently planned to determine if the protective effect seen *in vivo* is present when given a lower, more tolerable dose of 50mg/kg ip. Further scaffolding substitutions of MSK-M03 will also evaluate the necessity of the ethyl ester in hopes of circumventing the current lack of activity we are seeing in our standard rodent model.

UCF 201/UCF 501

A second natural product inspired library is the Asinex BioDesign library. This library combines natural product-based substructural moieties (Biocores) into synthetically tractable compounds. Filtering the BioDesign library for compounds enriched with saturated rings and removing any compounds containing peroxide bridges we were able to identify the novel antiplasmodial scaffolds UCF 201 and UCF 501.

Both UCF 201 and UCF 501 act on all stages in the intraerythrocytic life cycle. This presents an interesting task in determining the targets of these two compounds. While some level of resistance is developing for UCF 201, UCF 501 is behaving as most fast-acting antiplasmodial compounds do in showing a “resistance-proof” phenotype. While the inability for *P. falciparum* to acquire resistance *in vitro* is promising, *in vitro* resistant cultures are tested against 10^9 parasites and malarial infections can often reach 10^{19} parasites within the infected human host. And it must be admitted that this elevated number of parasites may allow for resistant mutants to arise under UCF 501 treatment. Throughout our study to identify the target of UCF 201 and UCF 501 we have primarily focused on protein targets, specifically on constitutively active proteins that also play a role in activated merozoite development or invasion. Plans to determine their effect on PfPKG (a known regulator of invasion) are already in motion. However it is possible that the targets of these compounds are not protein at all. There is some evidence that styryl compounds induce cell-cycle arrest, by decreasing cyclin expression levels ((Prasad, Park et al. 2009)), apoptosis, through induction of the release of cytochrome c ((Prasad, Park et al. 2009) & ((Mrozek-Wilczkiewicz, Spaczynska et al. 2015)))

and possibly through direct mitochondrial DNA intercalation ((Mrozek-Wilczkiewicz, Spaczynska et al. 2015)). Another possibility is that these compounds block critical nutrient transporters (glucose, sorbitol, etc.) and Styryl compounds like RH 421, have been used as fluorescent dyes to investigate membrane channels ((Clarke, Zouni et al. 1995)) or interact with membrane permeability ((Sivakumar, Wang et al. 2014)). Blocking of these membrane transporters could explain rapid inhibition of intracellular development at any stage after the compound was administered. It is possible, in the case of UCF 501 that cellular localization could be observed directly in the microscope due to the inherent fluorescent nature of the compound. However, this has not been observed in this study. This may be due to a quenching of fluorescent signaling or possible dissociation of the styryl group from the molecule post binding.

Breaking the Failing Paradigm of Current Antimalarials

With resistance to all known antimalarials emerging or widespread, the need for new chemical scaffolds with early-acting potential and novel mechanism of action is of the utmost importance. In this environment even a fully curative effect is insufficient. These next generation antimalarials need to expand beyond the current targeting limitations of electron transport chain, the digestive vacuole, or the apicoplast. There needs to be a greater diversity of targets, even more than the ATPase, mitochondrial chain and PI4K inhibitors which dominate the current antimalarial pipeline (Burrows, Duparc et al. 2017). The compounds identified from these libraries interact and block intraerythrocytic progression in unique patterns. This underscores the significance of the early acting ring activity of UCF 201 and UCF 501. It is noteworthy that both UCF 201 block at every

stage, including merozoite invasion (a yet unseen mechanism of antimalarial drugs) and promote these compounds as useful treatment candidates for acute infections that require rapid parasite clearance. The early acting ring activity of both of these is also of significance due to the fact that latent ring stage activity has been linked to *in vitro* resistance development of dihydroartemunate (Teuscher, Gatton et al. 2010) (Hoshen, Na-Bangchang et al. 2000). MSK-M03 blocks egress (also novel among current antimalarial drugs) and it remains to be seen if this is targeting known kinases (PfPKG/PfCDPK5) or if M03 is acting on some new molecular target. As aforementioned, true next generation antimalarial compounds will also need to demonstrate transmission blocking potential if global malaria eradication is ever to be achieved. Such activity is demonstrated for 2291-SB1 and UCF 501.

It is clear that the results described in this dissertation have identified previously unidentified antiplasmodial chemotypes with novel cellular action. Now the major challenge would be to improve both potency and pharmacological properties through iterative SAR and SPR studies. Identification of molecular target undoubtedly would help in improved inhibitor design.

Known Target Necessity

While these aforementioned studies are focused on determining the molecular target of the hits identified in this study, it is important to note that the lead optimization and further movement of these scaffolds down the antimalarial drug discovery pipeline can, and indeed should, run in parallel with these target identification studies. In the

antimalarial field, while a defined target will surely aid in lead optimization, the main criteria for lead optimization is *in vivo* activity/selectivity. In fact, the most successful antimalarial drugs, Chloroquine and Artemisinin, have been in clinical use for decades and only recently are studies beginning to tease out their molecular targets. It is therefore evident that even in the absence of a definitive target we can establish these pharmacophores as novel antimalarials, with unique cellular mechanisms of action.

REFERENCES

Alam, M. M., L. Solyakov, A. R. Bottrill, C. Flueck, F. A. Siddiqui, S. Singh, S. Mistry, M. Viskaduraki, K. Lee, C. S. Hopp, C. E. Chitnis, C. Doerig, R. W. Moon, J. L. Green, A. A. Holder, D. A. Baker and A. B. Tobin (2015). "Phosphoproteomics reveals malaria parasite Protein Kinase G as a signalling hub regulating egress and invasion." Nat Commun 6: 7285.

Alvarado, S., B. F. Roberts, A. E. Wright and D. Chakrabarti (2013). "The bis(indolyl)imidazole alkaloid nortopsentin exhibits antiplasmodial activity." Antimicrob Agents Chemother 57(5): 2362-2364.

Avdeef, A., M. Strafford, E. Block, M. P. Balogh, W. Chambliss and I. Khan (2001). "Drug absorption in vitro model: filter-immobilized artificial membranes. 2. Studies of the permeability properties of lactones in Piper methysticum Forst." Eur J Pharm Sci 14(4): 271-280.

Baggish, A. L. and D. R. Hill (2002). "Antiparasitic agent atovaquone." Antimicrob Agents Chemother 46(5): 1163-1173.

Blackman, M. J. (2008). "Malarial proteases and host cell egress: an 'emerging' cascade." Cell Microbiol 10(10): 1925-1934.

Bradley, J., A. Ogouyemi-Hounto, S. Cornelie, J. Fassinou, Y. S. S. de Tove, A. A. Adeothy, F. T. Tokponnon, P. Makoutode, A. Adechoubou, T. Legba, T. Houansou, D. Kinde-Gazard, M. C. Akogbeto, A. Massougboji, T. B. Knox, M. Donnelly and I. Kleinschmidt (2017). "Insecticide-treated nets provide protection against malaria to children in an area of insecticide resistance in Southern Benin." Malar J 16(1): 225.

Bullock, T. and W. Bagley (1997). The pioneer camp of the saints : the 1846 and 1847 Mormon trail journals of Thomas Bullock. Spokane, Wash., A.H. Clark Co.

Burkhard, P. and D. E. Lanar (2015). "Malaria vaccine based on self-assembling protein nanoparticles." Expert review of vaccines 14(12): 1525-1527.

Burrows, J. N., S. Duparc, W. E. Gutteridge, R. Hooft van Huijsduijnen, W. Kaszubska, F. Macintyre, S. Mazzuri, J. J. Mohrle and T. N. C. Wells (2017). "New developments in anti-malarial target candidate and product profiles." Malar J 16(1): 26.

Carter, R. and K. N. Mendis (2002). "Evolutionary and historical aspects of the burden of malaria." Clin Microbiol Rev 15(4): 564-594.

CDC. (2015, 10/07/12015). "Disease." Malaria: About Malaria Retrieved 5/25/2017, 2017, from <https://www.cdc.gov/malaria/about/disease.html>.

CDC. (2016, 03/11/2016). "The History of Malaria, an Ancient Disease." Malaria- About Malaria Retrieved 05/27/17, 2017, from [https://www.cdc.gov/malaria/about/history/ -mcwa](https://www.cdc.gov/malaria/about/history/-mcwa).

Celli, A. and A. Celli (1933). The history of malaria in the Roman Campagna from ancient times. London,, Bale & Danielsson.

Clarke, R. J., A. Zouni and J. F. Holzwarth (1995). "Voltage sensitivity of the fluorescent probe RH421 in a model membrane system." Biophys J 68(4): 1406-1415.

Collins, C. R., F. Hackett, M. Strath, M. Penzo, C. Withers-Martinez, D. A. Baker and M. J. Blackman (2013). "Malaria parasite cGMP-dependent protein kinase regulates blood stage merozoite secretory organelle discharge and egress." PLoS Pathog 9(5): e1003344.

Cordier, C., D. Morton, S. Murrison, A. Nelson and C. O'Leary-Steele (2008). "Natural products as an inspiration in the diversity-oriented synthesis of bioactive compound libraries." Nat Prod Rep 25(4): 719-737.

Dahl, E. L. and P. J. Rosenthal (2007). "Multiple antibiotics exert delayed effects against the Plasmodium falciparum apicoplast." Antimicrob Agents Chemother 51(10): 3485-3490.

Deng, W. and D. A. Baker (2002). "A novel cyclic GMP-dependent protein kinase is expressed in the ring stage of the Plasmodium falciparum life cycle." Mol Microbiol 44(5): 1141-1151.

Dvorin, J. D., D. C. Martyn, S. D. Patel, J. S. Grimley, C. R. Collins, C. S. Hopp, A. T. Bright, S. Westenberger, E. Winzeler, M. J. Blackman, D. A. Baker, T. J. Wandless and M. T. Duraisingh (2010). "A plant-like kinase in Plasmodium falciparum regulates parasite egress from erythrocytes." Science 328(5980): 910-912.

Famin, O. and H. Ginsburg (2002). "Differential effects of 4-aminoquinoline-containing antimalarial drugs on hemoglobin digestion in Plasmodium falciparum-infected erythrocytes." Biochem Pharmacol 63(3): 393-398.

Gamo, F. J., L. M. Sanz, J. Vidal, C. de Cozar, E. Alvarez, J. L. Lavandera, D. E. Vanderwall, D. V. Green, V. Kumar, S. Hasan, J. R. Brown, C. E. Peishoff, L. R. Cardon and J. F. Garcia-Bustos (2010). "Thousands of chemical starting points for antimalarial lead identification." Nature 465(7296): 305-310.

Guiguemde, W. A., A. A. Shelat, D. Bouck, S. Duffy, G. J. Crowther, P. H. Davis, D. C. Smithson, M. Connelly, J. Clark, F. Zhu, M. B. Jimenez-Diaz, M. S. Martinez, E. B. Wilson, A. K. Tripathi, J. Gut, E. R. Sharlow, I. Bathurst, F. El Mazouni, J. W. Fowble, I. Forquer, P. L. McGinley, S. Castro, I. Angulo-Barturen, S. Ferrer, P. J. Rosenthal, J. L. Derisi, D. J. Sullivan, J. S. Lazo, D. S. Roos, M. K. Riscoe, M. A. Phillips, P. K. Rathod, W. C. Van Voorhis, V. M. Avery and R. K. Guy (2010). "Chemical genetics of Plasmodium falciparum." Nature 465(7296): 311-315.

Gutierrez, M., C. Theoduloz, J. Rodriguez, M. Lolas and G. Schmeda-Hirschmann (2005). "Bioactive metabolites from the fungus Nectria galligena, the main apple canker agent in Chile." J Agric Food Chem 53(20): 7701-7708.

Guzman, E. A., K. Maers, J. Roberts, H. V. Kemami-Wangun, D. Harmody and A. E. Wright (2015). "The marine natural product microsclerodermin A is a novel inhibitor of the nuclear factor kappa B and induces apoptosis in pancreatic cancer cells." Invest New Drugs 33(1): 86-94.

Hawass, Z., Y. Z. Gad, S. Ismail, R. Khairat, D. Fathalla, N. Hasan, A. Ahmed, H. Elleithy, M. Ball, F. Gaballah, S. Wasef, M. Fateen, H. Amer, P. Gostner, A. Selim, A. Zink and C. M. Pusch (2010). "Ancestry and pathology in King Tutankhamun's family." JAMA 303(7): 638-647.

Hoshen, M. B., K. Na-Bangchang, W. D. Stein and H. Ginsburg (2000). "Mathematical modelling of the chemotherapy of Plasmodium falciparum malaria with artesunate: postulation of 'dormancy', a partial cytostatic effect of the drug, and its implication for treatment regimens." Parasitology 121 (Pt 3): 237-246.

Ishizuka, A. S., K. E. Lyke, A. DeZure, A. A. Berry, T. L. Richie, F. H. Mendoza, M. E. Enama, I. J. Gordon, L.-J. Chang, U. N. Sarwar, K. L. Zephir, L. A. Holman, E. R. James, P. F. Billingsley, A. Gunasekera, S. Chakravarty, A. Manoj, M. Li, A. J. Ruben, T. Li, A. G. Eappen, R. E. Stafford, N. K C, T. Murshedkar, H. DeCederfelt, S. H.

Plummer, C. S. Hendel, L. Novik, P. J. M. Costner, J. G. Saunders, M. B. Laurens, C. V. Plowe, B. Flynn, W. R. Whalen, J. P. Todd, J. Noor, S. Rao, K. Sierra-Davidson, G. M. Lynn, J. E. Epstein, M. A. Kemp, G. A. Fahle, S. A. Mikolajczak, M. Fishbaugher, B. K. Sack, S. H. I. Kappe, S. A. Davidson, L. S. Garver, N. K. Bjorkstrom, M. C. Nason, B. S. Graham, M. Roederer, B. K. L. Sim, S. L. Hoffman, J. E. Ledgerwood and R. A. Seder (2016). "Protection against malaria at 1 year and immune correlates following PfSPZ vaccination." Nature medicine 22(6): 614-623.

Jamet, H. P. (2016). "Insecticide Treated Bednets for Malarial Control." Outlooks on Pest Management 27(3): 5.

Janiszewski, J. S., K. J. Rogers, K. M. Whalen, M. J. Cole, T. E. Liston, E. Duchoslav and H. G. Fouda (2001). "A high-capacity LC/MS system for the bioanalysis of samples generated from plate-based metabolic screening." Anal Chem 73(7): 1495-1501.

Jones, W. H. S. and E. T. Withington (1909). Malaria and Greek history. Manchester,, The University press.

Kansy, M., F. Senner and K. Gubernator (1998). "Physicochemical high throughput screening: parallel artificial membrane permeation assay in the description of passive absorption processes." J Med Chem 41(7): 1007-1010.

Kombarov, R., A. Altieri, D. Genis, M. Kirpichenok, V. Kochubey, N. Rakitina and Z. Titarenko (2010). "BioCores: identification of a drug/natural product-based privileged structural motif for small-molecule lead discovery." Mol Divers 14(1): 193-200.

Konig, G. M., A. D. Wright and A. Linden (1998). "Antiplasmodial and cytotoxic metabolites from the Maltese sponge *Agelas oroides*." Planta Med 64(5): 443-447.

Leslie, B. J. and P. J. Hergenrother (2008). "Identification of the cellular targets of bioactive small organic molecules using affinity reagents." Chem Soc Rev 37(7): 1347-1360.

McNamara, C. W., M. C. Lee, C. S. Lim, S. H. Lim, J. Roland, A. Nagle, O. Simon, B. K. Yeung, A. K. Chatterjee, S. L. McCormack, M. J. Manary, A. M. Zeeman, K. J. Dechering, T. R. Kumar, P. P. Henrich, K. Gagaring, M. Ibanez, N. Kato, K. L. Kuhen, C. Fischli, M. Rottmann, D. M. Plouffe, B. Bursulaya, S. Meister, L. Rameh, J. Trappe, D. Haasen, M. Timmerman, R. W. Sauerwein, R. Suwanarusk, B. Russell, L. Renia, F. Nosten, D. C. Tully, C. H. Kocken, R. J. Glynn, C. Bodenreider, D. A. Fidock, T. T.

Diagana and E. A. Winzeler (2013). "Targeting Plasmodium PI(4)K to eliminate malaria." Nature 504(7479): 248-253.

Moura-Letts, G., C. M. Diblasi, R. A. Bauer and D. S. Tan (2011). "Solid-phase synthesis and chemical space analysis of a 190-membered alkaloid/terpenoid-like library." Proc Natl Acad Sci U S A 108(17): 6745-6750.

Mrozek-Wilczkiewicz, A., E. Spaczynska, K. Malarz, W. Cieslik, M. Rams-Baron, V. Krystof and R. Musiol (2015). "Design, Synthesis and In Vitro Activity of Anticancer Styrylquinolines. The p53 Independent Mechanism of Action." PLoS One 10(11): e0142678.

Najera, J. A., M. Gonzalez-Silva and P. L. Alonso (2011). "Some lessons for the future from the Global Malaria Eradication Programme (1955-1969)." PLoS Med 8(1): e1000412.

Ncokazi, K. K. and T. J. Egan (2005). "A colorimetric high-throughput beta-hematin inhibition screening assay for use in the search for antimalarial compounds." Anal Biochem 338(2): 306-319.

Nobel Foundation (1907). Nobel Lectures. Amsterdam, Elsevier Publishing Company

Pease, B. N., E. L. Huttlin, M. P. Jedrychowski, E. Talevich, J. Harmon, T. Dillman, N. Kannan, C. Doerig, R. Chakrabarti, S. P. Gygi and D. Chakrabarti (2013). "Global analysis of protein expression and phosphorylation of three stages of Plasmodium falciparum intraerythrocytic development." J Proteome Res 12(9): 4028-4045.

Peters, W. and B. L. Robinson (1988). "The chemotherapy of rodent malaria.XLIII. Indolo (3,2-c) quinoline-N-oxides." Ann Trop Med Parasitol 82(5): 423-427.

Prasad, A., I. W. Park, H. Allen, X. Zhang, M. V. Reddy, R. Boominathan, E. P. Reddy and J. E. Groopman (2009). "Styryl sulfonyl compounds inhibit translation of cyclin D1 in mantle cell lymphoma cells." Oncogene 28(12): 1518-1528.

Proksch, P., R. A. Edrada and R. Ebel (2002). "Drugs from the seas - current status and microbiological implications." Appl Microbiol Biotechnol 59(2-3): 125-134.

Rishton, G. M. (2008). "Molecular diversity in the context of leadlikeness: compound properties that enable effective biochemical screening." Curr Opin Chem Biol 12(3): 340-351.

Roberts, B. F., I. D. Iyamu, S. Lee, E. Lee, L. Ayong, D. E. Kyle, Y. Yuan, R. Manetsch and D. Chakrabarti (2016). "Spirocyclic chromanes exhibit antiplasmodial activities and inhibit all intraerythrocytic life cycle stages." Int J Parasitol Drugs Drug Resist 6(1): 85-92.

Roberts, B. F., Y. Zheng, J. Cleaveleand, S. Lee, E. Lee, L. Ayong, Y. Yuan and D. Chakrabarti (2017). "4-Nitro styrylquinoline is an antimalarial inhibiting multiple stages of Plasmodium falciparum asexual life cycle." Int J Parasitol Drugs Drug Resist 7(1): 120-129.

Rodrigues, T., D. Reker, P. Schneider and G. Schneider (2016). "Counting on natural products for drug design." Nat Chem 8(6): 531-541.

Rts, S. C. T. P., S. T. Agnandji, B. Lell, J. F. Fernandes, B. P. Abossolo, B. G. N. O. Methogo, A. L. Kabwende, A. A. Adegnika, B. Mordmuller, S. Issifou, P. G. Kremsner, J. Sacarlal, P. Aide, M. Lanaspá, J. J. Aponte, S. Machevo, S. Acacio, H. Bulo, B. Sigauque, E. Macete, P. Alonso, S. Abdulla, N. Salim, R. Minja, M. Mpina, S. Ahmed, A. M. Ali, A. T. Mtoro, A. S. Hamad, P. Mutani, M. Tanner, H. Tinto, U. D'Alessandro, H. Sorgho, I. Valea, B. Bihoun, I. Guiraud, B. Kabore, O. Sombie, R. T. Guiguemde, J. B. Ouedraogo, M. J. Hamel, S. Kariuki, M. Onoko, C. Odero, K. Otieno, N. Awino, M. McMorro, V. Muturi-Kioi, K. F. Laserson, L. Slutsker, W. Otieno, L. Otieno, N. Otsyula, S. Gondi, A. Otieno, V. Owira, E. Oguk, G. Odongo, J. B. Woods, B. Ogutu, P. Njuguna, R. Chilengi, P. Akoo, C. Kerubo, C. Maingi, T. Lang, A. Olotu, P. Bejon, K. Marsh, G. Mwambingu, S. Owusu-Agyei, K. P. Asante, K. Osei-Kwakye, O. Boahen, D. Dosoo, I. Asante, G. Adjei, E. Kwara, D. Chandramohan, B. Greenwood, J. Lusingu, S. Gesase, A. Malabeja, O. Abdul, C. Mahende, E. Liheluka, L. Malle, M. Lemnge, T. G. Theander, C. Drakeley, D. Ansong, T. Agbenyega, S. Adjei, H. O. Boateng, T. Rettig, J. Bawa, J. Sylverken, D. Sambian, A. Sarfo, A. Agyekum, F. Martinson, I. Hoffman, T. Mvalo, P. Kamthunzi, R. Nkomo, T. Tembo, G. Tegha, M. Tsidya, J. Kilembe, C. Chawinga, W. R. Ballou, J. Cohen, Y. Guerra, E. Jongert, D. Lapierre, A. Leach, M. Lievens, O. Ofori-Anyinam, A. Olivier, J. Vekemans, T. Carter, D. Kaslow, D. Leboulleux, C. Loucq, A. Radford, B. Savarese, D. Schellenberg, M. Sillman and P. Vansadia (2012). "A phase 3 trial of RTS,S/AS01 malaria vaccine in African infants." The New England journal of medicine 367(24): 2284-2295.

Russell, T. L., N. W. Beebe, R. D. Cooper, N. F. Lobo and T. R. Burkot (2013). "Successful malaria elimination strategies require interventions that target changing vector behaviours." Malar J 12: 56.

Salmon, B. L., A. Oksman and D. E. Goldberg (2001). "Malaria parasite exit from the host erythrocyte: a two-step process requiring extraerythrocytic proteolysis." Proc Natl Acad Sci U S A 98(1): 271-276.

Sandlin, R. D., M. D. Carter, P. J. Lee, J. M. Auschwitz, S. E. Leed, J. D. Johnson and D. W. Wright (2011). "Use of the NP-40 detergent-mediated assay in discovery of inhibitors of beta-hematin crystallization." Antimicrob Agents Chemother 55(7): 3363-3369.

Sibley, C. H., J. E. Hyde, P. F. Sims, C. V. Plowe, J. G. Kublin, E. K. Mberu, A. F. Cowman, P. A. Winstanley, W. M. Watkins and A. M. Nzila (2001). "Pyrimethamine-sulfadoxine resistance in *Plasmodium falciparum*: what next?" Trends Parasitol 17(12): 582-588.

Singh, N., R. Guha, M. A. Giulianotti, C. Pinilla, R. A. Houghten and J. L. Medina-Franco (2009). "Cheminformatic analysis of combinatorial libraries, drugs, natural products, and molecular libraries small molecule repository." J Chem Inf Model 49(4): 1010-1024.

Sivakumar, K., V. B. Wang, X. Chen, G. C. Bazan, S. Kjelleberg, S. C. Loo and B. Cao (2014). "Membrane permeabilization underlies the enhancement of extracellular bioactivity in *Shewanella oneidensis* by a membrane-spanning conjugated oligoelectrolyte." Appl Microbiol Biotechnol 98(21): 9021-9031.

Sonoiki, E., A. Palencia, D. Guo, V. Ahyong, C. Dong, X. Li, V. S. Hernandez, Y. K. Zhang, W. Choi, J. Gut, J. Legac, R. Cooper, M. R. Alley, Y. R. Freund, J. DeRisi, S. Cusack and P. J. Rosenthal (2016). "Antimalarial Benzoxaboroles Target *Plasmodium falciparum* Leucyl-tRNA Synthetase." Antimicrob Agents Chemother 60(8): 4886-4895.

Tan, D. S. (2005). "Diversity-oriented synthesis: exploring the intersections between chemistry and biology." Nat Chem Biol 1(2): 74-84.

Tanner, M. and D. de Savigny (2008). "Malaria eradication back on the table." Bull World Health Organ 86(2): 82.

Teuscher, F., M. L. Gatton, N. Chen, J. Peters, D. E. Kyle and Q. Cheng (2010). "Artemisinin-induced dormancy in plasmodium falciparum: duration, recovery rates, and implications in treatment failure." J Infect Dis 202(9): 1362-1368.

Thomas, K. D., A. V. Adhikari and N. S. Shetty (2010). "Design, synthesis and antimicrobial activities of some new quinoline derivatives carrying 1,2,3-triazole moiety." Eur J Med Chem 45(9): 3803-3810.

Tine, J. A., D. E. Lanar, D. M. Smith, B. T. Welde, P. Schultheiss, L. A. Ware, E. B. Kauffman, R. A. Wirtz, C. De Taisne, G. S. Hui, S. P. Chang, P. Church, M. R. Hollingdale, D. C. Kaslow, S. Hoffman, K. P. Guito, W. R. Ballou, J. C. Sadoff and E. Paoletti (1996). "NYVAC-Pf7: a poxvirus-vectored, multiantigen, multistage vaccine candidate for Plasmodium falciparum malaria." Infection and immunity 64(9): 3833-3844.

Trager, W. and J. B. Jensen (1976). "Human malaria parasites in continuous culture." Science 193(4254): 673-675.

Vasilevich, N. I., R. V. Kombarov, D. V. Genis and M. A. Kirpichenok (2012). "Lessons from natural products chemistry can offer novel approaches for synthetic chemistry in drug discovery." J Med Chem 55(16): 7003-7009.

WHO (2016). World Malaria Report 2016. France, World Health Organization.

WHO. (2017). "Malaria." Retrieved June 02, 2017, 2017, from <http://www.who.int/ith/diseases/malaria/en/>.

WHO. (2017, April 2017). "Malaria Fact Sheet." Retrieved 06/05/2017, 2017, from <http://www.who.int/mediacentre/factsheets/fs094/en/>.

Zhang, J. H., T. D. Chung and K. R. Oldenburg (1999). "A Simple Statistical Parameter for Use in Evaluation and Validation of High Throughput Screening Assays." J Biomol Screen 4(2): 67-73.